Salisbury, M.H., Shinohara, M., Richter, C., et al., 2002
Proceedings of the Ocean Drilling Program, Initial Reports Volume 195

1. Leg 195 Summary[1]

Shipboard Scientific Party[2]

INTRODUCTION

Ocean Drilling Program Leg 195 had three distinct objectives. The first segment of the leg was devoted to coring and setting a long-term geochemical observatory at the summit of South Chamorro Seamount (Site 1200), which is a serpentine mud volcano on the forearc of the Mariana subduction system (Fig. F1). The second segment was devoted to coring and casing a hole in the Philippine Sea abyssal seafloor (Site 1201) and the installation of broadband seismometers for a long-term subseafloor borehole observatory. During the third segment, an array of advanced piston corer/extended core barrel holes was cored at Site 1202 under the Kuroshio Current in the Okinawa Trough off the island of Taiwan.

The drilling and observatory installation program at South Chamorro Seamount was designed to (1) examine the processes of mass transport and geochemical cycling in the subduction zones and forearcs of nonaccretionary convergent margins; (2) ascertain the spatial variability of slab-related fluids in the forearc environment as a means of tracing dehydration, decarbonation, and water-rock reactions in subduction and suprasubduction zone environments; (3) study the metamorphic and tectonic history of nonaccretionary forearc regions; (4) investigate the physical properties of the subduction zone as controls over dehydration reactions and seismicity; and (5) investigate biological activity associated with subduction zone material from great depth.

The seismic observatory in the Philippine Sea is an important component of the International Ocean Network seismometer net. By filling a large gap in the global seismic station grid, the observatory will help increase the resolution of global tomographic studies, which have revolutionized our understanding of mantle dynamics and structure. Moreover, the observatory will allow more precise study of the seismic structure of the crust and upper mantle of the Philippine plate, as well as

F1. Location map showing sites drilled during Leg 195, p. 33.

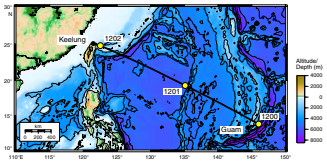

[1]Examples of how to reference the whole or part of this volume.
[2]Shipboard Scientific Party addresses.

Ms 195IR-101

better resolution of earthquake locations and mechanisms in the northwest Pacific subduction zone.

Drilling at Site 1201 was also designed to provide more precise basement age constraints for models of backarc spreading in the Philippine Sea as well as high-quality sediment sections that could be used to reconstruct the history of microplate motion, climate change, eolian transport, and arc volcanism in the region.

Drilling at Site 1202 was designed to obtain a high-resolution sediment record under the Kuroshio Current to study global climate change, sea level fluctuation, local tectonic development, and terrestrial environmental changes in East Asia over the past 2 m.y. The Okinawa Trough is one of the few locations in the Pacific where the seafloor under the Kuroshio Current lies above the carbonate compensation depth, allowing the calcareous microfossil record to be preserved, and it is the only location with a high sedimentation rate, allowing high-resolution studies.

SITE 1200: SERPENTINE MUD VOLCANO GEOCHEMICAL OBSERVATORY

South Chamorro Seamount, Mariana Forearc

Geologic processes at convergent plate margins control geochemical cycling, seismicity, and deep biosphere activity within subduction zones. The study of input into a convergent plate margin by sampling the downgoing plate provides the geochemical reference necessary to learn what factors influence the production of suprasubduction zone crust and mantle in these environments. The study of the output in terms of magma and volatiles in volcanic arcs and backarc basin settings constrains processes at work deep in the subduction zone, but these studies are incomplete without an understanding of the throughput, the nature of geochemical cycling that takes place between the time the subducting plate enters the trench and the time it reaches the zone of magma genesis beneath the arc. Tectonically induced circulation of fluids at convergent margins is a critical element in the understanding of chemical transport and cycling within convergent plate margins and, ultimately, in understanding global mass balance (e.g., COSOD II, 1987; Langseth et al., 1988; Kulm and Suess, 1990; Langseth and Moore, 1990; Martin et al., 1991). In the shallow to intermediate suprasubduction zone region, dehydration reactions release pore fluids from bound volatiles in oceanic sediments and basalts of the downgoing plate (Fryer and Fryer, 1987; Peacock, 1987, 1990; Mottl, 1992; Liu et al., 1996). Fluid production and transport affect the thermal regime of the convergent margin, metamorphism in the suprasubduction zone region, diagenesis in forearc sediments, biological activity in the region, and, ultimately, the composition of arc and backarc magmas. Furthermore, these fluids, their metamorphic effects, and the temperature and pressure conditions in the contact region between the plates (the décollement) affect the physical properties of the subduction zone, where most major earthquakes occur.

The discovery of Earth's deep biosphere is recognized as one of the most outstanding breakthroughs in the biological sciences. The extent of this biosphere is currently unknown, but we are becoming increasingly aware that life has persisted in environments ranging from active hydrothermal systems on mid-ocean ridges to deep ocean sediments,

but so far no detailed investigations have been made of the potential for interaction of the deep biosphere with processes active in convergent plate margins.

Determining unequivocally the composition of slab-derived fluids and their influences over the physical properties of the subduction zone, biological activity, or geochemical cycling in convergent margins requires direct sampling of the décollement region. To date, studies of décollement materials, mass fluxes, and geochemical interchanges have been based almost exclusively on data from drill cores taken in accretionary convergent margins (e.g., Kastner et al., 1993; Carson and Westbrook, 1995; Maltman et al., 1997). Large wedges of accreted sediment bury the underlying crystalline basement, making it inaccessible to drilling, and the wedges interact with slab-derived fluids, altering the original slab signal. The dehydration reactions and metamorphic interchanges in intermediate and deeper parts of the décollements have not been studied in these margins. By contrast, nonaccretionary convergent margins permit direct access to the crystalline basement and produce a more pristine slab-fluid signature for two reasons: the fluids do not suffer interaction with a thick accretionary sediment wedge, and they pass through fault zones that have already experienced water-rock interactions, thus minimizing interaction with subsequently escaping fluids. Regardless of the type of margin studied, the deeper décollement region is directly inaccessible with current or even foreseeable ocean drilling technologies. A locality is needed where some natural process brings materials from great depths directly to the surface. The Mariana convergent margin provides precisely the sort of environment needed.

Geologic Setting

The Mariana convergent plate margin system is nonaccretionary, and the forearc between the trench and the arc is pervasively faulted. It contains numerous large (30 km diameter and 2 km high) mud volcanoes (Fryer and Fryer, 1987; Fryer, 1992, 1996) (Fig. F2). The mud volcanoes are composed principally of unconsolidated flows of serpentine mud with clasts consisting predominantly of serpentinized mantle peridotite (Fryer, Pearce, Stokking, et al., 1990). Some have also brought up blueschist materials (Maekawa et al., 1995; Fryer and Todd, 1999). Faulting of the forearc to great depth produces fault gouge that when mixed with slab-derived fluids generates a thick gravitationally unstable slurry of mud and rock that rises in conduits along the fault plane to the seafloor (Fig. F3) (Fryer, 1992, 1996). These mud volcanoes are our most direct route to the décollement and, episodically, through protrusion events, open a window that provides a view of processes and conditions at depths as deep as 35 km beneath the forearc.

Prior to Leg 195, only one other active serpentine mud volcano (Conical Seamount) (see Fig. F2) had ever been sampled by drilling (Fryer, Pearce, Stokking, et al., 1990). Little was then known of either the processes that formed such seamounts, their distribution, and their relation to the tectonics of the forearc region or of the potential for understanding the deeper forearc processes they reflect. Recent advances in the understanding of the structure and tectonic evolution of nonaccretionary forearcs, the nature of geochemical cycling within them, and the various active thermal, hydrologic, metamorphic, and biological processes involved in the formation of mud volcanoes permitted the planning of comprehensive studies of the intermediate-depth processes occurring within the "subduction factory." By revisiting descriptions of

F2. Bathymetric map of the southern Mariana forearc, p. 34.

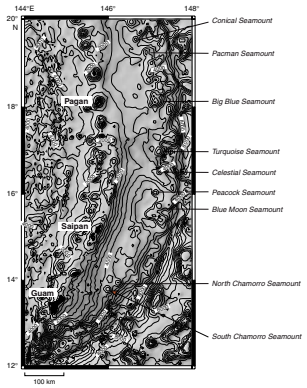

F3. Schematic cross section through the Mariana system, p. 35.

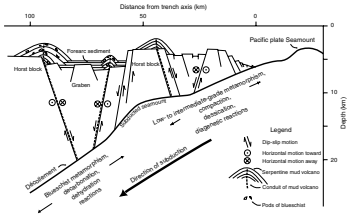

serpentine melanges and "sedimentary" serpentinite terranes from past literature (Lockwood, 1972), we now realize that serpentine mud volcanism in convergent margin settings is not merely a local curiosity of the Mariana system but occurs worldwide.

Site 1200 is located on a 200-m-high summit knoll on South Chamorro Seamount at 13°47′N, 146°00′E in a water depth of 2910 m, ~125 km east of Guam in the western Pacific Ocean. It lies 85 km from the trench, where the depth to the downgoing slab is ~26.5 km, based on studies by Isacks and Barazangi (1977). Pore fluids collected in gravity cores from this seamount exhibit a strong slab signal. It is the only known site of active blueschist mud volcanism in the world and supports the only documented megafaunal assemblages associated with serpentine/blueschist mud volcanism (Fryer and Mottl, 1997).

Side-scan surveys of this seamount (Fig. **F4**) show that the southeastern sector of the edifice has collapsed, and debris flows of serpentine material (dredged in 1981 and observed during *Shinkai 6500* dives in 1995) blanket the inner slope of the trench from the summit of the seamount to the trench axis. The summit knoll sits at the apex of the sector collapse, and its formation was most likely initiated in response to the collapse. Submersible observations show that the knoll's surface is broken into uplifted slabs of cohesive serpentine mud (Fryer, 1996) separated by meter-deep fissures with crosscutting orientations. Medium blue-green to dark blue serpentine mud and clasts of metamorphosed rocks are exposed. Low-temperature springs in the fissures support a vigorous biological community of mussels, gastropods, worm tubes, and galatheid crabs (Fryer and Mottl, 1997). The mussels are likely of the genus *Bathymodiolus,* one which contains methylotrophic symbionts in its gills and requires high ambient concentrations of methane in its feeding source (Fryer and Mottl, 1997). The pore fluid composition profiles and the presence of a vigorous biological community at the surface suggest that the summit knoll is a currently active seep region. The interior of the seamount shows little structure on six-channel seismic reflection profiles (Fryer and Mottl, 1997) (Fig. **F5**). This seamount is likely an active serpentine mud volcano similar to Conical Seamount, drilled during Leg 125 (Sites 778–780), and thus provides an excellent drill target for studies of the active processes of these mud volcanoes. It has the strongest slab signature in pore fluids from among the seamounts sampled in 1997 and is comparable to Conical Seamount in the strength of its slab signal.

F4. HMR-1 side-scan imagery of South Chamorro Seamount, p. 36.

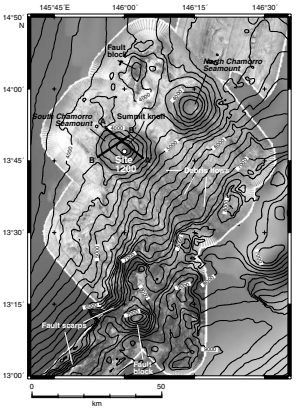

F5. Multichannel seismic reflection profiles over South Chamorro Seamount, p. 37.

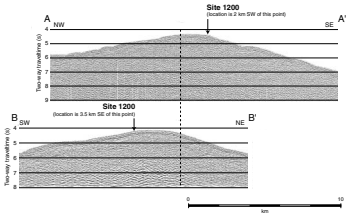

Scientific Objectives

The overall objectives of drilling at South Chamorro Seamount were to (1) study geochemical cycling and mass transport in the subduction zones and forearcs of nonaccretionary convergent margins; (2) determine the spatial variability of slab-related fluids within the forearc environment as a means of tracing dehydration, decarbonation, and water-rock reactions both in the subduction zone and the overlying suprasubduction zone environments; (3) study the metamorphic and tectonic history of nonaccretionary forearc regions; (4) investigate the physical properties of the subduction zone and their influence on dehydration reactions and seismicity; and (5) investigate biological activity associated with subduction zone material from great depth.

To achieve these scientific objectives, operations during Leg 195 were designed to recover sufficient materials to permit petrologic and mineralogic characterization of the serpentine mud flow units, to analyze

their pore fluid compositions, to collect any biological material contained in the muds, and to deploy a long-term geochemical observatory at South Chamorro Seamount.

Establishment of a Seafloor Geochemical Observatory

The primary objective at South Chamorro Seamount was to deploy a long-term geochemical observatory in a cased reentry hole in the central conduit of the serpentine mud volcano. The reentry hole for the installation of a downhole thermistor string, pressure sensor, and osmotic fluid samplers was designed to be sealed with a circulation obviation retrofit kit (CORK). The techniques that were used to install the CORK were similar to those used for successful installations during Legs 139, 164, 168, and 174B (Davis et al., 1992). The hole at Site 1200 was CORKed with a thermistor cable to obtain a long-term record of the temperature variations in the sealed hole as the natural hydrologic system reestablishes itself after drilling. This installation will provide a long-term record of (1) the rebound of temperatures toward formation conditions after the emplacement of the seal; (2) possible temporal variations in temperature and pressure due to lateral flow in discrete zones, regional and/or local seismicity, and short-term pressure effects; and (3) the composition of deep circulating fluids obtained with the osmotic samplers. Data from the downhole instruments will be collected during an NSF-funded *Jason/DSL 120* cruise that is tentatively scheduled to be conducted 18 months after Leg 195.

Fluid Transport

The drill site on South Chamorro Seamount was designed to help assess the variability of fluid transport and composition within the forearc. Previous field studies indicate that most of the fluid flow in the Mariana forearc is channeled along forearc faults and fault-controlled conduits in mud volcanoes. The pore fluid compositions are expected to vary depending on the nature of the channeling structures (diffuse network of small faults, major faults, and mud volcano conduits). In particular, fluids ascending through mud volcano conduits along well-established paths in contact with previously metamorphosed wall rock should carry the most pristine slab signature. This was certainly the case at Conical Seamount, drilled during Leg 125. The summit Site 780 produced by far the purest deep slab-derived fluids, based on their much lower chlorinity and higher K, Rb, B, H_2S, and sulfate, whereas the flank Sites 778 and 779 produced combinations of slab-derived fluid and seawater that had reacted with peridotite and basalt at shallower crustal levels (Mottl, 1992).

Fluid Budgets

Although total fluid budgets are difficult to ascertain in any convergent margin, they are likely to be more readily determined at nonaccretionary active margins because the hydrologic flow systems operate on longer timescales than do those at accretionary margins. Attempts to determine the total fluid budgets at accretionary active margins have been hindered by the presence of lateral heterogeneity and transient flow processes. Lateral heterogeneity results in different flow rates and compositions along the strike of the margin. Transient flow apparently

results largely from the valvelike influence of the accretionary complexes themselves.

Sediment properties vary with fluid pressure, and fluid pressure varies as a function of fluid production rate and transient hydrologic properties. Thus, the accretionary system acts as both a seal and a relief valve on the fluid flow system. The absence of such a short timescale, fluid pressure, and formation-properties modulator at nonaccretionary systems should allow fluids to escape more steadily. To test this hypothesis, the physical nature of fluid flow at nonaccretionary settings must be determined. Then fluid budgets can be constructed to determine whether the expected long-term flow is consistent with observations or if the flow must occur in transient pulses. The CORK experiment planned for the South Chamorro Seamount site will address this problem.

Along-Strike Variability

The composition of slab-derived fluids and deep-derived rock materials may differ along the strike of the forearc, reflecting regional variations in composition within the slab and suprasubduction zone lithosphere. The pore fluids from several of the forearc mud volcanoes already sampled are chemically distinct, and it was anticipated that the pore waters from South Chamorro Seamount would also be chemically distinct. These differences are probably associated not only with the depth to the slab but also with the physical conditions under which water-rock reactions occur and the variations in the regional composition of the plate and overriding forearc wedge.

The geochemistry of the fluids from Conical Seamount is described in detail in several publications (Fryer et al., 1990; Haggerty, 1991; Haggerty and Chaudhuri, 1992; Haggerty and Fisher, 1992; Mottl, 1992; Mottl and Alt, 1992). These papers show the origin of the Conical Seamount fluids to be from dehydration of oceanic crustal basalt and sediment at the top of the subducting lithospheric slab. The compositions of the fluids from the PACMANUS hydrothermal field and seamounts farther south are reported in Fryer et al. (1999). Pore fluids from these indicate a slab source, as shown by their lower chlorinity and higher K and Rb, similar to that observed at Conical Seamount by Mottl (1992).

Pressure and Temperature Indicators from Fluids

The composition of slab-derived and deep-derived metamorphosed rock is useful in defining geochemical processes and estimates of the thermal and pressure regime at depth, and thus, for determining the physical properties of the décollement region. It was hoped that it would also be possible to constrain some of the pressure and temperature conditions under which certain dehydration reactions take place in the subducted slab. Pore fluids from Ocean Drilling Program (ODP) Site 780 at the summit of Conical Seamount are unusual because of geochemical and physical processes at depth. The observed enrichments in alkali elements and B in fluids from Site 780 are unambiguous indicators of a source temperature in excess of 150°C, yet the fact that these elements are depleted at Sites 778 and 779 on the flanks of Conical Seamount, relative to their concentrations in seawater, indicates that the deep slab signal can be readily overprinted by local peridotite-seawater reactions at lower temperatures. Not all chemical spe-

cies are affected by this overprinting, however (i.e., sulfur isotopic composition of dissolved sulfate) (Mottl and Alt, 1992). Thus, to avoid potential reactions between sediment and slab-derived fluids, we planned to collect fluids from mud volcano conduits, where continued focused flow provides a pathway for slab-derived "basement" fluids to reach the seafloor.

Metamorphic Parageneses

Studies of deep-derived minerals and metamorphic rock fragments brought to the surface in mud flows in serpentine seamounts can be used to constrain the pressure and temperature regimes under which the metamorphism that formed them took place. It is known, for instance, that the minimum pressures of formation for incipient blueschist materials from Conical Seamount are 6–7 kbar (Maekawa et al., 1995). Similarly, from the paragenesis of crossite schist recovered in cores from South Chamorro Seamount, it can be shown that pressures >7 kbar are consistent with their metamorphism. Examination of a more extensive collection of the muds and clasts from South Chamorro Seamount should make it possible to quantify the assemblages of muds and xenoliths present in the flows and constrain the ranges of pressure and temperature that exist in the source regions for these materials.

Biological Activity Associated with Deep-Derived Subduction Zone Material

Interest in the deep subsurface biosphere has grown dramatically as a result of recent studies linking extreme environments to the first living organisms that inhabited the Earth. The search for the last common ancestor in the geologic record is moving toward high-temperature environments, such as those at spreading centers and hotspots both on the ocean floor and on land. Microbes and microbial products are abundant in oceanic hydrothermal environments and are presumed to be representative of a community of thermophilic and hyperthermophilic organisms that originated beneath the seafloor (Fisk et al., 1998). Microbes are also involved in the transformation of minerals in the oceanic crust and in the cycling of elements in the crust; however, the origin of these microbes is much more controversial.

Drilling at Chamorro Seamount provides a unique opportunity to determine the nature of microbiological activity in a very different kind of extreme environment, the high-pH, low-temperature environment associated with serpentine/blueschist mud volcanism (Fryer and Mottl, 1997; Fryer et al., 1999), and to reexamine the hypothesis that microbes are capable of using alternative energy sources that would support a heterotrophic subsurface ecosystem. In addition, because the pore fluids are more pristine in nonaccretionary convergent margins, it should be easier to assess from the chemistry of both the muds and the fluids whether organic syntheses capable of supporting life are active in these settings.

Understanding the origin of the deep biosphere is a fundamental ODP objective and will further address the compelling question of whether life arose in extreme environments rather than on the surface of the early Earth. Although several experimental studies indicate that a thermophilic origin of life is possible, definitive proof must await an assessment of the full range of conditions in which life exists and the nature of life in these environments.

Mechanics and Rheology

The mechanics and rheology of serpentine muds in the Mariana forearc seamounts control the processes that formed the seamounts and their morphology. It was thus planned to conduct a rheological study of the serpentine muds to place realistic constraints on the mechanisms governing the ascent of the muds to the surface, the maintenance of the conduits, and the construction of the seamounts.

Shipboard torsion-vane testing during Leg 125 at Conical Seamount in the Mariana forearc and at Torishima Forearc Seamount in the Bonin forearc showed that the serpentine muds are plastic solids with a rheology that bears many similarities to the idealized Cam clay model and is well described by critical-state soil mechanics (Phipps and Ballotti, 1992). These muds are thus orders of magnitude weaker than salt and are, in fact, comparable in strength to common deep-sea pelagic clays. The rate at which the muds rise relative to the fluids will likely influence the water-rock reactions and the character of the slab signal in fluids from these mud volcanoes. Better constraints on the nature of the fluids will permit a more accurate determination of the physical conditions of the décollement, where the fluids originate.

Drilling Strategy and Operations

After steaming to the site and lowering the pipe to the summit of the seamount, we planned to conduct a brief seafloor television survey of the conduit to locate the springs and mussel beds identified in *Shinkai 6500* dives and to identify sites near the springs for rotary core barrel (RCB) coring and logging and relatively clast-free sites for advanced piston corer/extended core barrel (APC/XCB) coring, jet-in tests, and the establishment of a reentry hole. After conducting a jet-in test to establish the depth of the first casing string for the reentry hole, we planned to core and log an RCB pilot hole to 450 meters below seafloor (mbsf) to determine the nature of the formation and the ease of drilling on the seamount, a major concern because drilling during Leg 125 at Conical Seamount had been plagued with drilling problems.

Depending on the results of the RCB hole, we then planned to offset and jet in a reentry cone and 20-in casing to ~25 mbsf and then drill a hole in stages to 420 mbsf for the CORK installation. In anticipation of hole instability problems, an elaborate casing program was envisioned, with cemented 16-in casing to 200 mbsf followed by 10.75-in casing to 400 mbsf, including 23 m of screened casing and a casing shoe at the bottom to prevent the serpentine mud from slowly invading the installation from below. After the hole was drilled and cased, the instrumentation installed, and the remotely operated vehicle (ROV) platform emplaced, we planned to drill an APC/XCB hole to 420 mbsf to collect a continuous, undisturbed section for petrologic and pore water studies. By drilling the APC/XCB hole last, the time allocated for APC/XCB coring could be held in reserve as contingency time if it took longer than anticipated to drill the reentry hole and install the observatory. Not surprisingly, the actual operations at Site 1200 unfolded rather differently.

The *JOIDES Resolution* arrived at Site 1200 (proposed Site MAF-4B) at 2100 hr on 11 March 2001. Following a 4-hr camera survey, Hole 1200A was spudded adjacent to a vent mussel community at the top of South Chamorro Seamount at 2200 hr on 11 March with the RCB and cored to a depth of 147.2 mbsf (Fig. F6; Table T1). High torque and lost rotation at this depth resulted in a stuck drill string that ultimately forced

F6. Location of Holes 1200A–1200E on the summit knoll of South Chamorro Seamount, p. 38.

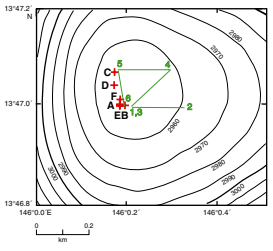

T1. Leg 195 coring summary, p. 63.

us to abandon the hole. Recovery in Hole 1200A was poor (147.2 m cored; 9.4% recovered), with little recovery of the mud matrix material surrounding the hard ultramafic clasts. The drill string was pulled out of the hole, and the seafloor was cleared at 1535 hr, ending Hole 1200A.

The ship was then offset 25 m to the east, and Hole 1200B was spudded at 1640 hr on 13 March. Our intention was to wash to 147.2 mbsf and then start coring to the target depth of 450 m. By 1615 hr on 14 March, the hole had been advanced to a depth of 98.0 mbsf. Once again, high torque and overpull began to plague the hole. Despite consistent mud sweeps and multiple reaming attempts, the hole could not be stabilized. At 0645 hr on 14 March, we decided to abandon further drilling/coring efforts in the pilot hole and to start the reentry hole because it was obvious that deep penetration could not be achieved without the use of casing.

Once the drill string was pulled out of the hole with the top drive, the ship was offset to the north and Hole 1200C was spudded at 0450 hr with the 20-in casing attached to the reentry cone. After a total of 18.25 hr of drilling with an 18.5-in bit, 22-in underreamer, and drilling motor, the reentry cone base reached the seabed, placing the 20-in casing shoe at 23.7 mbsf. Drilling of the 22-in hole for the 16-in intermediate casing string, without the motor this time, advanced smoothly and without incident. At 0130 hr on 18 March, the hole reached a depth of 140 mbsf. While we washed/lowered the casing string into the hole, however, the casing shoe encountered an obstruction 6 m off bottom that prevented the casing hanger from landing. After three futile hours, the drill string was recovered and one joint of casing was removed from the string. The shortened string was run back into the hole and washed down without incident. With the 16-in casing shoe placed at a depth of 107.4 mbsf, the casing string was cemented in place. The drilling process was then reinitiated using a 14.75-in drill bit and 20-in underreamer, dressed with 20-in cutter arms, and advanced to a depth of 266.0 mbsf. The penetration rate deteriorated to zero at that point, and a subsequent wiper trip found 9 m of soft fill at the bottom of the hole that was easily removed by circulation. Upon reaching the rig floor, the underreamer was missing two out of three cutters. Because the hole had penetrated below the base of the summit knoll but could not be deepened further, the 10.75-in casing was deployed, reaching a depth of 224.0 mbsf by 0300 hr on 24 March without incident. However, progress beyond this point was not possible, and the string was pulled out of the hole to remove three joints of casing. The shortened casing string finally placed the shoe at 202.8 mbsf, with the screened interval extending from 202.3 to 148.8 mbsf (Fig. **F7**).

The CORK assembly, with two stands of 5.5-in drill pipe used as the stinger, was run in the hole, and the drill string was lowered to 53.0 mbsf. This left the CORK shy of landing out by ~8 m. At 1300 hr on 25 March, the thermistor/osmotic sampler assembly was slowly run in the hole, and at 1430 hr the data logger was landed in the CORK body. After 1 hr of pressure transducer calibration, the data logger was latched and the CORK body was then lowered the final few meters and latched in place as in Figure **F8.** The CORK installations at Hole 1200C ended with a successful free-fall deployment of the ROV platform. The pipe was then returned to the surface; not counting the pilot holes, nine round pipe trips totaling 52 pipe-km of tripping pipe were required to deploy the observatory.

After the successful installation of the geochemical observatory, the vessel was offset 40 m to the south and Hole 1200D was spudded with

F7. Casing configuration for the geochemical observatory, p. 39.

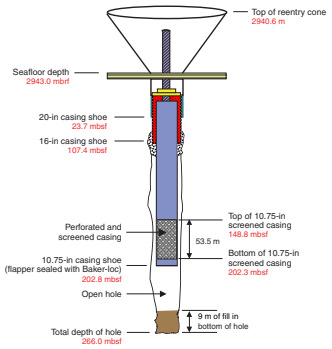

F8. CORK configuration in Hole 1200C, p. 40.

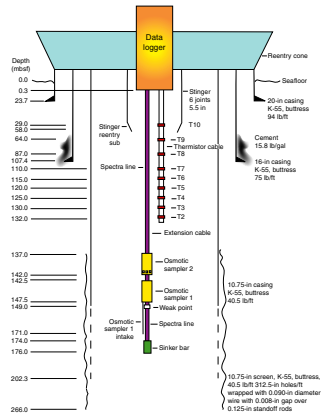

the APC to sample the serpentine muds for petrology, pore water, and microbiology studies at 1415 hr on 26 March. Coring continued to a depth of 44.4 mbsf using the APC advance-by-recovery method. Hard clasts were drilled with an XCB center bit assembly. After coring was halted by a hard clast at 44.4 mbsf, the XCB was used to deepen the hole. After advancing 9.0 m, however, the penetration rate fell to zero and the decision was made to abandon Hole 1200D.

The vessel was then offset back to the location of the earlier identified mussel beds, and Hole 1200E was spudded with the APC for further pore water studies. Coring with the APC/XCB continued, again using the advance-by-recovery method for the APC cores, to a depth of 50.4 mbsf, where the scientific objectives of the hole were met.

The ship was then offset 20 m to the north, and Hole 1200F was spudded at 1315 hr. Coring proceeded until the time allocated for operations at Site 1200 ran out. The hole depth reached 16.3 mbsf, with the recovery of APC Cores 195-1200F-1H through 3H. At 0200 hr on 29 March 2001, the ship was under way to the Guam pilot station.

Principal Results

The principal objective at Site 1200 was to install a borehole geochemical observatory at the summit of South Chamorro Seamount to sample fluids from the décollement below the Mariana forearc. Although this objective was achieved, no data will be recovered from the observatory until it is revisited by an ROV in 2003. As was to be expected in such an exotic environment, however, the drilling and coring undertaken to install the observatory and document its setting produced unexpected and often spectacular results.

Perhaps the most fundamental achievement at Site 1200 was the documentation of the muds, xenoliths, and fluids rising to the surface from the mantle and the décollement zone through the central conduit of the mud volcano. The recovery in all cored holes consisted of poorly sorted, dark blue-gray to black serpentine mud breccia (Fig. F9) in which the muds are composed predominantly of silty clay–sized serpentine, and the clasts, which range up to a meter across, consist largely of serpentinized ultramafics.

F9. Serpentine mud breccia from South Chamorro Seamount, p. 41.

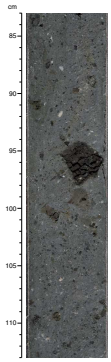

Well-preserved and diversified subtropical assemblages of planktonic foraminifers and calcareous nannofossils were found in the top 0.1–0.3 m of the holes that were APC cored (Holes 1200D, 1200E, and 1200F), indicating that the surface of the summit is blanketed with a veneer of calcareous microfossil-bearing deposits. A few species of benthic foraminifers are also present in small quantities in all holes. Samples farthest away from the vent communities contain more abundant, diversified, and better-preserved microfossil fauna. The downcore sections in these three holes are virtually barren of microfossils, except for a peculiar interval with folded color bands between 11 and 13 mbsf in Hole 1200D, which is interpreted as a paleosurface that has been covered or folded into the mud by the flow of serpentine. This interval contains abundant and diversified calcareous microfossils comparable to the core tops. The major difference is that these fossils tend to be robust species overgrown by calcite on the original structures, whereas the more delicate species have been dissolved. All the fossils are late Quaternary in age.

With the exception of the two calcareous intervals noted above, which are light yellow-brown to pink due to their microfossil content, and a 10- to 20-m-thick zone of strongly reduced, black serpentine

muds starting about a meter below the seafloor, the mud breccia in the conduit displays no stratigraphy, which is consistent with its mud volcano origin. It has been divided into two facies, however, on the basis of the abundance of clasts (<10% and 10%–30%); based on recovery, the average is ~7%. The smaller ultramafic clasts tend to be angular with planar external surfaces along early serpentine veins, whereas the larger clasts are subrounded to rounded, suggesting comminution by collisions during ascent.

The mineralogy and composition of the muds and clasts almost all attest to a deep origin along the décollement zone or the overlying mantle, regardless of the particle or clast size, from silty clay to boulder. With the exception of aragonite produced at the mudline, where rising pore fluids interact with seawater to produce carbonates and rare zeolites (analcime) found farther down in the section, X-ray diffraction (XRD) analysis shows that the muds are dominated by serpentine minerals formed by the hydration of ultramafics + accessory glaucophane, spinel, garnet, chlorite, and talc derived from the metamorphism of mafic rocks along the décollement. Optical examination on board ship suggests lizardite/antigorite > chrysotile > brucite.

The dual origin of the materials making up the mud breccia is even more clearly revealed in the grit fraction (0.1–1.5 cm). About 90% by volume of the grit fraction consists of partially to completely serpentinized ultramafic rocks, but 10% consists of metabasites, including glaucophane schist (Fig. **F10**), crossite/white-mica/chlorite schist, chlorite schist (Fig. **F11**), white-mica schist, and amphibolite schist containing blue-green to black amphibole and interstitial mica. These lithologies, especially the blueschists, are indicative of a high-pressure, low-temperature origin (Fryer et al., 1999; Fryer and Todd, 1999; Todd and Fryer, 1999), and we interpret them as metamorphosed basic rocks from the descending slab. About 1% of the serpentine mud consists of blue sodic amphibole. Analysis of similar grains in gravity cores from South Chamorro Seamount showed a crossitic composition (Fryer et al., 1999). The mineral grains are zoned with blue rims and lighter blue-green cores, implying relatively rapid ascent with the rising serpentine muds. The rationale for this interpretation is that if the grains had been in contact with rising fluids having the extreme compositions observed in the pore water analyses (see below) for geologically significant periods of time, they would have likely back-reacted and would show retrograde metamorphic effects.

Although retrograde reactions are generally sluggish, the primary reason for this is the lack of reactive fluids in a system that has previously experienced prograde regional metamorphism. Such metamorphism drives volatiles out of the rocks, resulting in a dry system, which is far less likely to undergo retrograde metamorphism despite changes in pressure and temperature. The presence of highly reactive fluids in intimate contact with the serpentine muds at Site 1200, however, would make the possibility of retrograde reactions far more likely. None of the materials studied previously by Fryer and colleagues (Fryer et al., 1999; Todd and Fryer, 1999) have ever shown any indication of retrograde effects. The mineral grains from Site 1200 also lack retrograde effects.

Although the grit fraction contains a rich and varied population of high P-T samples from the décollement, such samples appear to be absent from the large clasts, suggesting that the metabasites reaching the surface are preferentially smaller pieces. The abundance of phyllosilicate minerals in the schists may contribute to the comminution of these samples as they rise from the source region. Pressure release as the

F10. Glaucophane schist in serpentine mud, p. 42.

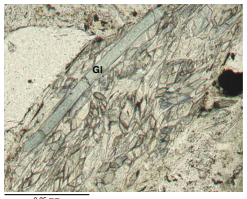

F11. Tremolite-rich chlorite schist in serpentine mud, p. 43.

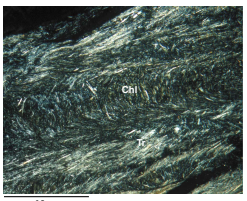

rock fragments rise may cause the phyllosilicates to expand and disintegrate, and the continual collisions and mechanical grinding within the rising muds may cause the more friable rocks to break up into small fragments.

As noted earlier, about 7% of the material recovered at Site 1200 consists of large clasts of partially to completely serpentinized ultramafic rocks from the mantle wedge under the Mariana forearc. Whereas serpentinization has been extensive in all samples (40%–100%; average = ~75%), there are sufficient relict minerals present in many of the samples to assess the original grain size (0.01–5.0 mm) and to determine that harzburgite is the dominant protolith, dunite is much less common, and lherzolite is rare. This is consistent with the whole-rock chemistry of the samples, which suggests that the ultramafics underwent 20%–25% melt extraction at some point during the formation of the arc (Fig. **F12**). The actual percentage of relict minerals is extremely variable, with olivine ranging from 0% to 40%, orthopyroxene (enstatite) from 0% to 35%, clinopyroxene from 0% to 5%, and chrome spinel from 0% to 3%, depending on the original mineralogy and the degree of serpentinization. In general, olivine and enstatite were the least stable minerals, with olivine altering readily to serpentine (lizardite) or brucite + magnetite and enstatite altering to serpentine ± tremolite/actinolite, whereas clinopyroxene and spinel were usually the most resistant to alteration. Olivine often developed mesh and hourglass textures during serpentinization, whereas enstatite is commonly replaced by bastitic textures. The serpentinization appears to have occurred in stages, because lizardite veins are often cut orthogonally by chrysotile veins, producing spectacular "Frankenstein veins" consistent with uniform dilation during late-stage serpentinization along grain boundaries. Interestingly, most of the ultramafics and all of the dunites show evidence of deformation prior to serpentinization: the olivines commonly show kink banding and granulation and the enstatites (or their bastite replacements) often display undulatory extinction.

The pore waters from Site 1200 revealed two distinct phenomena, a deep-sourced fluid that is believed to be upwelling from the top of the subducting slab 25–30 km below the seafloor and a new and exotic extremophile microbial community at 0–20 mbsf that is chemically manipulating its environment. As can be seen in Figure **F13,** most pore water vs. composition profiles for the site represent nearly ideal advection-diffusion curves and the gradients in the top few meters are so steep that they can only be maintained by upwelling from below. The deep fluid is similar in many ways to that sampled at Conical Seamount to the north during Leg 125 (Fryer, Pearce, Stokking, et al., 1990). It has a pH of 12.5 because it is in equilibrium with brucite, making it, along with the Conical Seamount fluids, the most alkaline pore water ever sampled in the deep sea. The pore water is also enriched in (mainly carbonate) alkalinity (60 mmol/kg), Na (610 mmol/kg), Na/Cl (1.2), K (19 mmol/kg), B (3.2 mmol/kg), ammonia (0.22 mmol/kg), methane (2 mmol/kg), and C_2 through C_6 hydrocarbons, all components that are virtually absent in depleted harzburgites and therefore require a different source. The pore water is highly depleted in Mg, Ca, Sr, and Li and has low concentrations of Si, Mn, Fe, Ba, and phosphate. It is slightly depleted in chloride (510 mmol/kg in seawater) and enriched in sulfate (by 7% relative to chloride). This chloride depletion is much smaller than in the deep fluid from Conical Seamount, suggesting that the Conical conduit is more heavily serpentinized and less reactive, allowing more of the H_2O from the deep source to arrive at the seafloor with-

F12. Composition diagrams for Mariana forearc peridotites showing degrees of partial melting, p. 44.

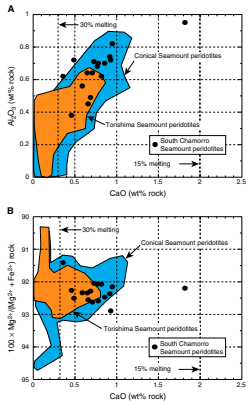

F13. Pore water composition vs. depth curves, p. 45.

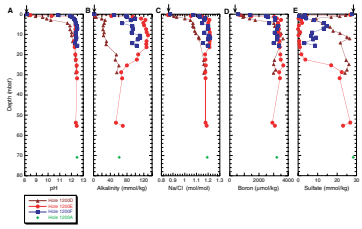

out being lost to serpentinization along the way, or that the fluids are rising more rapidly at Conical Seamount and have had less time to react.

Pore water composition vs. depth profiles also reveal that these deep fluids feed an active microbial community that is oxidizing light hydrocarbons from the fluid while reducing sulfate within the black serpentine mud in the upper 20 mbsf. This is a true extremophile community, operating at and probably driving the pH to 12.5, thus perpetuating its own ecosystem. Sulfate reduction is most active at two levels. Microbes within the upper level at 3 mbsf reduce seawater sulfate that diffuses downward against the ascending flow. Those within the lower level at 13 mbsf reduce sulfate that is supplied from the subducting slab by the upwelling fluid. As organic carbon is virtually absent within the depleted, serpentinized harzburgite, the microbes rely on methane and the C_2 through C_6 thermogenic hydrocarbons for their source of organic carbon and ammonia for their source of nitrogen. Both are supplied by the upwelling fluid. The microbial community intercepts these nutrients and effectively traps them within the ecosystem, where they can be recycled and continually enriched. This process explains the enrichment in organic carbon in the uppermost sediment. Iron sulfides and $CaCO_3$ in the form of aragonite needles and chimneys are also enriched there by reaction between the ascending fluid, the microbial community, and the overlying seawater.

As would be expected, the physical properties of the serpentine muds and clasts at Site 1200 are quite different and both are strongly influenced by the properties of serpentine. The velocities of the clasts, for example, range from 3.8 to 5.5 km/s and average 4.9 km/s, consistent with extensive serpentinization. Whereas the mud and the clasts have the same average grain density (2.64 g/cm^3), the average bulk densities of the clasts and the muds are lower and quite different, 2.49 and 1.87 g/cm^3, respectively. This is due primarily to differences in porosity between the clasts, which have low porosities, and the muds, which range from 40% to 60% porosity. Assuming the mud constitutes 93% of the breccia, the material in the conduit has an average density of 1.91 g/cm^3. If the average density of the crust is 2.75 g/cm^3, then the buoyancy of the serpentine mud breccia in the upper crust would be ~0.8 g/cm^3 before consolidation, or four times the density contrast between the salt in diapirs and most sedimentary rocks. Similarly, the buoyancy of completely consolidated serpentine mud breccia with a bulk density of 2.64 g/cm^3 (the grain density) in fresh ultramafics (~3.2 g/cm^3) would be ~0.5 g/cm^3, or more than twice the buoyancy of salt in sedimentary rocks. Whereas the average shear strength of the serpentine mud (52.5 kPa) is high for sediments, it is orders of magnitude lower than that for rocks, which is consistent with their extrusion on the seafloor as mud volcanoes.

Interestingly, although vent communities are observed on the summit, the borehole temperatures are very low in the upper 50 m in all of the holes measured at Site 1200, ranging from 2° to 3°C, or ~1.3°C above seafloor values. The heat flow values are quite variable, however, with those measured in Holes 1200A and 1200E near the springs averaging 15 mW/m^2, considerably below the global average of 50 mW/m^2, whereas the value measured in Hole 1200F, which was farther away, was ~100 mW/m^2. The thermal conductivities of the muds are not unusual, ranging from 1.04 to 1.54 W/(m·K) with an average of ~1.32 W/(m·K), but the hydraulic conductivities are extremely low, ~0.6 cm/yr.

Unlike the physical properties discussed above, the magnetic properties of the clasts and muds are similar: the average natural remanent magnetization (NRM) intensities of both are high (0.49 and 0.44 A/m for the clasts and muds, respectively), as are their average susceptibilities (5.58×10^{-3} and 6.81×10^{-3}, respectively). In both cases, the magnetization disappears at a Curie temperature of 585°C, indicating that the dominant magnetic mineral is magnetite produced by serpentinization. The only significant difference is that the NRM in the serpentine muds is unstable, whereas that in the clasts tends to be stable, with a high Koenigsberger ratio (average = 2.4). The NRM inclination and declination vary randomly with depth in single long pieces, however, indicating that the magnetization was acquired (i.e., serpentinization occurred) over a relatively long period or when the rock was being deformed or tumbled in the décollement or the conduit of the seamount.

SITE 1201: ION SEISMIC OBSERVATORY

West Philippine Basin

Tomographic studies using earthquake waves propagating through the Earth's interior have revolutionized our understanding of mantle structure and dynamics. High-quality digital seismic data obtained from seismic stations on land, for example, have been used to identify zones of anomalous velocity and anisotropy in the mantle, and from these, to determine patterns of mantle flow. In particular, Tanimoto (1988) has demonstrated the existence of a strong pattern of deep (>550 km) high-velocity anomalies in the western Pacific, suggesting complex interaction between subducting slabs and the surrounding mantle, whereas more recent studies in areas of dense seismic coverage have provided crude images of subducting plates extending to the 670-km discontinuity (van der Hilst et al., 1991; Fukao et al., 1992) and of deep velocity anomalies extending beneath ridges (Zhang and Tanimoto, 1992; Su et al., 1992).

One of the critical problems facing seismologists who wish to improve such tomographic models is the uneven global distribution of seismic stations. Few seismic stations are located on the 71% of the Earth's surface covered by oceans, and this problem is particularly acute in large expanses of ocean such as the Pacific. The scientific importance of establishing long-term geophysical observatories at deep ocean sites to understand the dynamic processes occurring in the Earth's interior through seismic imaging has long been recognized by the earth science and ocean drilling communities (COSOD II, 1987; JOI-ESF, 1987; Purdy and Dziewonski, 1988; JOI/USSAC, 1994; Montagner and Lancelot, 1995). The International Ocean Network (ION) project has identified the western Pacific and the Philippine Sea as a particularly important gap in the global seismic network. By installing long-term borehole seismic observatories in the seafloor in this region, the ION project is attempting to fill this gap so that high-resolution tomographic images of slab–mantle interaction zones can be obtained at great depth in the most active system of subduction complexes in the world. To this end, borehole seismic observatories were installed at ODP Sites 1150 and 1151 (Stations JT-1 and JT-2 in Fig. F14) on the inner wall of the Japan Trench during Leg 186 (Suyehiro, Sacks, Acton, et al., 2000) and another observatory was successfully installed at Site 1179 in the western

F14. Location of seismic station coverage in the northwest Pacific region, p. 46.

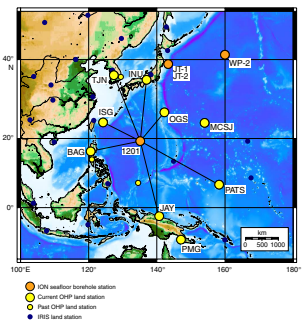

Pacific (Station WP-2 in Fig. F14) during ODP Leg 191 (Kanazawa, Sager, Escutia, et al., 2001).

A major objective of the ION project was to establish a borehole seismic observatory at a quiet site in the middle of the Philippine Sea on the upper plate of the Mariana subduction system to determine whether the Pacific plate is penetrating into the lower mantle below the 670-km discontinuity under the Mariana Trench but not under the Izu-Ogasawara (Bonin) Trench. A high-quality digital seismic observatory was thus installed during Leg 195 at Site 1201 in the West Philippine Basin west of the Kyushu-Palau Ridge between existing stations at Inuyama (IMA) and Taejon (TJN) to the north, Minami Torishima (MCSJ) and Chichijima (OGS) to the east, Ponphei (PATS) and Jayapura (JAY) to the south, and Ishigakishima (ISG) and Baguio (BAG) to the west (Fig. F14). The observatory is designed as a stand-alone system with its own battery pack and recorder at the seafloor so that it can be serviced and interrogated by an ROV. Like the borehole observatories installed at Sites 1150 and 1151, however, there is a coaxial transoceanic telephone cable (TPC-2) near Site 1201 that can be used eventually for data recovery and power. There are plans to connect data, control, and power lines to the TPC-2 cable, which is owned by the University of Tokyo, after confirmation of data retrieval. This is done under the auspices of the Ocean Hemisphere Network Project, a national program from 1995 to 2001 in Japan. The data will eventually become accessible worldwide through the Internet.

Geologic Setting

Site 1201 is located in the West Philippine Basin in 5711 m of water ~100 km west of the inactive Kyushu-Palau Ridge and 450 km north of the extinct Central Basin Fault (Fig. F15). Early interpretations of magnetic lineations (Hilde and Lee, 1984) indicated that the site lies on 49-Ma crust near Chron 21 and formed by northeast-southwest spreading on the Central Basin Fault. The spreading direction then changed to north-south at ~45 Ma, and spreading finally ceased at ~35 Ma as volcanism stopped on the Kyushu-Palau Ridge. Because the earliest magnetic anomalies in the region predate the initiation of subduction at ~45 Ma along the Kyushu-Palau Ridge, Hilde and Lee (1984) considered that the Philippine Sea initially formed by entrapment of an older Pacific spreading ridge. More recent bathymetric and magnetic surveys (Okino et al., 1999) show that the site lies at the transition from well-defined anomalies south of the Oki-Daito Ridge to more complicated anomalies to the north, which implies that the crust to the north may have formed at a different spreading center. Analysis of paleolatitude and declination data from the Philippine plate and its margins suggests that the plate has drifted about 15° to the north and rotated clockwise by up to 90° since the middle Eocene (Hall et al., 1995).

The sediment section at Site 1201 was predicted to be ~400 m thick based on recent seismic reflection surveys showing a two-way traveltime to basement of 0.45 s (Fig. F16). Drilling at other sites in the region during Deep Sea Drilling Project (DSDP) Legs 31 and 59 (Karig, Ingle, et al., 1975; Kroenke, Scott, et al., 1981) recovered a relatively barren deepwater section dominated by Holocene to Eocene–Paleocene(?) brown pelagic clays overlying basement near the Oki-Daito Ridge (DSDP Sites 294 and 295). At DSDP Sites 290 and 447 to the south, the section consists of a barren interval of Pliocene clays underlain by Oligocene nannofossil-bearing silty clays mixed with ash. This

F15. Location map showing DSDP and ODP sites in the Philippine Sea, p. 47.

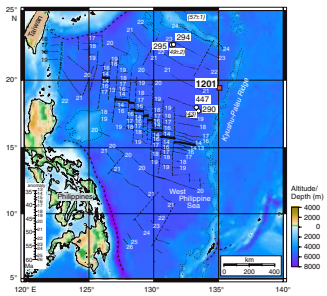

F16. Reflection line OT97 showing the location of Site 1201, p. 48.

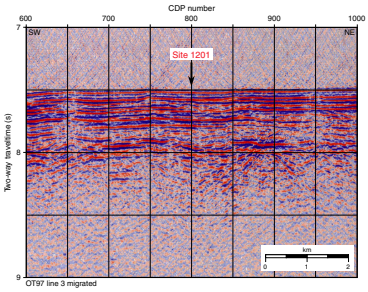

was underlain by a thick section of polymict and volcanic breccia presumably derived from the Kyushu-Palau Ridge to the east. The underlying basement consists of 80% basalt pillows and 20% diabase. Because Site 1201 lies in a similar setting at the foot of the Kyushu-Palau Ridge, it was considered likely that the section would be similar to that at Sites 290 and 447.

Scientific Objectives

The principal objective at Site 1201 was to install a long-term borehole seismic observatory in the middle of the Philippine plate to improve global seismic coverage, to study the structure of the upper mantle under the Philippine Sea, and to study plate interactions in the western Pacific. It was also expected that drilling at Site 1201 would provide samples representative of the Eocene/Paleocene crust of the northern West Philippine Basin. Results from this site would thus augment those obtained during DSDP Legs 31 and 59, which were the first legs to sample and estimate the age of basement in the region and to confirm that the seafloor formed by backarc spreading. Results from this site will also add to our knowledge of backarc crustal structure and geochemistry, microplate tectonics, magnetic lineations, and sedimentation. Because core quality and dating techniques have vastly improved since these early legs, it was also anticipated that drilling at Site 1201 would provide better age control on backarc spreading as well as detailed records of Northern Hemisphere climate change, eolian transport, and arc volcanism in the region during the Tertiary.

Establishment of a Borehole Seismic Observatory

As outlined above, one of the main reasons for installing a borehole seismic observatory in the middle of the Philippine plate was to achieve homogeneous seismic coverage of the Earth's surface with at least one station per 2000 km in the northwestern Pacific area (Fig. **F14**). Aside from plugging an important gap in the global seismic array, the Site 1201 observatory will produce high-quality seismic data. Tests with other borehole seismometers show that the noise level for oceanic borehole instruments is much lower than for most land stations (e.g., Stephen et al., 1999). High-quality seismic data from this site will be used for several purposes.

Earthquake Mechanisms

First, an observatory at Site 1201 will provide data from the backarc side of the Izu-Ogasawara and Mariana Trenches, giving greater accuracy and resolution of earthquake locations and source mechanisms. The observatory will also be valuable for resolving events in the Ryukyu and Philippine Trenches because its location is analogous to that of station WP-2 off the Japan Trench.

Structure of the Philippine Plate

Observations of seismic surface waves as well as various phases of body waves from earthquakes along the margins of the Philippine plate will provide sufficient data to map differences in plate structure among the different basins comprising the plate (e.g., the West Philippine, Shikoku, Japan, and Parece Vela Basins). Only a few previous studies with limited resolution exist on the lithospheric structure of these areas (Seekins and Teng, 1977; Goodman and Bibee, 1991). Surface wave data

suggest that the plate is only ~30 km thick (Seekins and Teng, 1977). Such a value is inconsistent with predicted values from age vs. heat flow and age vs. depth curves (Louden, 1980). A long-line (500 km) seismic refraction experiment in the West Philippine Basin could not image the lithosphere/asthenosphere boundary (Goodman and Bibee, 1991).

Mantle Structure and Dynamics

Finally, Site 1201 will provide higher seismic resolution of mantle and lithosphere structures in key areas that are now poorly imaged. There are indications that the subducting Pacific plate does not penetrate below the 670-km discontinuity and that it extends horizontally (Fukao et al., 1992; Fukao, 1992), but the resolution of these studies is poor (>1000 km) beneath the Philippine Sea and the northwestern Pacific, especially in the upper mantle, where significant discontinuities and lateral heterogeneities exist (Fukao, 1992). Data from Site 1201 will be crucial in determining whether the Pacific plate is penetrating into the lower mantle in the Mariana Trench but not in the Izu-Ogasawara (Bonin) Trench (van der Hilst et al., 1991; Fukao et al., 1992; van der Hilst and Seno, 1993) and in determining how the stagnant slab eventually sinks into the lower mantle (Ringwood and Irifune, 1988). Detailed images of mantle flow patterns may also help explain how backarc basins open and close and explain the mantle heterogeneity that causes the basalts sampled from western Pacific marginal basins to have Indian Ocean Ridge isotopic characteristics (Hickey-Vargas et al., 1995).

In addition to the seismic objectives at Site 1201, we recognized that coring at the site might accomplish a number of important geologic objectives.

Age of Basement

Although the age of the basement in the northern West Philippine Sea has been estimated from magnetic anomalies, paleontologic confirmation has been imprecise because of spot coring, core disturbance, and poor preservation of microfossils. By continuous coring to basement using modern coring techniques, we hoped to obtain an accurate basement age from undisturbed microfossils, magnetostratigraphy, or radiometric dating of ash horizons. This information would be of considerable importance in constraining models of backarc spreading.

Basalt Chemistry and Crustal Thickness

Recent studies on the relationship between mid-ocean-ridge basalt (MORB) chemistry and crustal thickness indicate that the degree of partial melting is strongly controlled by the temperature of the upwelling mantle at the ridge. The volume of the melt (represented by the crustal thickness) and its chemical composition are sensitive to the temperature. This means that a knowledge of crustal thickness in an ocean basin makes it possible to estimate the temperature at which the crust was formed and the concentration of major and minor chemical elements in the resulting basalts (e.g., Klein and Langmuir, 1987; White and Hochella, 1992). To date, these studies have concentrated on young MORBs. The chemical model on which these predictions are based still has large uncertainties, partly because there are few cases off ridge where rock samples and high-quality seismic data have been collected at the same location. Chemical analysis of the basalt samples from Site

1201 should provide clues as to why the crust in the Philippine Basin is 3 to 4 km thinner than normal.

Tertiary Climate Record

Previous drilling in the West Philippine Sea was conducted during DSDP Legs 31 and 59 before the advent of piston coring, and many of the holes were only spot cored. As a consequence, the available core from the region is almost useless for stratigraphic and paleontologic reconstructions. By obtaining a continuous, high-quality record of pelagic sedimentation supplemented by high-quality logs, we hoped to obtain a proxy record of Tertiary climate change for the region. It was anticipated that the upper levels of the section might also contain a record of eolian transport from Eurasia.

Ash Fall Record

Although ash and tuff were present in the sediments recovered in the region during previous legs, it was impossible to reconstruct the ash fall stratigraphy because of core disturbance and the discontinuous nature of the coring. By continuous coring using APC and XCB techniques and correlation with high-resolution Formation MicroScanner (FMS), natural gamma spectrometry tool (NGT), and ultrasonic borehole imager (UBI) logs, we hoped to obtain a detailed record of arc volcanism around the Philippine Sea.

Philippine Plate Paleolatitude, Rotation, and Tectonic Drift

Paleomagnetic measurements of sediments and basalt cores are important because oriented samples are difficult to obtain from the oceans. The basalts record the direction of the magnetic field at the time the basalts were emplaced and can be used to infer the paleolatitude of the site (e.g., Cox and Gordon, 1984). Although it was unlikely that enough flow units would be cored at Site 1201 to average secular variation adequately, it was thought that the results would be useful in determining a Paleogene paleomagnetic pole for the Philippine plate. Sediments are typically a good recorder of the Earth's magnetic field and should contain a continuous record of the movement of the Philippine plate through the Cenozoic. By collecting oriented sediment cores, we hoped to study the rotation of the Philippine plate and the initiation of subduction of the Pacific plate.

Drilling Strategy and Operations

After arriving on site, we planned to drill and core two pilot holes to determine the geology of the formation and to establish the casing requirements for the reentry hole that was to house the borehole seismic observatory. The first was to be APC cored to refusal (estimated at 200 mbsf) with the Tensor core orientation tool then XCB cored to basement, estimated at ~370 mbsf. After a jet-in test, a second pilot hole was to be drilled to basement and then cored 100 m into basement using the RCB to determine the nature of the basement. This hole would then be logged to identify a suitable interval for setting the seismometer package.

Once the pilot holes had been completed, we planned to offset and jet in a reentry cone and ~60 m of 16-in casing. The hole would then be

reentered and deepened to ~425 mbsf with a 14.75-in tricone bit to lower a 410-m string of 10.75-in casing ~40 m into basement and cement it in place. The hole would then be reentered again and deepened to ~100 m in basement for the seismometers. After the seismometer package had been made up, lowered into the hole, and cemented in place, a battery package would be lowered into the throat of the reentry cone and acoustically released. The pipe would then be tripped to the surface, bringing the deployment to completion so that it could be activated by an ROV at a later time. As at Site 1200, however, the actual operations at Site 1201 departed significantly from those that had been planned.

The *JOIDES Resolution* arrived on site at 1600 hr on 31 March 2001, following a 2-day transit from Guam. After the pipe was lowered to the seafloor, Hole 1201A was spudded with the APC/XCB to study the sediment section but the hole was abandoned after one core because of a premature APC shear pin failure. APC coring was then initiated in Hole 1201B at 1905 hr on 1 April and continued to a depth of 46.7 mbsf, after which the hole was deepened with the XCB to 90.3 mbsf (Table **T1**). The vessel was then offset 15 m to the west and a third APC hole, 1201C, was spudded and cored to refusal at 48.1 mbsf to provide a repeat section through the soft sediments. The Tensor core orientation tool was used on the third, fourth, and fifth cores in both Holes 1201B and 1201C, and a temperature measurement was taken with the Adara shoe at a depth of 44.6 mbsf in Hole 1201C.

A problem with the spooling of the coaxial cable used for the undersea television camera became apparent during the deepwater operations at the site. Since the undersea camera was required for reentry and the deployment of the seismic observatory, we decided to search for a deepwater pocket where we could fully extend and retension the cable in an attempt to correct the problem. After steaming 204 nmi northwest to a small basin indicated on Japanese hydrographic charts, we deployed the coaxial cable to a depth of 6183 m and fixed the spooling problems.

At 0718 hr on 5 April, the vessel was back at Site 1201 and the main pilot hole, Hole 1201D, was spudded 120 m south of Hole 1201C. The hole was drilled with a center bit to a depth of 80.4 mbsf, where RCB coring was initiated. Coring proceeded without incident to basement at 510 mbsf, which was considerably deeper than initially predicted, and then continued another 90 m into the basement to a total depth of 600 mbsf. After releasing the bit, Hole 1201D was logged with the triple combination (triple combo) tool from 80 mbsf to total depth. A second logging run with the FMS-sonic tool could not pass an obstruction at 366 mbsf because of deteriorating hole conditions. After completing the run in what was left of the open hole, the pipe was lowered again in an attempt to reopen the hole for logging but an impassable bridge was reached at a depth of 90 mbsf. At that point, a 50-m plug of cement was set to prevent future fluid communication with the cased reentry hole and seismometer.

The hole for the seismometer was initiated at 1600 hr on April 14, when Hole 1201E was spudded with a reentry cone and 16-in casing and jetted in to a depth of 39.1 m. The hole was then drilled to 543.0 mbsf and cased with 10.75-in casing to a depth of 527.0 mbsf, or 15 m into basement. After cementing the casing in basement, the 9.875-in ION installation hole was drilled to a total depth of 580 mbsf. By 1230 hr on 23 April, the seismometer instrument string was assembled and final electrical integrity checks were completed (Fig. **F17**). Hole 1201E was then reentered and the instrument package was lowered into the

F17. Borehole seismometer instrument package, p. 49.

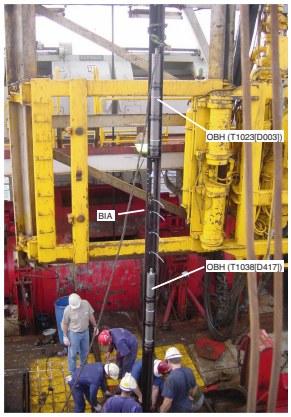

hole without incident. The seismometer package was cemented in place with the end of the stinger located at a depth of 568.7 mbsf (Fig. F18). The top of the uppermost seismometer was placed ~558.4 mbsf, or ~46.4 m below the basement contact. At 0830 hr on 24 April, the battery platform was lowered through the moonpool and landed in the reentry cone at 1400 hr (Fig. F19). A handheld acoustic command unit was used to release the platform. Proper platform installation was confirmed with the subsea television camera, and by 1100 hr on 25 April, the ship was secured for transit and under way to Site 1202 (alternate Site KS-1).

Principal Results

The principal objective at Site 1201 was to install a long-term borehole seismic observatory in the middle of the Philippine plate. Although this was successfully accomplished, the observatory will not be activated until its brains are installed during an ROV visit in the spring of 2002 and no data will be recovered until it is revisited in 2002 or 2003. In the meantime, the core recovered during the course of preparing the hole for the observatory produced striking and, in some cases, unexpected results.

Drilling at Site 1201 yielded a composite 600-m-thick section consisting of 510 m of Miocene through late Eocene sediments and 90 m of basalt. The sedimentary section consists of two lithostratigraphic units (Fig. F20). The uppermost unit (0–53 mbsf) consists of soft pelagic clays, cherts, and interbedded sandstones and silty claystones that contain significant amounts of red clay. The underlying unit (53–510 mbsf) is composed of a thick section of interbedded turbidites composed of detrital volcaniclastic material and traces of reef detritus from the Kyushu-Palau Ridge, which range in size from coarse sandstones and breccia through silty claystone to claystone. The individual turbidite layers range from tens of meters to a few millimeters in thickness and tend to decrease in thickness and grain size downsection (Figs. F21, F22), reflecting a gradual change from high-energy to low-energy deposition. The basal 20–30 m of the unit consists of interbedded turbidites and reddish tan to chocolate-brown claystones deposited in a quiet marine environment. One of the most striking features of the entire sediment section at Site 1201 is the color of the turbidites, which range from dark gray to dark greenish gray in the upper 240 m of the unit, where the volcaniclastics are (relatively) fresh, and then range from deep green to gray-green to the base of the unit. Thin section and XRD analyses show that these changes are related to progressive alteration with depth, including the devitrification of glass, the replacement of the calcic cores of plagioclase by clays, and the infilling of voids and vesicles by clays and zeolites in the upper part of the unit, and the wholesale replacement of volcaniclastic material in the lower part of the unit by smectite, chlorite, and zeolites (chabazite, erionite, heulandite/clinoptilolite, and analcime/wairakite) during diagenesis.

The composition of the interstitial water at Site 1201 is very unusual for deep-sea sediments and reflects the profound diagenesis that has occurred in the turbidites in the lower part of the section. The most striking feature is an extremely large increase in pH, Ca, and chlorinity with depth in the pore water; whereas seawater is mainly a sodium chloride solution, the altered seawater near the base of the sediments is mainly a calcium chloride solution (Fig. F23). Calcium increases to 270 mmol/kg, 27 times the concentration in seawater, by leaching from the volca-

F18. Configuration of reentry cone, casing, and ION seismic observatory components, p. 50.

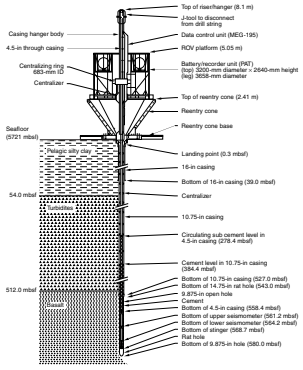

F19. ROV landing platform, p. 51.

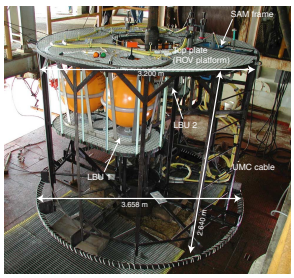

F20. Lithology, color, natural gamma count, and mineralogy vs. depth and age, p. 52.

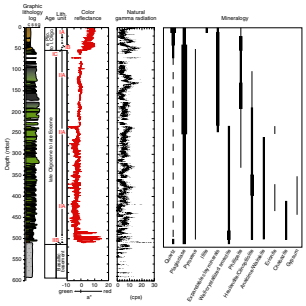

F21. Laboratory multisensor track measurements, p. 53.

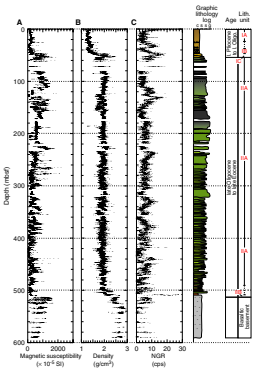

niclastic material. Similarly, chlorinity increases to 645 mmol/kg, 20% higher than seawater values, due to the removal of water during the formation of hydrous minerals such as clays and zeolites. The gain in Ca is balanced by the removal of 70% of the Na (to 140 mmol/kg) and the loss of nearly all of the Mg and K from the seawater during the formation of clay, smectite, and zeolites. Sulfate decreases as well, from 28 to 15 mmol/kg, by the precipitation of gypsum in response to the elevated Ca concentration. Alkalinity falls from the seawater value of 2.4 to <1 meq/kg as it is consumed by the precipitation of authigenic minerals. The rise in pH to 10.0 from the seawater value of 8.1 also reflects extreme alteration. Many of the pore water gradients in the top of the turbidite section can only be supported by ongoing reactions, which is consistent with the fact that the volcaniclastics at this level are not yet completely altered. Deeper in the section, however, many of the geochemical gradients approach zero, implying that equilibrium has been achieved and that the geochemistry observed is that of "fossil" pore water.

To reconstruct the geological history of the site and determine the timing of diagenesis, it is necessary to look at the microfossil and paleomagnetic record. The topmost (0–29 mbsf) and lowermost (462–509 mbsf) sections are barren of nannofossils, but moderately to poorly preserved nannofossils in the middle section allowed us to recognize six biozones spanning Zones NP19/NP20 to NP25 (Fig. **F24**). The turbidites between 53 and 462 mbsf represent an expanded sequence of late Eocene to early Oligocene age. Separated by a short hiatus and lying on top of the turbidites is a 25-m sequence of upper Oligocene (Zone NP25) red claystone. Compared to DSDP drilling results at Sites 290 and 447 (Karig, Ingle, et al., 1975; Kroenke, Scott, et al., 1981), the upper Eocene sediments (>34.3 Ma) recovered at this site are the oldest so far identified on the sedimentary apron of the Kyushu-Palau Ridge. Because the 47-m interval overlying basement at the site could not be dated on board ship, this is clearly a minimum age; dating of this critical interval must await the results of shore-based radiolarian studies.

Preliminary interpretation of the magnetic inclination record identified 64 reversals of the geomagnetic timescale in the sediment section. Although the Pliocene–Pleistocene section (0–5 m.y.) is apparently missing, the barren pelagic sediments in the top 29 mbsf provided an excellent record from the Thvera Subchron (C3n.4n) through the late and middle Miocene polarity intervals to Subchron C5Bn.1n or close to the base of the middle Miocene (Fig. **F25**). Major unconformities are present between 14.8 and 24.1 Ma and in the top section of Biozone NP24 at ~25–30 Ma. Surprisingly, the magnetic inclination record in the turbidites between 100 and 500 mbsf defines several long normal and reversed polarity chrons (C12n–C16n.2n) that are well constrained by biostratigraphic ages. The combined biostratigraphic and paleomagnetic results show that the sedimentation rates were moderate (35 m/m.y.) in the late Eocene, then very high (109 m/m.y.) in late Eocene–early Oligocene time, when the turbidites were being deposited, and then decreased to very low values (3 m/m.y.) during the Miocene, when the pelagic sediments at the top of the section were being deposited (Fig. **F26**).

Although the age of the basement could not be determined aboard ship, its composition and provenance are clear. The 90 m of basement drilled at Site 1201 consists of altered pillow basalts having a composition that is transitional between that of arc tholeiites and MORB and backarc basin basalts (Fig. **F27**). Geochemical and thin section analysis

F22. Logging results from Hole 1201D, p. 54.

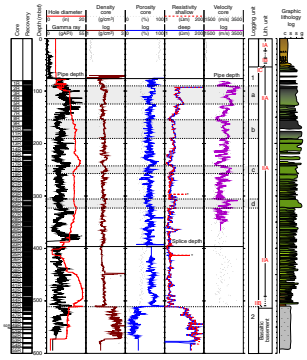

F23. Pore water Mg, Ca, Na, and alkalinity concentrations vs. depth, p. 55.

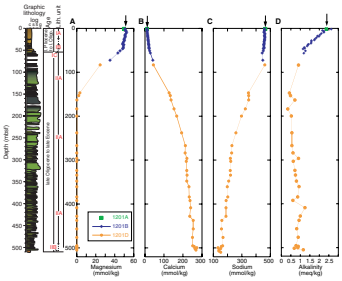

F24. Nannofossil ranges at Site 1201, p. 56.

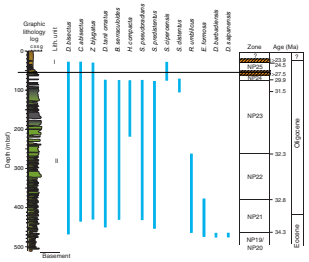

F25. Magnetic inclination and declination record in pelagic sediments, p. 57.

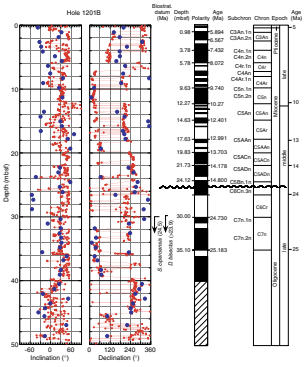

shows that the basalts have been strongly weathered, especially at the contact with the overlying sediments, where they show significant Na uptake and depletion in Ca. Hyaloclastites in the section have been palagonitized and altered to smectite, and interpillow sediments recovered from within the upper 10 m of basement contain marine microfossils, indicating eruption in a marine environment. Magnetic inclinations in the basaltic basement are shallow and indicate a position of the Philippine plate near the equator, at ~7° paleolatitude, during the Eocene.

From the data provided above, it is evident that the basement at Site 1201 formed near the equator by submarine eruption during the Eocene before 34.3 Ma. The composition of the basalts, which are transitional between island arc tholeiites and MORB or backarc basin basalts, suggests they erupted in an arc or backarc setting. The absence of calcareous nannofossils and the presence of siliceous microfossils in the interpillow sediments and pelagic sediments immediately overlying the basement suggests that the basement formed in a deep water environment below the carbonate compensation depth (CCD) (Fig. F28).

Beginning in the late Eocene and continuing into the early Oligocene (from ~35 to 30 Ma), pelagic sedimentation at the site became mixed with, and was finally overwhelmed by, increasingly thick, coarse, and energetic turbidites composed of arc-derived volcaniclastics and reef detritus. The composition and timing of the turbidites is consistent with a source to the east in the Kyushu-Palau Ridge, which was an active arc from ~48 to 35 Ma (Arculus et al., 1995) and only began to subside at ~28 Ma (Klein and Kobayashi, 1980). The presence of scoria and rounded lithic clasts in the volcaniclastic breccia at Site 1201 is consistent with subaerial erosion, but the absence of plutonic fragments indicates that the ridge remained undissected (Dickinson, 1985; Valloni, 1985). The upward coarsening of the turbidites can be attributed to many possible causes, including changes in arc elevation and erosion, sediment supply, proximity to source, tectonics, sea level, and slope gradient. Alteration of the volcaniclastics would have commenced immediately after deposition and is continuing to the present in the upper part of the section, but diagenesis would only have begun when the turbidite section became sufficiently thick for the temperature in the lower part of the section to reach 85° to 125°C (Fisher and Schminke, 1984).

Between the late Oligocene and early Pliocene, the Kyushu-Palau Ridge subsided, the deposition of turbidites came to an end, and pelagic sedimentation resumed at Site 1201 as the Parece Vela Basin opened and arc volcanism moved eastward relative to the Kyushu-Palau Ridge in response to plate reorganization. Finally, even pelagic sedimentation ceased at ~5 Ma, presumably in response to bottom currents caused by a change in bottom-water circulation.

SITE 1202: KUROSHIO CURRENT

The Kuroshio (Black) Current is the biggest western boundary surface current in the western Pacific. Because of its high speed (2.7–3.6 km/hr), great thickness (1.0 km) and width (150–200 km), and high temperature (28°–29°C in summer and 22°–25°C in winter), it plays an important role in the meridional transport of heat, mass, momentum, and moisture from the western Pacific warm pool to high latitudes in the north Pacific. Although its role in the Pacific is as important as that of the Gulf Stream in the North Atlantic, almost nothing has been learned

F26. Sedimentation rates at Site 1201, p. 58.

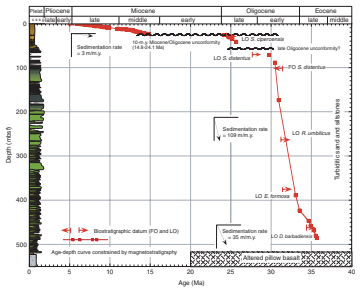

F27. V vs. Ti tectonic discrimination diagram, p. 59.

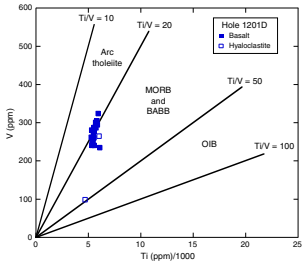

F28. Geological interpretation of the sediment and basement section, p. 60.

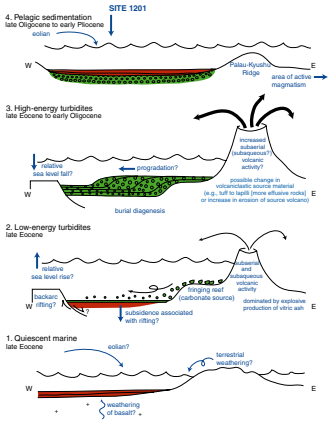

about its evolution during the past 32 yr of drilling by DSDP and ODP because there are almost no locations beneath the Kuroshio Current where a deep-sea sedimentary section with high sedimentation rates can contain well-preserved calcareous microfossils. Because the CCD is shallow in the western Pacific (<3500 m) and the water depth is great (generally >4000 m), foraminifers and calcareous nannofossils are rarely preserved. Conditions appear to be ideal for obtaining a such a section, however, in the southern Okinawa Trough. As the Kuroshio Current passes between the eastern side of the island of Taiwan and the southernmost part of the Ryukyu Island arc, it is deflected upward when it approaches the Ilan Ridge and then flows northeastward in the Okinawa Trough (Ono et al., 1987; Chen et al., 1992) (Fig. F29). The seafloor in the Okinawa Trough lies above the CCD, and sedimentation rates are high because of terrigenous input from the East China Sea shelf and the island of Taiwan (Boggs et al., 1979; Lin and Chen, 1983). Site 1202 was accordingly proposed on the southern slope of the Okinawa Trough to obtain a high-resolution record of the history of the Kuroshio Current during the Quaternary.

F29. Location of Site 1202 in the Okinawa Trough, p. 61.

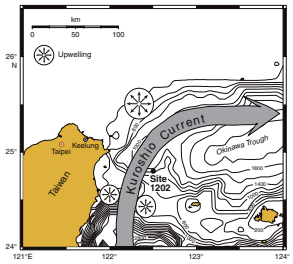

Geologic Setting

The Okinawa Trough, which extends from southwestern Kyushu, Japan, to the northeastern side of the island of Taiwan, is an active, incipient, intracontinental backarc basin formed behind the Ryukyu arc-trench system in the western Pacific (Lee et al., 1980; Letouzey and Kimura, 1985; Sibuet et al., 1987). The trough was formed by extension within continental lithosphere already intruded by arc volcanism (Uyeda, 1977; Sibuet and Hsu, 1997). Although there is considerable controversy about the age of early rifting, most researchers agree that the most recent phases of extension have taken place since 2 Ma (Sibuet et al., 1998). The southernmost part of the Okinawa Trough is characterized as a rifting basin with incipient arc volcanism opening in the middle of a foundered orogen caused by previous arc-continent collision (Teng, 1996).

The recent phase of extension of the Okinawa Trough occurred in the late Pleistocene (~0.1 Ma) (Furukawa et al., 1991), based on seismic correlation with drilling stratigraphy (Tsuburaya and Sata, 1985), but the exact timing of this recent phase of extension in the area of the site is unknown. The extension is characterized by normal faulting on both sides of the trough. The amount of extension during this recent phase has been estimated to be 5 km, both in the middle and the southwest end of the Okinawa Trough (Sibuet et al., 1995, 1998). Based on the coincidence in timing between the development of the sedimentary basins in the Okinawa Trough (Kimura, 1985) and the uplift of the Ryukyu arc at the Pliocene/Pleistocene boundary (Ujiie, 1980), Sibuet et al. (1998) concluded that the penultimate phase of rifting, including subsidence and block faulting along the central axis of the trough, started at ~2 Ma. The total amount of extension in the area is ~30 km.

It has been suggested that the Okinawa Trough changed from an open-sea environment to a semienclosed marginal basin because of a 120-m drop in sea level (Fairbanks, 1989) during the last glacial maximum (Ujiie et al., 1991). Consequently, the Kuroshio Current may have been located on the trench side of the Ryukyu arc until ~7.5 ka during the Holocene (Ujiie et al., 1991; Ahagon et al., 1993; Shieh and Chen, 1995). Glacial–interglacial sea level fluctuations are likely to have caused significant changes in the configuration and distribution of continental shelves in the region, particularly in the South China Sea, and

these changes must have caused dramatic hydrographic changes and sediment redistribution in the Okinawa Trough.

The southern Okinawa Trough is currently an area of high sedimentation because of the enormous terrigenous sediment supply from the East China shelf and the island of Taiwan. Modern sediments in this area consist mainly of clay- to silt-sized terrigenous sediments with a moderate (~20%) biogenic carbonate content (Chen et al., 1992; Lou and Chen, 1996). Sediment trap studies in the southern Okinawa Trough (Hung et al., 1999) indicate that the abundance of suspended particulate material decreases with increasing distance from the East Asian continent but increases with depth, implying effective resuspension and lateral transport across the area. Studies of short piston cores (Lou and Chen, 1996; Shieh et al., 1997; Ujiie and Ujiie, 1999) taken from the area suggest that sedimentation rates during the Holocene were ~20 cm/ky.

Extensive geophysical surveys conducted in the area (Sibuet et al., 1998; Liu et al., 1998) show that the trough is marked by a series of normal faults dipping toward the center and a series of volcanic edifices and hydrothermal vents piercing through the sedimentary layer. Based on low interval velocities (<2.0 km/s) determined from the analysis of seismic data, a prominent series of reflectors is observed from 250 to 350 mbsf (Fig. F30). This prominent reflection has been suggested to be the unconformity marking the onset of the most recent phase of extension of the Southern Okinawa Trough (Hsu, 1999). Site 1202 was proposed to penetrate this sequence to a depth of ~410 mbsf, not only to study the paleoceanography of the Kuroshio Current but to provide constraints on the timing of the most recent phase of extension in the Okinawa Trough.

F30. North-south seismic profile EW95091 at Site 1202, p. 62.

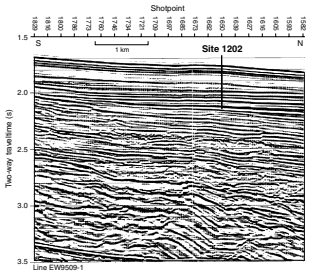

Scientific Objectives

The primary objective of drilling at Site 1202 was to obtain a high-resolution record of the paleoceanographic history of the Kuroshio Current. Such a record might make it possible to identify long-term patterns of climate change associated with the western Pacific boundary current during the past 1.5 m.y. For example, the Kuroshio Current passes over the Ryukyu arc and into the Okinawa Trough before turning northeast and continuing toward Japan, but changes in sea level associated with glacial–interglacial cycles could well redirect the Kuroshio Current outside the arc and isolate the Okinawa Trough on a cyclic basis. Changes in sedimentation caused by such deflections, coupled with periodic exposure of the continental shelf to the northwest during low sea level stands, should be easily detectable by drilling at Site 1202.

We also hoped that drilling at Site 1202 would enable us to detect the effects of orbital forcing in the Pacific during the mid-Pleistocene (~0.7 Ma), when the Earth's climate system switched from a regime of dominant 41-k.y. cycles to 100-k.y. cycles. Oxygen isotope measurements on foraminifers from Site 1202, for example, should reflect surface temperature cycles over a large area of the western equatorial Pacific because the Kuroshio Current is a composite current assembled from numerous smaller currents before it reaches the site.

We also hoped to document the temporal and spatial variability of millenial climate changes in the Kuroshio Current and the catchment basins that deliver sediments to the Okinawa Trough. These changes should be reflected not only in the oxygen isotopic composition of microfossils but in the grain size and composition of sediments from some

of the largest river systems in east Asia, including the Yangtze, which rises in Tibet and samples much of southern China.

Finally, we hoped to examine long-term changes in El Niño/La Niña–style climate oscillations in the low-latitude Pacific by comparing the Kuroshio Current record to other Pacific ODP records (Andreasen and Ravelo, 1997; Clement et al., 1999).

Drilling Strategy and Operations

After arriving on station and lowering the pipe, we planned to triple–APC core the sediment section to refusal, which was estimated to be at ~250 mbsf, to obtain overlapping, and thus complete, coverage for high-resolution paleoenvironmental studies. If time allowed, we planned to deepen the third hole to 410 mbsf using the XCB. We then hoped to log the open hole using the triple combo and the FMS-sonic tools to provide a quantitative basis for comparison with the multisensor track (MST) data, which could be used to reconstruct a continuous sediment section for the site.

The transit to Site 1202 (proposed Site KS-1) was made in good time with fair seas and favorable currents. The 784-nmi distance was covered in 64.9 hr at an average speed of 12.1 kt. At 0254 hr on the morning of 28 April, the vessel arrived at 24°48.24′N, 122°30.00′E, the coordinates for the drilling location. The crew began lowering thrusters and hydrophones, and at 0515 hr on 28 April the positioning beacon was deployed.

A standard APC/XCB bottom-hole assembly (BHA), including a lockable float valve (LFV) to allow wireline logging of the deepest hole of the site, was made up. The drill string was tripped to the bottom, and Hole 1202A was spudded at 0810 hr. APC coring continued through Core 195-1202A-9H to a depth of 83.1 mbsf (Table **T1**) when the APC failed to stroke out. Core 195-1202A-10H fully stroked; however, Cores 11H and 12H did not fully advance. Advance by recovery was used for the two incomplete cores in the hope that the hard layer would be limited in thickness and piston coring would once again become viable. APC refusal was finally accepted when Core 195-1202A-13H at 119.5 mbsf had not only failed to scope, but the core liner failed at the midpoint of the barrel. Core orientation using the Tensor tool was initiated with Core 195-1202A-4H and continued through Core 13H. Temperature measurements were taken on Cores 195-1202A-4H, 7H, 10H, and 13H using the Adara temperature tool. Two of the four temperature measurements were good (see **"Physical Properties,"** p. 11, in the "Site 1202" chapter). The developmental APC-methane tool was deployed on Core 195-1202A-4H and then on Cores 7H through 13H. All runs were successful in acquiring data. Hole 1202A officially ended with the clearing of the seafloor at 1900 hr on 28 April.

The vessel was offset 15 m to the east, and Hole 1202B was spudded at 1935 hr on 28 April. APC coring continued through Core 195-1202B-13H to a depth of 111.6 mbsf (Table **T1**) before APC refusal was defined by two successive incomplete strokes on Cores 195-1202B-12H and 13H. Because the ultimate depth objective at this site was 410 mbsf, we decided to cut three XCB cores before terminating the hole to obtain an idea about penetration rates, core recovery, and quality. Coring continued with the XCB through Core 195-1202B-16X to a depth of 140.5 mbsf. The drill string was pulled clear of the seafloor, officially ending Hole 1202B at 0445 hr on 29 April.

The ship was offset 15 m to the east, and Hole 1202C was spudded at 0540 hr on 29 April. APC coring continued through Core 195-1202C-11H to a depth of 97.5 mbsf (Table T1), where APC refusal was encountered as defined by three consecutive incomplete strokes. Core orientation using the Tensor tool was initiated with Core 195-1202C-4H and continued through Core 11H. The drill string was pulled clear of the seafloor, officially ending Hole 1202C at 1215 hr on 29 April.

For the third time, the ship was offset 15 m to the east, and Hole 1202D was spudded with the APC at 1245 hr on 29 April. Recovery of the first core was only 15 cm. APC coring continued in this hole through Core 195-1202D-9H to a depth of 76.2 mbsf (Table T1), when the first core did not achieve full stroke. Coring with the XCB proceeded through Core 195-1202D-32X to a depth of 297.4 mbsf, where a short wiper trip was made to 221.3 mbsf, above an area of poor recovery. The wiper trip was uneventful, and coring continued through Core 195-1202-44X to a depth of 410.0 mbsf, the approved target depth for Site 1202.

In preparation for logging, a wiper trip was initiated at 1930 hr on 30 April and reached the logging depth of 80.0 mbsf without incident. The hole was displaced with 150 bbl of sepiolite logging mud, and the bit was pulled back to a logging depth of 80.0 mbsf.

The triple combo tool string was made up with the Lamont Doherty Earth Observatory (LDEO) temperature/acceleration/pressure (TAP) tool. A nuclear source was not incorporated because the loss of density data did not outweigh the risk of losing the source in disputed waters under hostile current conditions. Throughout operations at the site, the Kuroshio Current was strong. Heavy pipe vibration was experienced continually, while the currents varied cyclically between 2.6 and nearly 4.0 kt. The first tool string was deployed to a depth of ~215 meters below rig floor. At that point, the logging engineer reported losing all power to the logging tools. After bringing the tool string to the surface, the tools showed several loose connections caused by the current-induced drill sting vibrations. All joints were retightened and taped with duct tape. The tool string was once again deployed inside the drill pipe; however, the winch operator only reached 72 mbsf before losing weight with the logging line, as if setting down on an obstruction. Upon recovery, the connections were once again found to be loose and the lower portion of the TAP tool was missing.

At 0430 hr, the circulating head was rigged up and the coring line was run in the hole to determine if the TAP tool was lodged in the drill string. Results were inconclusive. We decided to abandon further wireline logging efforts because of the intensity of the current-induced drill string vibration. The drill string was pulled clear of the seafloor by 0730 hr. By 1100 hr, preparations were under way to secure and clean the ship for transit into port. The ~55-nmi transit to Keelung, Taiwan, was made at reduced speed for an 0815-hr arrival at the pilot station on 2 May 2001. The ship was dockside at 0904 hr, ending Leg 195.

Principal Results

The principal objective at Site 1202 was to obtain a continuous sediment section deposited beneath the Kuroshio Current that would allow high-resolution studies of climate change in East Asia associated with late Quaternary glaciation and deglaciation cycles. The strategy adopted was to drill at an extremely high sedimentation rate site in relatively

shallow water above the CCD in the Okinawa Trough where calcareous microfossils would be preserved in an expanded section.

The objective was met with the recovery of a 410-m section of dark grayish green, bioturbated clayey silt with abundant sandy turbidites between 220 and 280 mbsf and occasional thin (<1 cm) turbidites scattered throughout the rest of the section. The sediments were rich in organic carbon and charged with H_2S. Smear slide analysis shows that the nonbiogenic component of the sediments is composed predominantly of quartz, feldspar, and detrital carbonate, whereas the turbidites also contain micas, heavy minerals (green hornblende, tourmaline, epidote, and zircon), and opaques. Surprisingly, no tephra layers were observed and glass shards are rare. Although the site is located in the Okinawa Trough, heat flow values (0.040 W/m^2) were slightly lower than the global average and no evidence of diagenesis was observed.

As anticipated, the preservation of calcareous microfossils was excellent, with planktonic and benthic foraminifers and calcareous nannofossils present in small amounts (<1% by volume) throughout the section, except in the turbidites, where they are abundant. Also present, especially in the turbidites, are diatoms, ostracodes, radiolarians, sponge spicules, the plates and spines of echinoderms, fragments of molluscs and pteropods, copepod remains, and fragments of bark, roots, and leaves, the latter indicating rapid burial and high sedimentation rates.

Despite the excellent preservation of microfossils, shipboard determination of the age of the section proved difficult. The presence of *Emiliania huxleyi* throughout the section suggests that the section is very young (<0.26 Ma, or latest Quaternary) and the absence of pink *G. ruber* indicates that the entire section is younger than 127 ka. This is consistent with shipboard paleomagnetic inclination data, which shows that the entire 410-m section lies within the Brunhes C1n normal polarity chron and is thus <0.78 Ma in age. Several excursions are seen in the data, including one at 110 m, which may correspond to the Laschamps event (40–45 ka), but given the absence of biostratigraphic markers and reversals, an accurate age determination for the section will have to be based on paleointensities.

If the age of the section is <127 ka, as suggested by the absence of pink *G. ruber,* then the sedimentation rate at the site was at least 3 m/k.y., one of the highest rates ever observed in the ocean basins for fine-grained, fossiliferous sediments. Given the relatively low biogenic content of the sediments, this requires a large terrigenous source. We infer that the section is composed of reworked sediments from the Chinese mainland that were delivered to the East China shelf by the Yangtze River. The presence of mica and other metamorphic minerals in the coarse fraction of the turbidites suggests that an additional component is derived from nearby metamorphic terrains on the island of Taiwan.

If this initial interpretation is borne out, then the section recovered at Site 1202 is almost ideal for studying climate change associated with glaciation and deglaciation in East Asia during the Holocene and latest Pleistocene. The section is relatively homogeneous; it is continuous, at least in the top 130 m where it was APC cored; it contains excellent paleomagnetic, lithologic, and biogenic proxies for climate; and it displays extraordinarily high resolution (<100 yr, assuming bioturbation to 20 cm). In principle, this resolution should be sufficient to study the influence of climate on the rise of Chinese civilization.

REFERENCES

Ahagon, N., Tanaka, Y., and Ujiie, H., 1993. *Florisphaera profunda,* a possible nannoplankton indicator of late Quaternary changes in sea-water turbidity at the northwestern margin of the Pacific. *Mar. Micropaleontol.,* 22:255–273.

Andreasen, D.H., and Ravelo, A.C., 1997. Tropical Pacific Ocean thermocline depth reconstructions for the last glacial maximum. *Paleoceanography,* 12:395–413.

Arculus, R.J., Gill, J.B., Cambray, H., Chen, W., and Stern, R.J., 1995. Geochemical evolution of arc systems in the western Pacific: the ash and turbidite record recovered by drilling. *In* Taylor, B., and Natland, J. (Eds.), *Active Margins and Marginal Basins of the Western Pacific*. Am. Geophys. Union, 88:45–65.

Boggs, S., Jr., Wang, W.C., Lewis, F.S., and Chen, J.-C., 1979. Sediment properties and water characteristics of the Taiwan shelf and slope. *Acta Oceanogr. Taiwanica,* 10:10–49.

Carson, B., and Westbrook, G.K., 1995. Modern fluid flow in the Cascadia accretionary wedge: a synthesis. *In* Carson, B., Westbrook, G.K., Musgrave, R.J., and Suess, E. (Eds.), *Proc. ODP, Sci. Results,* 146 (Pt 1): College Station, TX (Ocean Drilling Program), 413–421.

Chen, M.-P., Lo, S.-C., and Lin, K.-L., 1992. Composition and texture of surface sediment indicating the depositional environments off northeast Taiwan. *TAO,* 3:637–642.

Clement, A.C., Seager, R., and Cane, M.A., 1999. Orbital controls on the El Nino/Southern Oscillation and the tropical climate. *Paleoceanography,* 14:441–456.

COSOD II, 1987. *Rep. 2nd Conf. Scientific Ocean Drilling:* Washington/Strasbourg (JOIDES/European Sci. Found.).

Cox, A., and Gordon, R.G., 1984. Paleolatitudes determined from paleomagnetic data from vertical cores. *Rev. Geophys. Space Phys.,* 22:47–72.

Davis, E.E., Becker, K., Pettigrew, T., Carson, B., and MacDonald, R., 1992. CORK: a hydrologic seal and downhole observatory for deep-ocean boreholes. *In* Davis, E.E., Mottl, M.J., Fisher, A.T., et al., *Proc. ODP, Init. Repts.,* 139: College Station, TX (Ocean Drilling Program), 43–53.

Dickinson, W.R., 1985. Interpreting provenance relations from detrital modes of sandstones. *In* Zuffa, G.G. (Ed.), *Provenance of Arenites:* Dordrecht (D. Riedel), 333–361.

Fairbanks, R.G., 1989. A 17,000-year glacio-eustatic sea level record: influence of glacial melting rates on the Younger Dryas event and deep-ocean circulation. *Nature,* 342:637–642.

Fisher, R.V., and Schmincke, H.-U., 1984. *Pyroclastic Rocks:* New York (Springer-Verlag).

Fisk, M.R., Giovannoni, S.J., and Thorseth, I.H., 1998. Alteration of oceanic volcanic glass: textural evidence of microbial activity. *Science,* 281:978–980.

Fryer, P., 1992. A synthesis of Leg 125 drilling of serpentine seamounts on the Mariana and Izu-Bonin forearcs. *In* Fryer, P., Pearce, J.A., Stokking, L.B., et al., *Proc. ODP, Sci. Results,* 125: College Station, TX (Ocean Drilling Program), 593–614.

————, 1996. Tectonic evolution of the Mariana convergent margin. *Rev. Geophys.,* 34:89–125.

Fryer, P., and Fryer, G.J., 1987. Origins of nonvolcanic seamounts in a forearc environment. *In* Keating, B.H., Fryer, P., Batiza, R., and Boehlert, G.W. (Eds.), *Seamounts, Islands, and Atolls*. Geophys. Monogr., Am. Geophys. Union, 43:61–69.

Fryer, P., and Mottl, M., 1997. Shinkai 6500 investigations of a resurgent mud volcano on the southeastern Mariana forearc. *JAMSTEC J. Deep Sea Res.,* 13:103–114.

Fryer, P., Pearce, J.A., Stokking, L.B., et al., 1990. *Proc. ODP, Init. Repts.,* 125: College Station, TX (Ocean Drilling Program).

Fryer, P., Saboda, K.L., Johnson, L.E., Mackay, M.E., Moore, G.F., and Stoffers, P., 1990. Conical Seamount: SeaMARC II, *Alvin* submersible, and seismic reflection studies.

In Fryer, P., Pearce, J.A., Stokking, L.B., et al., *Proc. ODP, Init. Repts.,* 125: College Station, TX (Ocean Drilling Program), 69–80.

Fryer, P., and Todd, C., 1999. Mariana blueschist mud volcanism sampling the subducted slab. *Eos,* 80:S349.

Fryer, P., Wheat, C.G., and Mottl, M.J., 1999. Mariana blueschist mud volcanism: implications for conditions within the subduction zone. *Geology,* 27:103–106.

Fukao, Y., 1992. Seismic tomogram of the Earth's mantle: geodynamic implications. *Science,* 258:625–630.

Fukao, Y., Obayashi, M., Inoue, H., and Nenbai, M., 1992. Subducting slabs stagnant in the mantle transition zone. *J. Geophys. Res.,* 97:4809–4822.

Furukawa, M., Tokuyama, H., Abe, S., Nishizawa, A., and Kinoshita, H., 1991. Report of DELP 1988 cruises in the Okinawa trough. *Bull. Earthquake Res. Inst., Univ. Tokyo,* 66:17–36.

Goodman, D., and Bibee, L.D., 1991. Measurements and modelling of possible mantle constituents from a long-line seismic refraction experiment in the West Philippine Basin. *Geophys. J. Int.,* 106:667–675.

Haggerty, J.A., 1991. Evidence from fluid seeps atop serpentine seamounts in the Mariana forearc: clues for emplacement of the seamounts and their relationship to forearc tectonics. *Mar. Geol.,* 102:293–309.

Haggerty, J.A., and Chaudhuri, S., 1992. Strontium isotopic composition of the interstitial waters from Leg 125: Mariana and Bonin forearc. *In* Fryer, P., Pearce, J.A., Stokking, L.B., et al., *Proc. ODP, Sci. Results,* 125: College Station, TX (Ocean Drilling Program), 397–400.

Haggerty, J.A., and Fisher, J.B., 1992. Short-chain organic acids in interstitial waters from Mariana and Bonin forearc serpentines: Leg 125. *In* Fryer, P., Pearce, J.A., Stokking, L.B., et al., *Proc. ODP, Sci. Results,* 125: College Station, TX (Ocean Drilling Program), 387–395.

Hall, R., Fuller, M., Ali, J., and Anderson, C., 1995. The Philippine Sea plate: magnetism and reconstructions. *In* Taylor, R.B., and Natland, J. (Eds.), *Active Margins and Marginal Basins of the Western Pacific.* Geophys. Monogr., Am. Geophys. Union, 88:371–404.

Hickey-Vargas, R., Hergt, J.M., and Spadea, P., 1995. The Indian Ocean-type isotopic signature in western Pacific marginal basins: origin and significance. *In* Taylor, B., and Natland, J. (Eds.), *Active Margins and Marginal Basins of the Western Pacific.* Geophys. Monogr., Am. Geophys. Union, 88:175–197.

Hilde, T.W.C., and Lee, C.-S., 1984. Origin and evolution of the West Philippine Basin: a new interpretation. *Tectonophysics,* 102:85–104.

Hsu, B.-H., 1999. Geological structure of South Okinawa Trough: a reflection seismic interpretation [MS Thesis]. National Central Univ., Taiwan. (In Chinese).

Hung, J.-J., Lin, C.S., Hung, G.-W., and Chung, Y.-C., 1999. Lateral transport of lithogenic particles from the continental margin of the southern East China Sea. *Estuarine Coastal Shelf Sci.,* 49:483–499.

Isacks, B.L., and Barazangi, M., 1977. Geometry of Benioff zones: lateral segmentation and downwards bending of the subducted lithosphere. *In* Talwani, M., and Pitman, W.C., III (Eds.), *Island Arcs, Deep Sea Trenches, and Back Arc Basins.* Am. Geophys. Union, Maurice Ewing Ser., 1:94–114.

Ishii, T., Robinson, P.T., Maekawa, H., and Fiske, R., 1992. Petrological studies of peridotites from diapiric serpentinite seamounts in the Izu-Ogasawara-Mariana forearc, Leg 125. *In* Fryer, P., Pearce, J.A., Stokking, L.B., et al., *Proc. ODP, Sci. Results,* 125: College Station, TX (Ocean Drilling Program), 445–485.

JOI-ESF, 1987. Report of the Second Conference on Scientific Ocean Drilling. Washington (JOI, Inc.).

JOI/USSAC, 1994. BOREHOLE: a plan to advance post-drilling sub-seafloor science. *JOI/USSAC Workshop Rep.,* Univ. Miami, FL, 1–83.

Kanazawa, T., Sager, W., Escutia, C., et al., 2001. *Proc. ODP, Init. Repts.,* 191 [CD-ROM]. Available from: Ocean Drilling Program, Texas A&M University, College Station TX 77845-9547, USA.

Karig, D.E., Ingle, J.C., Jr., et al., 1975. *Init. Repts. DSDP,* 31: Washington (U.S. Govt. Printing Office).

Kastner, M., Elderfield, H., Jenkins, W.J., Gieskes, J.M., and Gamo, T., 1993. Geochemical and isotopic evidence for fluid flow in the western Nankai subduction zone, Japan. *In* Hill, I.A., Taira, A., Firth, J.V., et al., *Proc. ODP, Sci. Results,* 131: College Station, TX (Ocean Drilling Program), 397–413.

Kimura, M., 1985. Back-arc rifting in the Okinawa Trough. *Mar. Pet. Geol.,* 2:222–240.

Klein, E.M., and Langmuir, C.H., 1987. Global correlations of ocean ridge basalt chemistry with axial depth and crustal thickness. *J. Geophys. Res.,* 92:8089–8115.

Klein, G.deV., and Kobayashi, K., 1980. Geological summary of the north Philippine Sea, based on Deep Sea Drilling Project Leg 58 results. *In* Klein, G.deV., Kobayashi, K., et al., *Init. Repts. DSDP,* 58: Washington (U.S. Govt. Printing Office) 951–962.

Kroenke, L., Scott, R., et al., 1981. *Init. Repts. DSDP,* 59: Washington (U.S. Govt. Printing Office).

Kulm, L.D., and Suess, E., 1990. Relationship between carbonate deposits and fluid venting: Oregon accretionary prism. *J. Geophys. Res.,* 95:8899–8915.

Langseth, M.G., and Moore, J.C., 1990. Fluid in accretionary prisms. *Eos,* 71:245–246.

Langseth, M.G., Mottl, M.J., Hobart, M.A., and Fisher, A., 1988. The distribution of geothermal and geochemical gradients near Site 501/504: implications for hydrothermal circulation in the oceanic crust. *In* Becker, K., Sakai, H., et al., *Proc. ODP, Init. Repts.,* 111: College Station, TX (Ocean Drilling Program), 23–32.

Lee, C.-S., Shor, G.-G., Bibee, L.D., Jr., Lu, R.-S., and Hilde, Y.W.C., 1980. Okinawa Trough: origin of a back-arc basin. *Mar. Geol.,* 35:219–241.

Letouzey, J., and Kimura, M., 1985. Okinawa trough genesis: structure and evolution of a back arc basin developed in a continent. *Mar. Pet. Geol.,* 2:111–130.

Lin, F.-T., and Chen, J.-C., 1983. Textural and mineralogical studies of sediments from the southern Okinawa Trough. *Acta Oceanogr. Taiwanica,* 14:26–41.

Liu, C.-S., Liu, S.Y., Lallemand, S.E., Lundberg, N., and Reed, D., 1998. Digital elevation model offshore Taiwan and its tectonic implications. *TAO,* 9:705–738.

Liu, J., Bohlen, S.R., and Ernst, W.G., 1996. Stability of hydrous phases in subducting oceanic crust. *Earth Planet. Sci. Lett.,* 143:161–171.

Lockwood, J.P., 1972. Possible mechanisms for the emplacement of alpine-type serpentinite. *Mem.—Geol. Soc. Am.,* 132:273–287.

Lou, J.-Y., and Chen, A.C.-T., 1996. A paleoenvironmental record during 7–21 Ka BP in the sediments off northern Taiwan. *Le Mer,* 34:237–245.

Louden, K.E., 1980. The crustal and lithospheric thickness of the Philippine Sea as compared to the Pacific. *Earth Planet. Sci. Lett.,* 50:275–288.

Maekawa, H., Fryer, P., Ozaki, M., 1995. Incipient blueschist-facies metamorphism in the active subduction zone beneath the Mariana Forearc. *In* Taylor, B., and Natland, J. (Eds.), *Active Margins and Marginal Basins of the Western Pacific.* Geophys. Monogr., Am. Geophys. Union, 88:281–290.

Maltman, A., Labaume, P., and Housen, B., 1997. Structural geology of the décollement at the toe of the Barbados accretionary prism. *In* Shipley, T.H., Ogawa, Y., Blum, P., and Bahr, J.M. (Eds.), *Proc. ODP, Sci. Results,* 156: College Station, TX (Ocean Drilling Program), 279–292.

Martin, J.B., Kastner, M., and Elderfield, H., 1991. Lithium: sources in pore fluids of Peru slope sediments and implication for oceanic fluxes. *Mar. Geol.,* 102:281–292.

Montagner, J.-P., and Lancelot, Y. (Eds.), 1995. Multidisciplinary observatories on the deep seafloor. *INSU/CNRS, IFREMER, ODP-France, OSN/USSAC, ODP-Japan.*

Mottl, M.J., 1992. Pore waters from serpentinite seamounts in the Mariana and Izu-Bonin forearcs, Leg 125: evidence for volatiles from the subducting slab. *In* Fryer, P., Pearce, J.A., Stokking, L.B., et al., *Proc. ODP, Sci. Results,* 125: College Station, TX (Ocean Drilling Program), 373–385.

Mottl, M.J., and Alt, J.C., 1992. Data report: Minor and trace element and sulfur isotopic composition of pore waters from Sites 778 through 786. *In* Fryer, P., Pearce, J.A., Stokking, L.B., et al., *Proc. ODP, Sci. Results,* 125: College Station, TX (Ocean Drilling Program), 683–688.

Okino, K., Ohara, Y., Kasuga, S., and Kato, Y., 1999. The Philippine Sea: new survey results reveal the structure and the history of marginal basins. *Geophys. Res. Lett.,* 26:2287–2290.

Ono, T., Yamamoto, S., and Ujiie, H., 1987. Fluctuation of carbonate and interstitial exchangeable elements in sediments from the ocean surrounding the Ryukyu Islands. *Compass,* 64:195–206.

Parkinson, I.J., and Pearce, J.A., 1998. Peridotites from the Izu-Bonin-Mariana forearc (ODP Leg 125); evidence for partial melting and melt-mantle interactions in a suprasubduction zone setting. *J. Petrol.,* 39:1577–1618.

Peacock, S.M., 1987. Creation and preservation of subduction-related inverted metamorphic gradients. *J. Geophys. Res.,* 92:12763–12781.

————, 1990. Fluid processes in subduction zones. *Science,* 248:329–337.

Phipps, S.P., and Ballotti, D., 1992. Rheology of serpentinite muds in the Mariana-Izu-Bonin forearc. *In* Fryer, P., Pearce, J.A., Stokking, L.B., et al., *Proc. ODP, Sci. Results,* 125: College Station, TX (Ocean Drilling Program), 363–372.

Purdy, G.M., and Dziewonski, A.M., 1988. *Proc. of a Workshop on Broadband Downhole Seismometers in the Deep Ocean.* Joint Oceanogr. Inst. and U.S. Sci. Advisory Comm.

Ringwood, A.E., and Irifune, T., 1988. Nature of the 650 km seismic discontinuity: implications for mantle dynamics and differentiation. *Nature,* 331:131–136.

Seekins, L.C., and Teng, T.L., 1977. Lateral variations in the structure of the Philippine Sea plate. *J. Geophys. Res.,* 82:317–324.

Shieh, Y.-T., and Chen, M.-P., 1995. The ancient Kuroshio Current in the Okinawa Trough during the Holocene. *Acta Oceanogr. Taiwanica,* 34:73–80.

Shieh, Y.-T., Wang, C.-H., Chen, M.-P., and Yung, Y.-L., 1997. The last glacial maximum to Holocene environment changes in the southern Okinawa Trough. *J. Asian Earth Sci.,* 15:3–8.

Sibuet, J.-C., Deffontaines, B., Hsu, S.-K., Thareau, N., Formal, J.-P., Liu, C.-S., and the ACT party, 1998. Okinawa Trough backarc basin: early tectonic and magmatic evolution. *J. Geophys. Res.,* 103:30245–30267.

Sibuet, J.-C., and Hsu, S.-K., 1997. Geodynamics of the Taiwan arc-arc collision. *Tectonophysics,* 274:221–251.

Sibuet, J.-C., Hsu, S.-K., Shyu, C.-T., and Liu, C.-S., 1995. Structural and kinematic evolution of the Okinawa Trough backarc basin. *In* Taylor, B. (Ed.), *Backarc Basins: Tectonics and Magmatism:* New York (Plenum Press), 343–378.

Sibuet, J.-C., Letouzey, J., Barbier, F., Charvet, J., Foucher, J.-P., Hilde, T.W.C., Kimura, M., Ling-Yun, C., Marsett, B., Muller, C., and Stephan, J.-F., 1987. Back arc extension in the Okinawa Trough. *J. Geophys. Res.,* 92:14041–14063.

Stephen, R.A., Collins, J.A., and Peal, K.R., 1999. Seafloor seismic stations perform well. *Eos,* 80:592.

Su, W.-J., Woodward, R.L., and Dziewonski, A.M., 1992. Deep origin of mid-ocean-ridge velocity anomalies. *Nature,* 360:149–152.

Suyehiro, K., Sacks, S., Acton, G.D., et al., 2000. *Proc. ODP, Init. Repts,* 186 [CD-ROM]. Available from: Ocean Drilling Program, Texas A&M University, College Station TX 77845-9547, USA.

Tanimoto, T., 1988. The 3-D shear wave structure in the mantle by overtone waveform inversion, II: inversion of X-waves, R-waves, and G-waves. *J. Geophys.,* 93:321–333.

Teng, L.S., 1996. Extensional collapse of the northern Taiwan mountain belt. *Geology,* 24:949–952.

Todd, C., and Fryer, P., 1999. Blueschist mud volcanism in the Mariana forearc: sampling the subducted slab. *Geol. Soc. Am. Abstr. Progr.,* 31:7.

Tsuburaya, H., and Sata, T., 1985. Petroleum exploration well Miyakojima-Oki. *J. Japanese Assoc. Petrol. Technol.,* 50:25–53.

Ujiié, H., 1980. Significance of "500 m deep island shelf" surrounding the southern Ryukyu Island arc for its Quaternary history. *Quat. Res.,* 18:209–219.

Ujiié, H., Tanaka, Y., and Ono, T., 1991. Late Quaternary paleoceanographic record from the middle Ryukyu Trench slope, northwest Pacific. *Mar. Micropaleontol.,* 18:115–128.

Ujiié, H., and Ujiié, Y., 1999. Late Quaternary course changes of the Kuroshio Current in the Ryukyu arc region, northwestern Pacific Ocean. *Mar. Micropaleontol.,* 37:23–40.

Uyeda, S., 1977. Some basic problems in trench-arc-back-arc systems. *In* Talwani, M., and Pitman, W.C., II (Eds.), *Island Arcs, Deep Sea Trenches, and Back-arc Basins.* Geophys. Monogr., Maurice Ewing Ser., Am. Geophys. Union, 1:1–14.

Valloni, R., 1985. Reading provenance from modern marine sands. *In* Zuffa, G.G. (Ed.), *Provenance of Arenites.* NATO ASI Ser. C, 148:309–332.

van der Hilst, H., Engdahl, R., Spakman, W., and Nolet, G., 1991. Tomographic imaging of subducted lithosphere below northwest Pacific island arcs. *Nature,* 353:37–43.

van der Hilst, R.D., and Seno, T., 1993. Effects of relative plate motion on the deep structure and penetration depth of slabs below the Izu-Bonin and Mariana Island arcs. *Earth Planet. Sci. Lett.,* 120:395–407.

White, A.F., and Hochella, M.F., 1992. Surface chemistry associated with the cooling and subaerial weathering of Recent basalt flows. *Geochim. Cosmochim. Acta,* 56:3711–3721.

Zhang, Y.S., and Tanimoto, T., 1992. Ridges, hotspots and their interaction as observed in seismic velocity maps. *Nature,* 355:45–49.

Figure F1. Location map showing sites drilled during Leg 195. The geochemical observatory was installed at Site 1200, and the International Ocean Network (ION) seismic observatory was installed at Site 1201. Site 1202 was drilled to study the history of the Kuroshio Current.

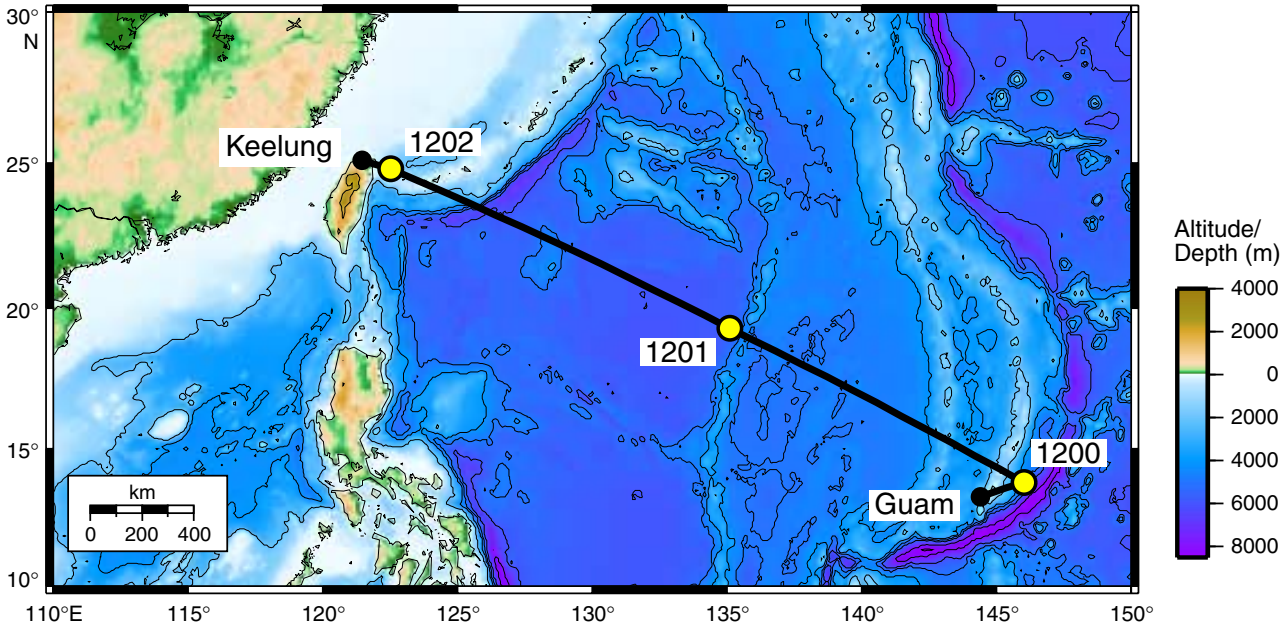

Figure F2. Bathymetric map of the southern Mariana forearc (250-m contour intervals) showing locations of all forearc seamounts sampled to date. Site 1200 was drilled on South Chamorro Seamount during Leg 195.

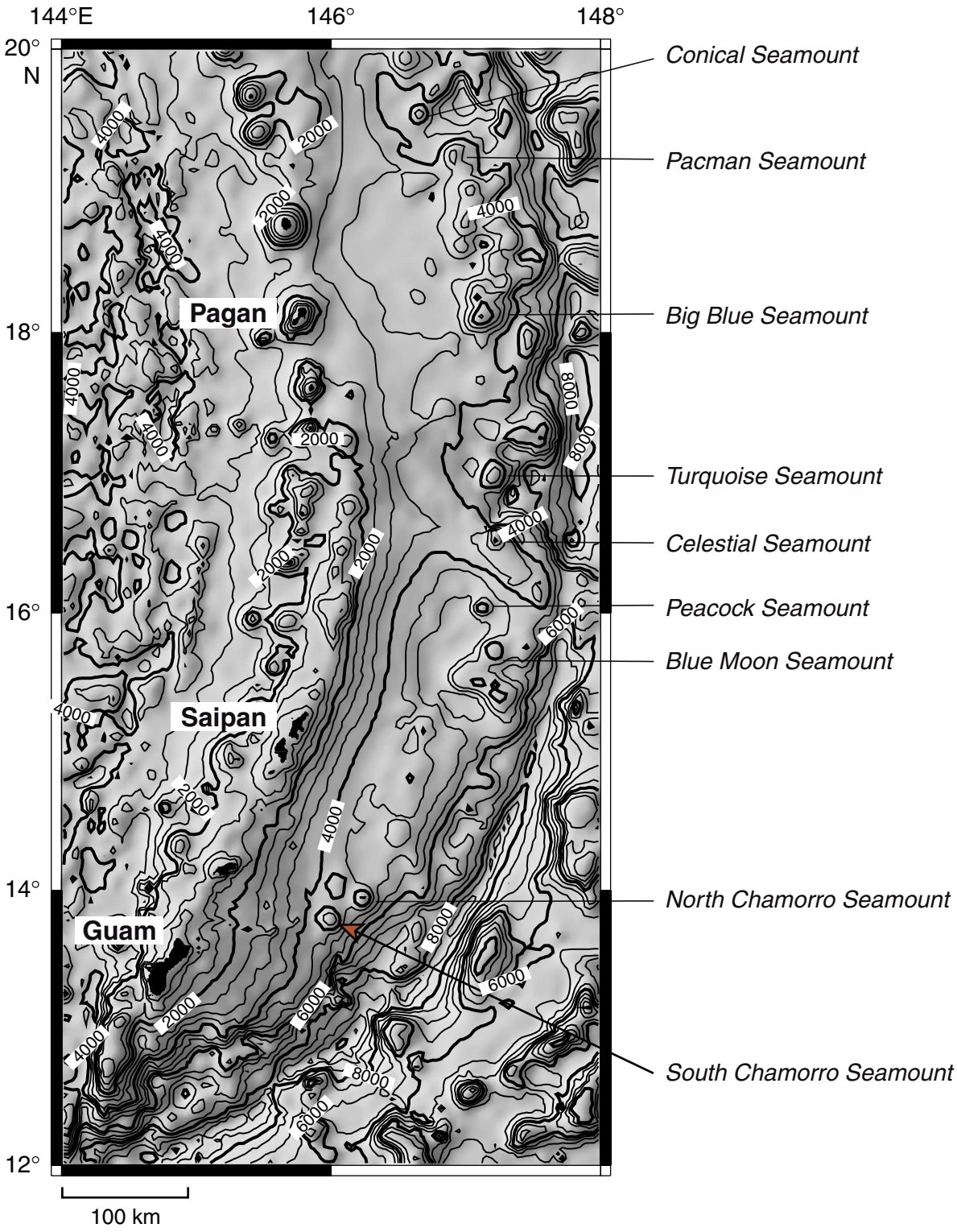

Figure F3. Schematic cross section through the Mariana system showing various types of associations of serpentine mud volcanoes, with faulting in the forearc wedge. Strike-slip faulting associated with along-strike extension and vertical tectonics related to seamount subduction both play a part in the tectonic deformation of the forearc and provide avenues for the ascent of slab-derived fluids and fault gouge from both the décollement and the lithosphere of the overriding plate. Decarbonation reactions in the downgoing plate probably take place between depths of ~15 and 20 km.

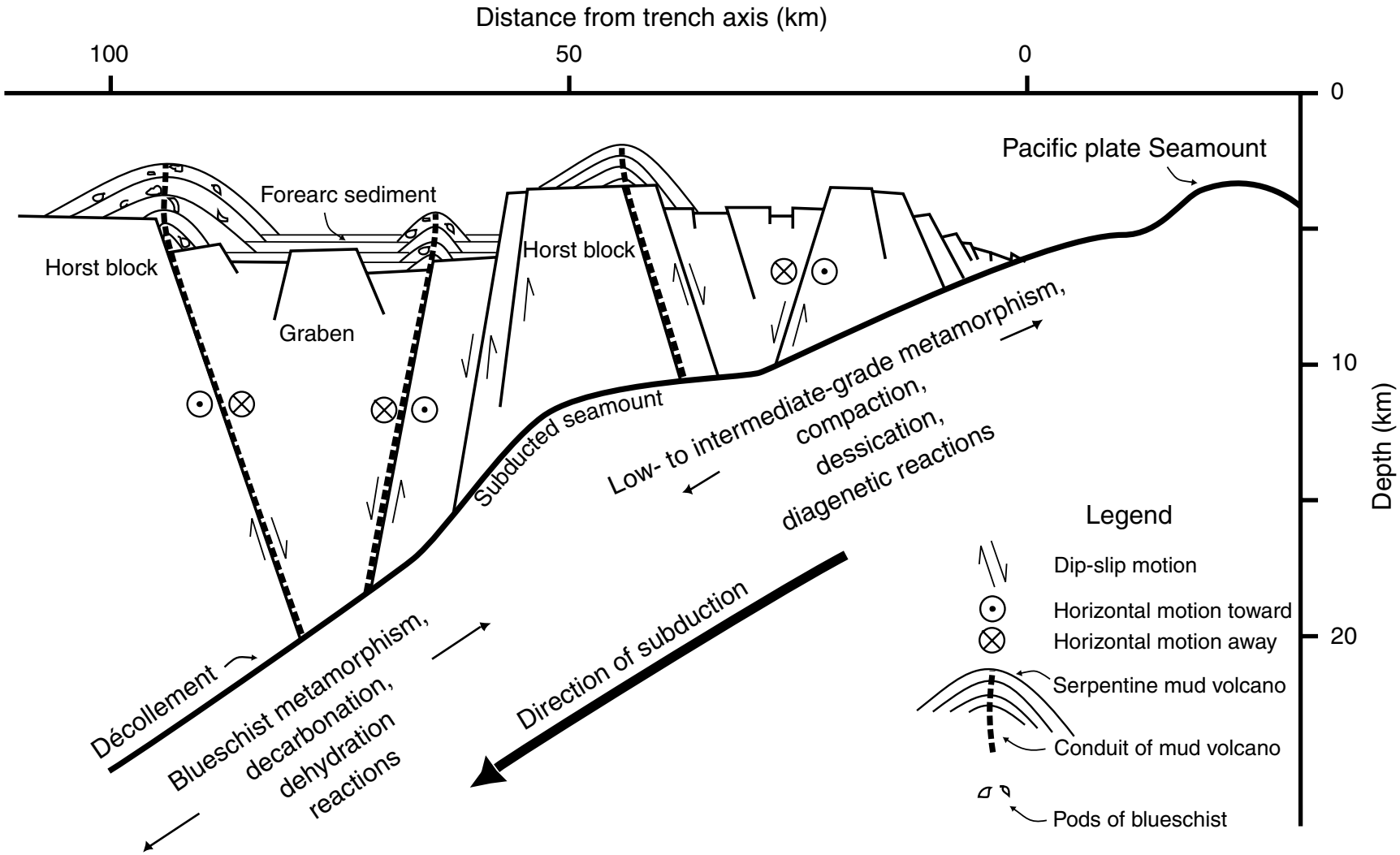

Figure F4. HMR-1 side-scan imagery of South Chamorro Seamount showing the locations of six-channel seismic reflection profiles shown in Figure F5, p. 37. Contour intervals are given in meters.

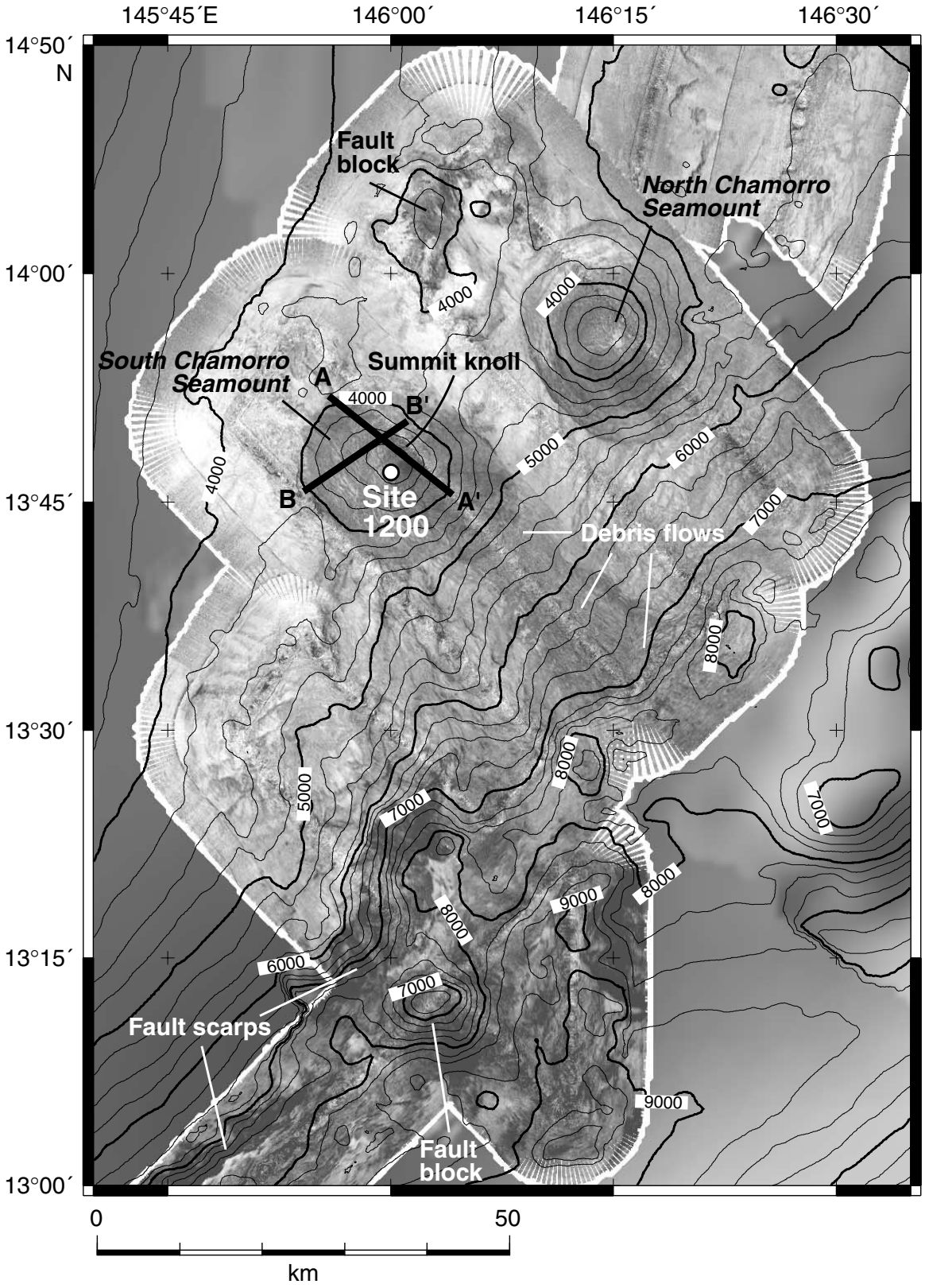

Figure F5. Multichannel seismic reflection profiles over South Chamorro Seamount (locations are shown in Fig. F4, p. 36).

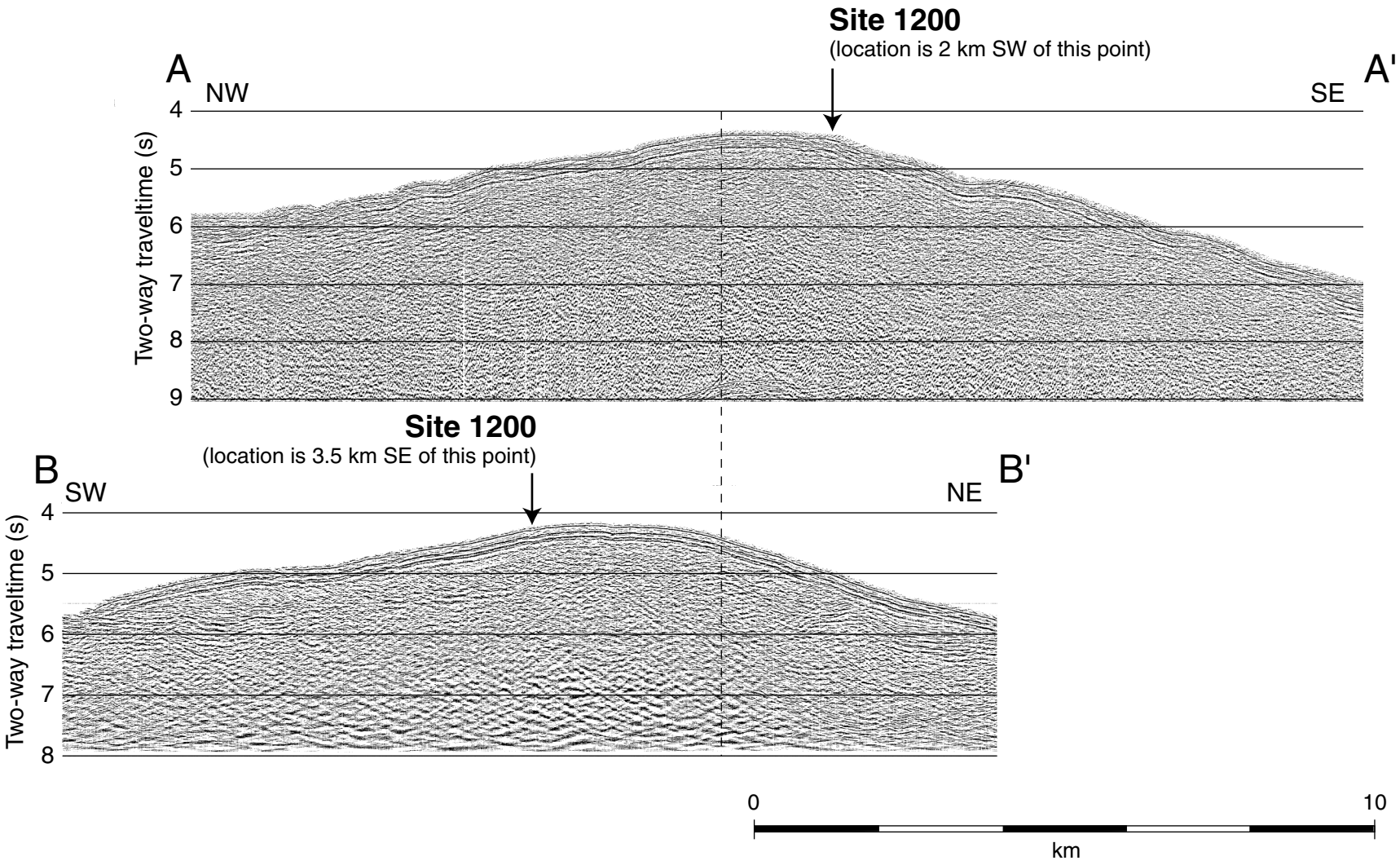

Figure F6. Locations of Holes 1200A–1200F drilled on the summit knoll of South Chamorro Seamount. Also shown is the location of the seafloor television survey conducted before drilling. Contours are given in meters.

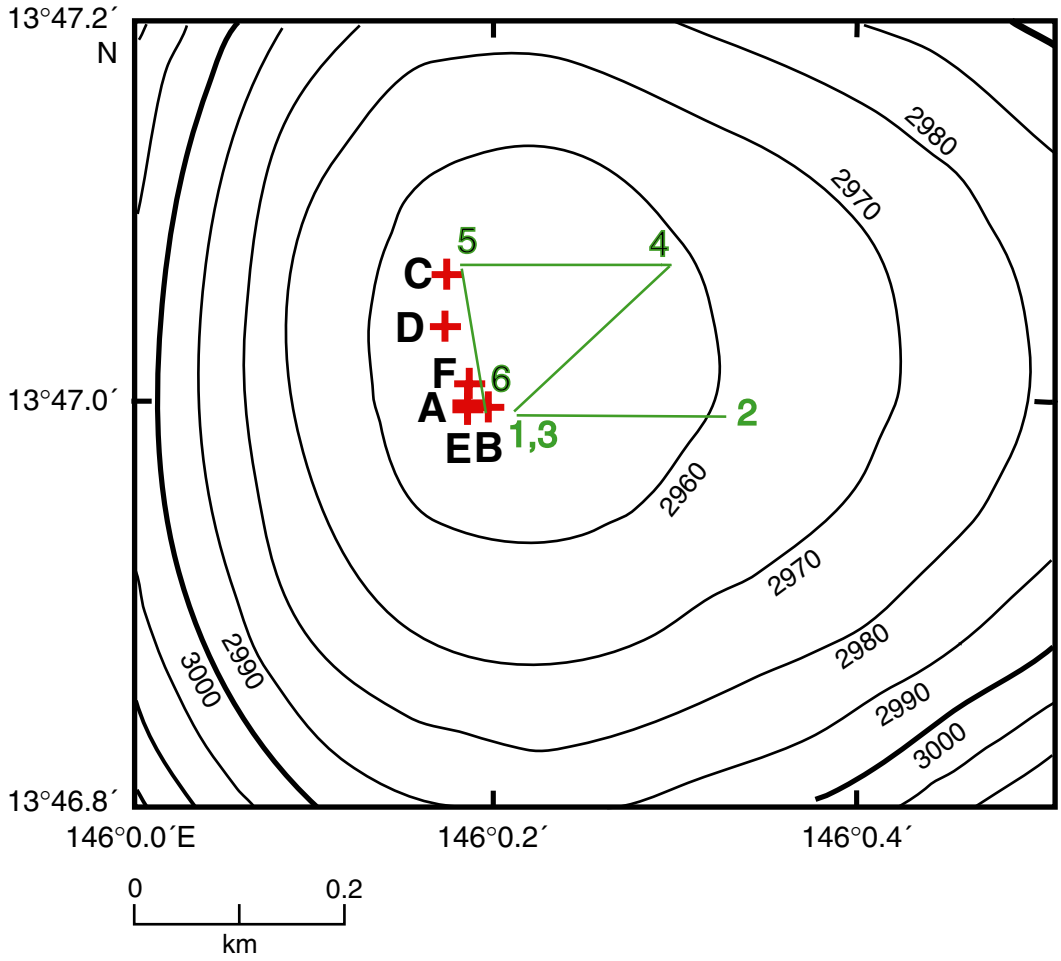

Figure F7. Casing configuration for the geochemical observatory installed in Hole 1200C on South Chamorro Seamount.

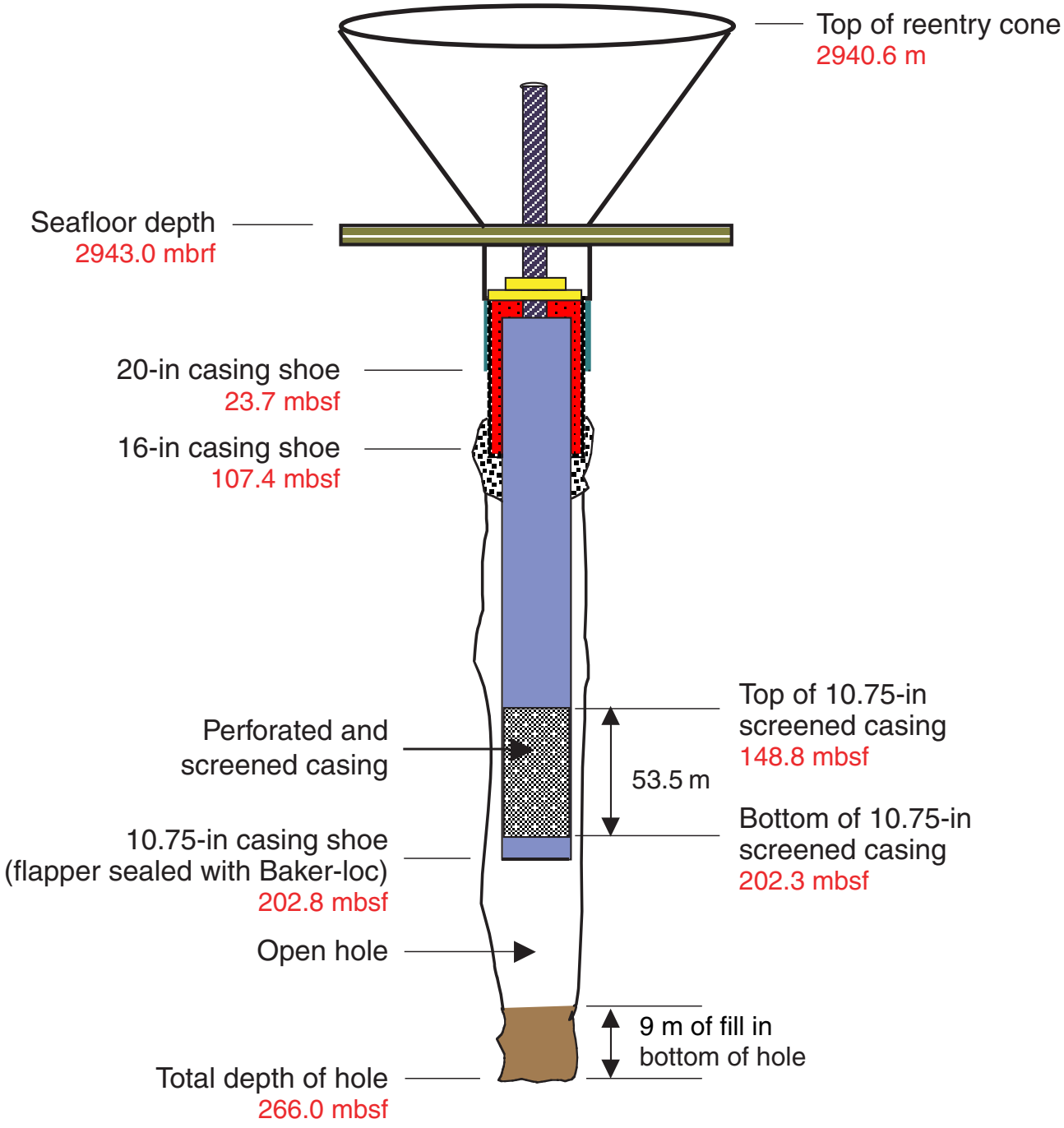

Figure F8. Geochemical observatory (CORK) configuration in Hole 1200C, South Chamorro Seamount.

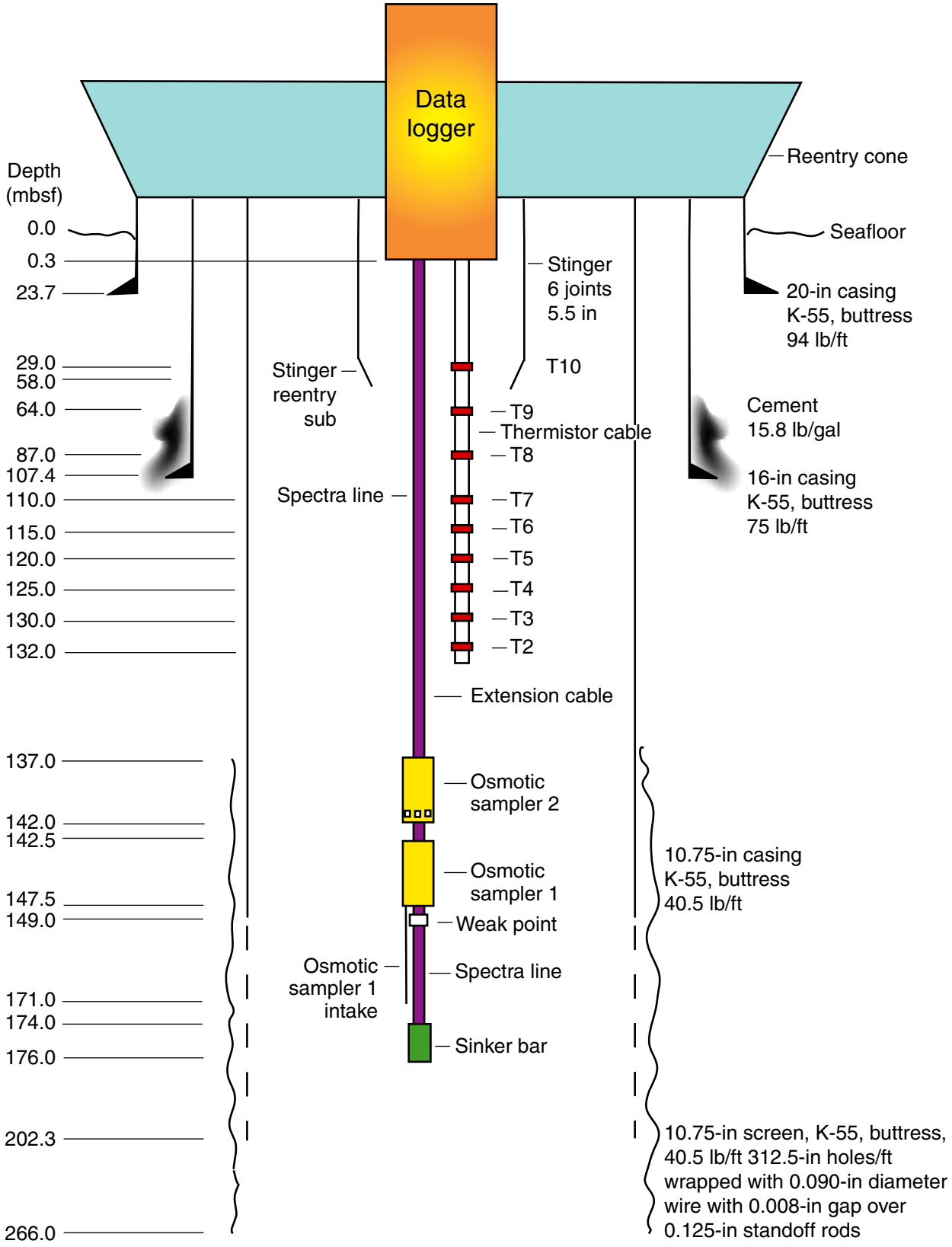

Figure F9. Close-up photograph of serpentine mud breccia from South Chamorro Seamount (interval 195-1200E-10H-2, 83–113 cm).

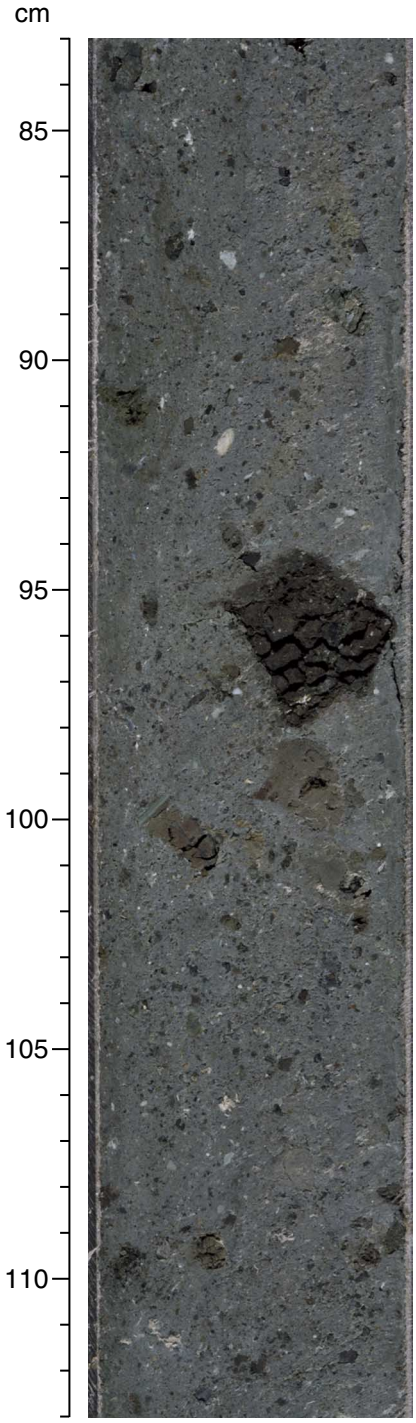

Figure F10. Photomicrograph of glaucophane (Gl) schist in serpentine mud (Sample **195-1200F-1H-4, 34–36 cm**).

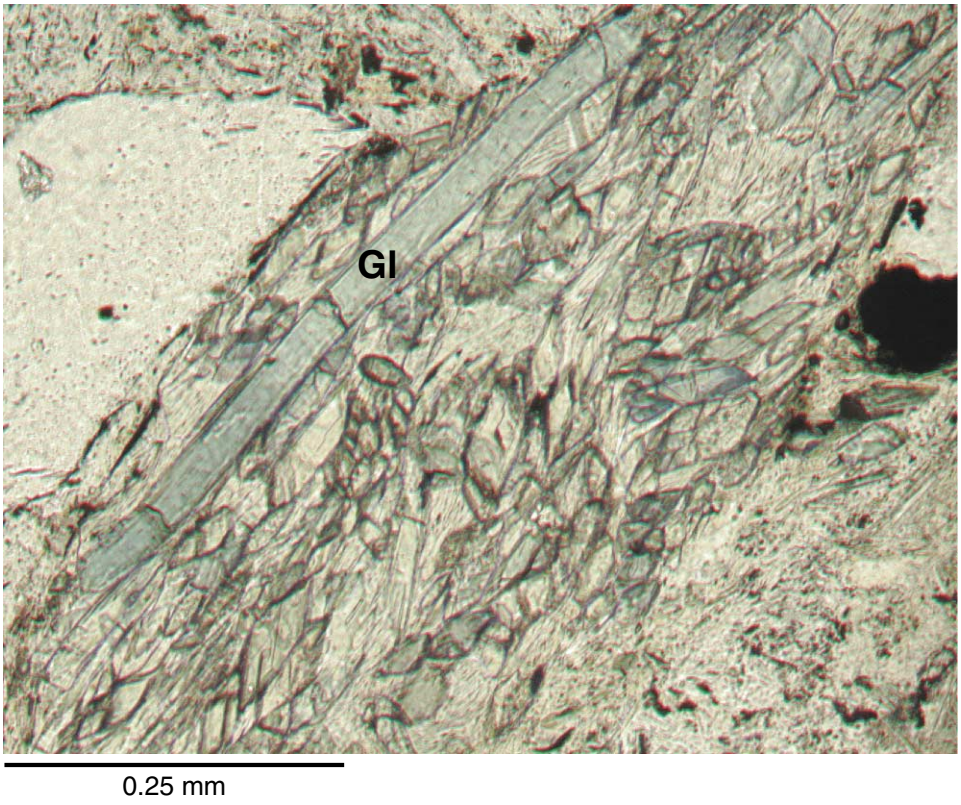

Figure F11. Photomicrograph of tremolite (Tr)-rich chlorite (Chl) schist in serpentine mud (Sample 195-1200F-1H-4, 34–36 cm).

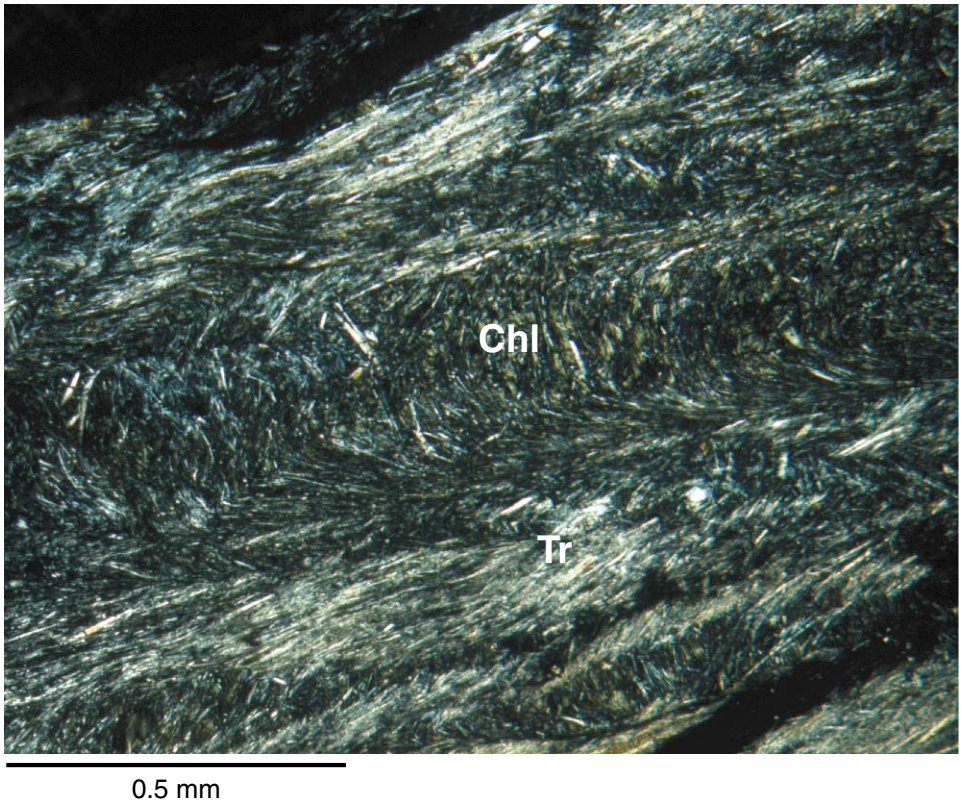

Figure F12. (**A**) Al_2O_3 and (**B**) $Mg^{2+}/(Mg^{2+}+Fe^{2+})$ diagrams for Mariana forearc peridotites, showing degrees of partial melting. Conical and Torishima Forearc Seamount data are from Ishii et al. (1992) and Parkinson and Pearce (1998).

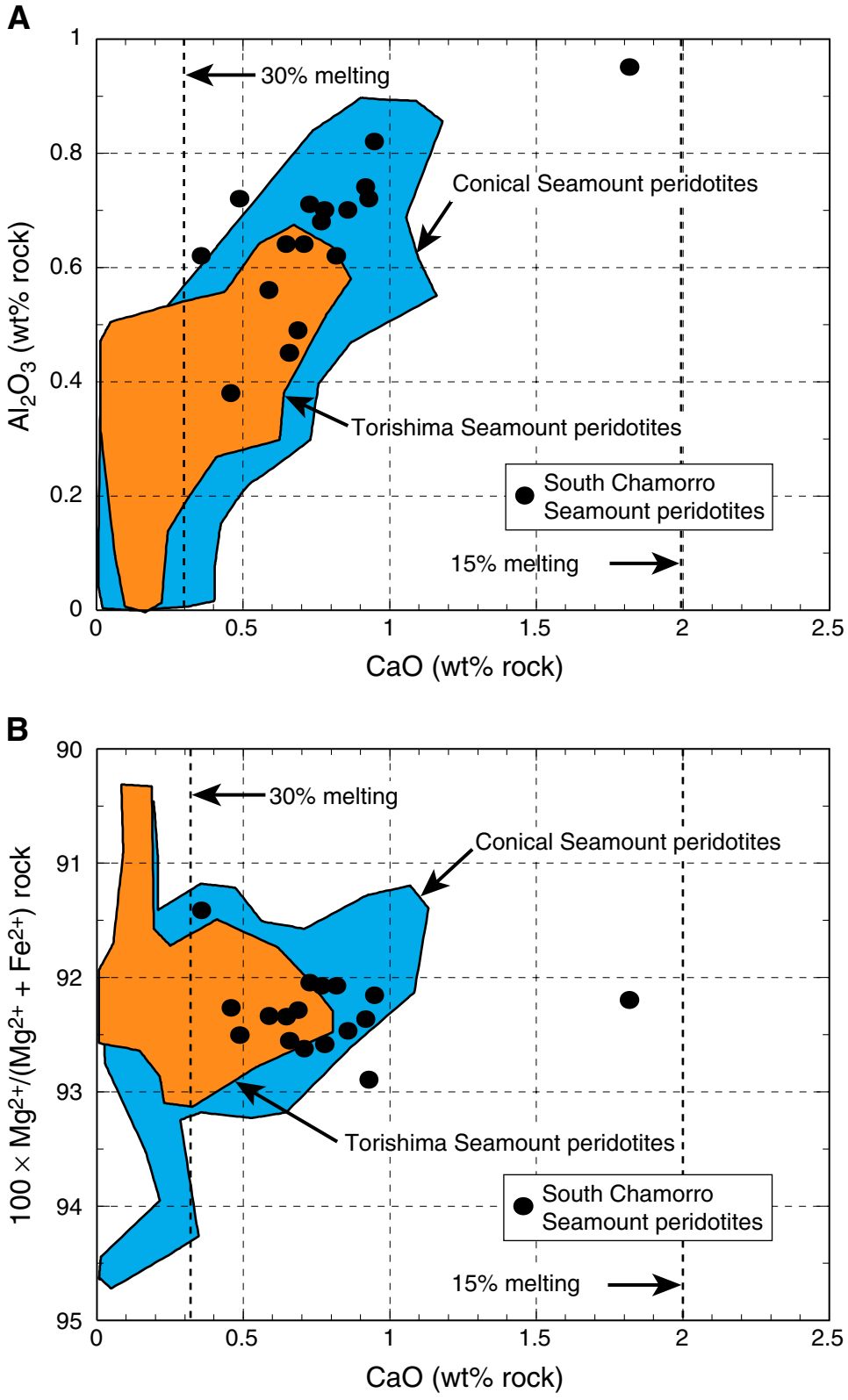

Figure F13. Pore water composition vs. depth curves for Holes 1200D, 1200E, and 1200F. **A.** pH. **B.** Alkalinity. **C.** Sodium/chloride. **D.** Boron. **E.** Sulfate. Hole 1200E is closest to the vent community on the summit of South Chamorro Seamount; Hole 1200D is the most distant. Arrow = seawater value.

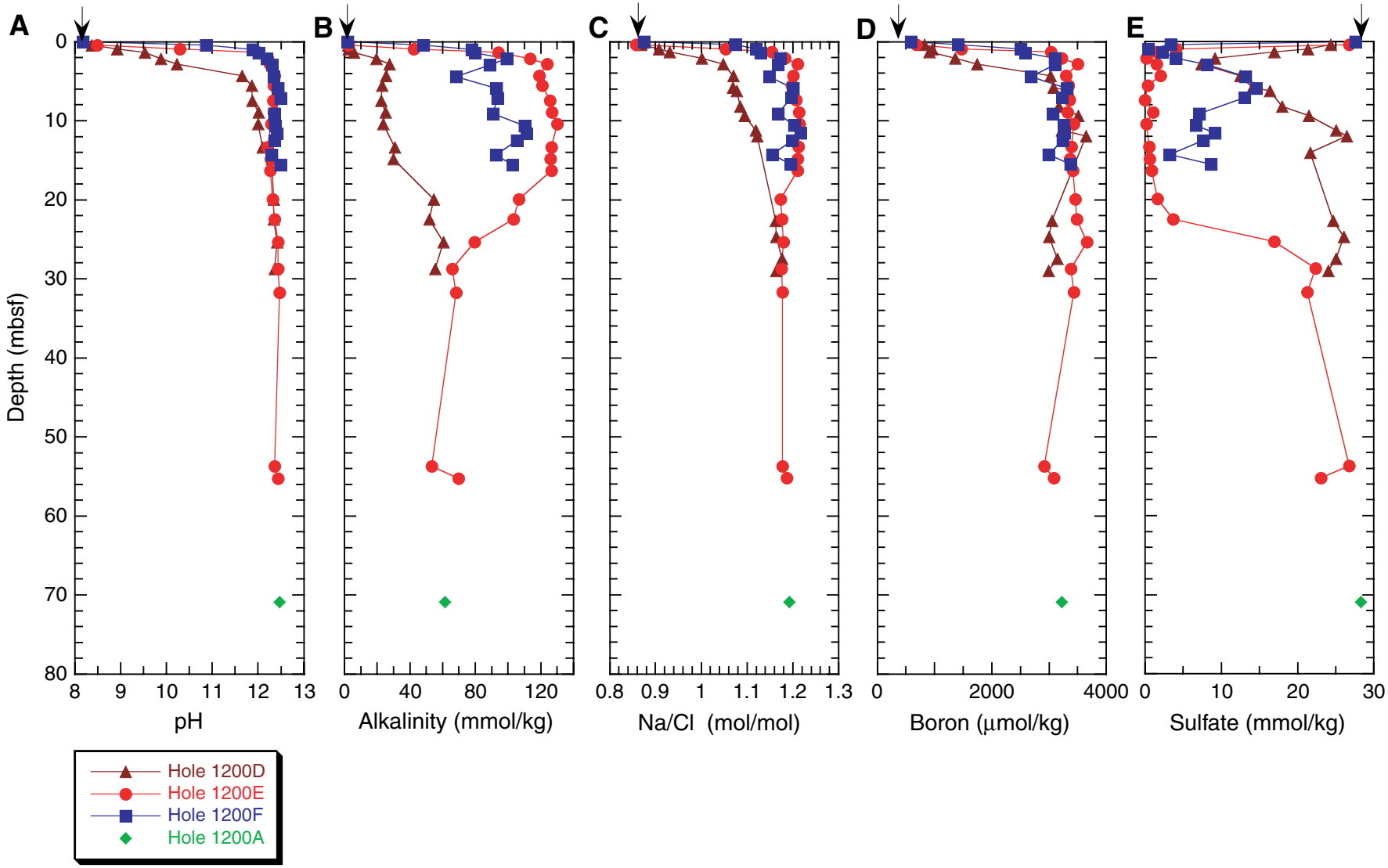

Figure F14. Location of seismic station coverage in the northwest Pacific region. At least five major plates with consuming boundaries interact in the northwest Pacific, causing subduction, backarc spreading, slab collisions, terrane accretion, and island arc development. Blue and yellow circles = land seismic stations. Orange circles = International Ocean Network (ION) seafloor observatories JT-1 and JT-2 (Japan Trench), WP-2 (northwest Pacific), and Site 1201 (this site). OHP = Ocean Hemisphere Network Project, IRIS = Incorporated Research Institutions for Seismology. TJN = Taejon, South Korea; INU = Inuyama, Japan; ISG = Ishigakijima, Japan; OGS = Chichijima, Japan; MCSJ = Minami Torishima, Japan; BAG = Baguio, Philippines; PATS = Pohnpei, Micronesia; JAY = Jayapura, Indonesia; PMG = Port Moresby, Papua New Guinea.

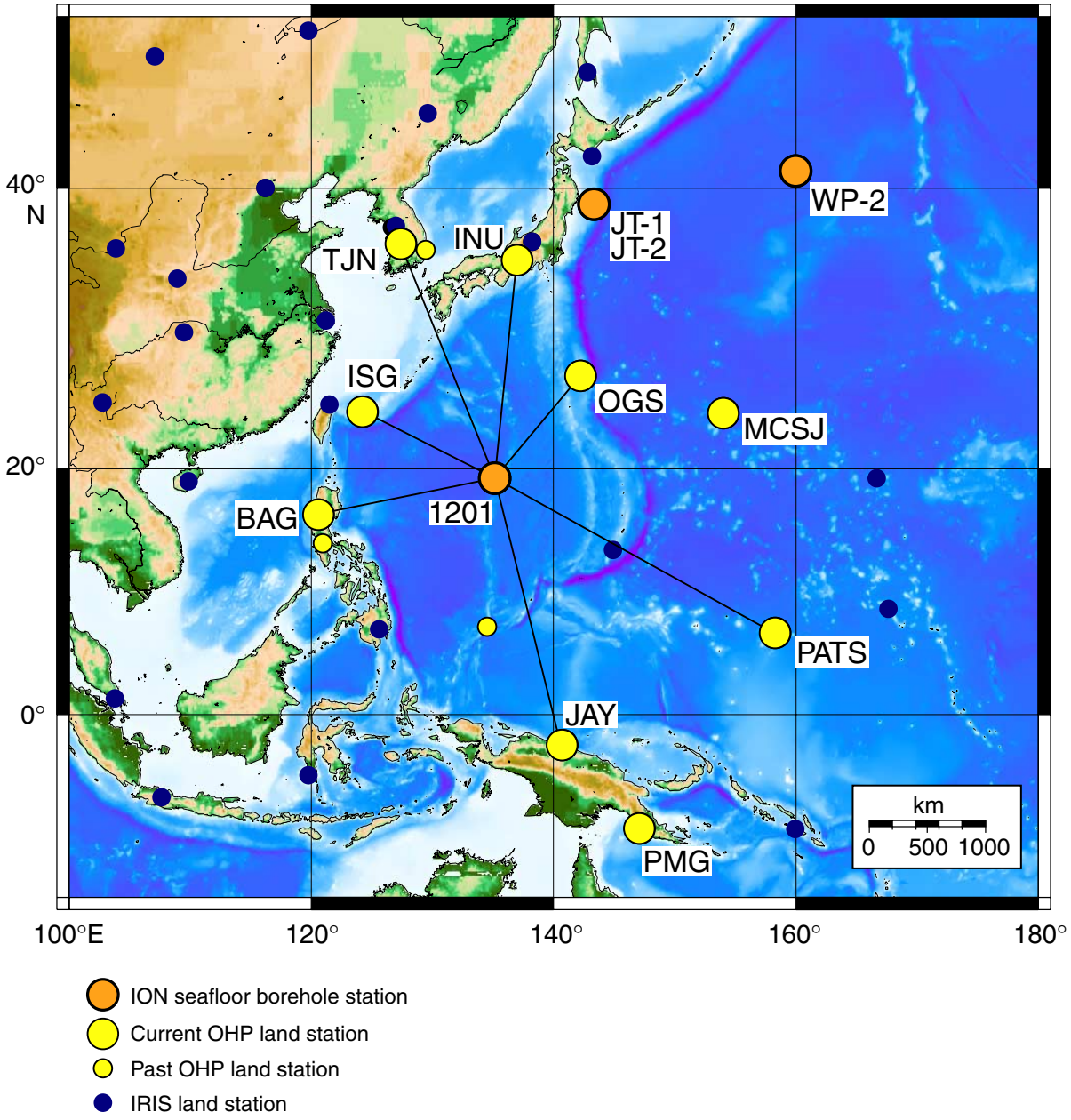

Figure F15. Location map showing DSDP Sites 290, 294, 295, and 447 and ODP Site 1201 in the Philippine Sea. Also shown are magnetic lineations from Hilde and Lee (1984). Basement ages in parentheses. The Central Basin Fault (the former spreading center) is shown as a series of heavy solid lines with offsets along transform faults.

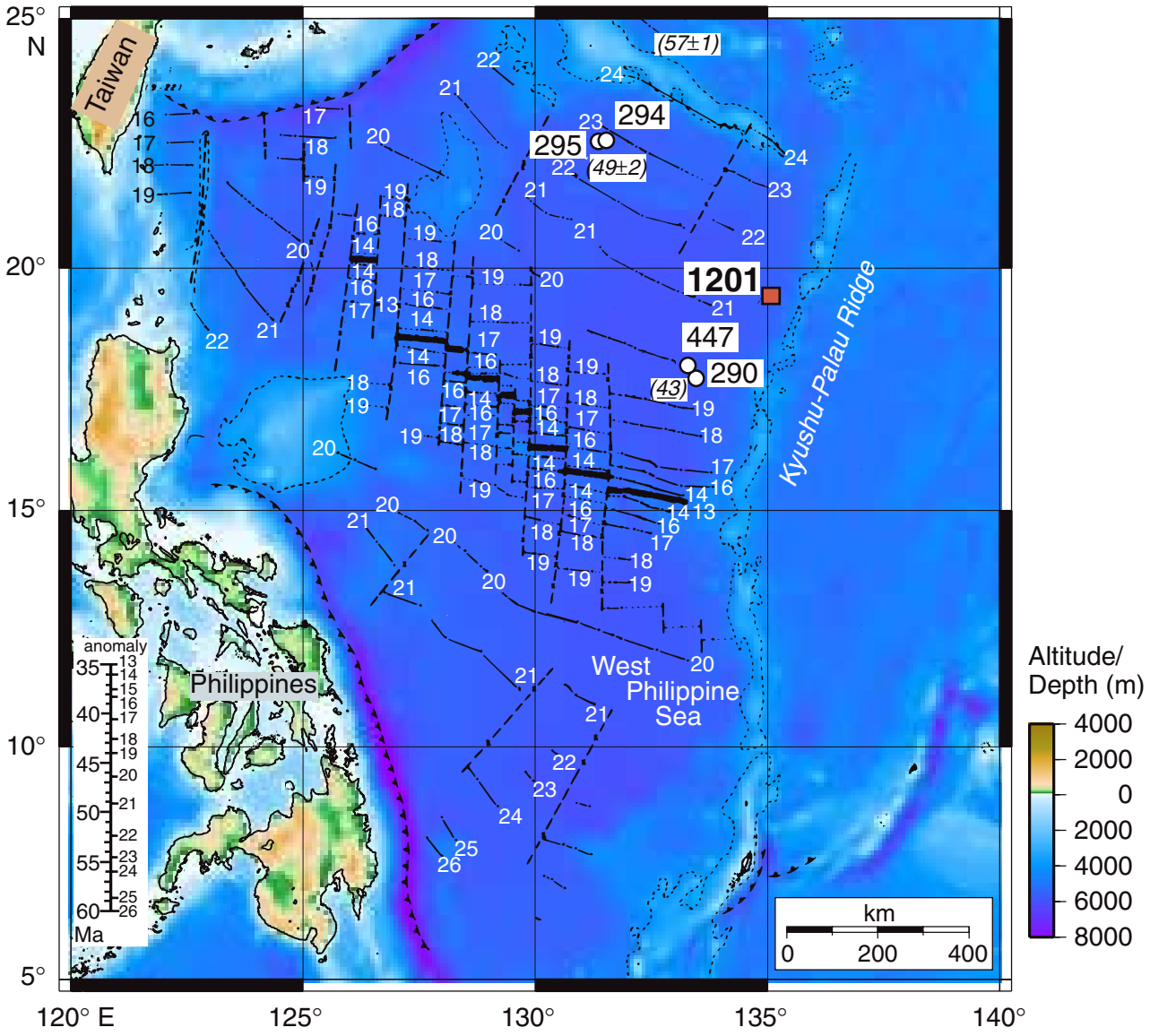

Figure F16. Reflection line OT97 showing the location of Site 1201. Basement lies about 0.45 s (two-way traveltime) below seafloor and was reached at 510 mbsf. CDP = common depth point.

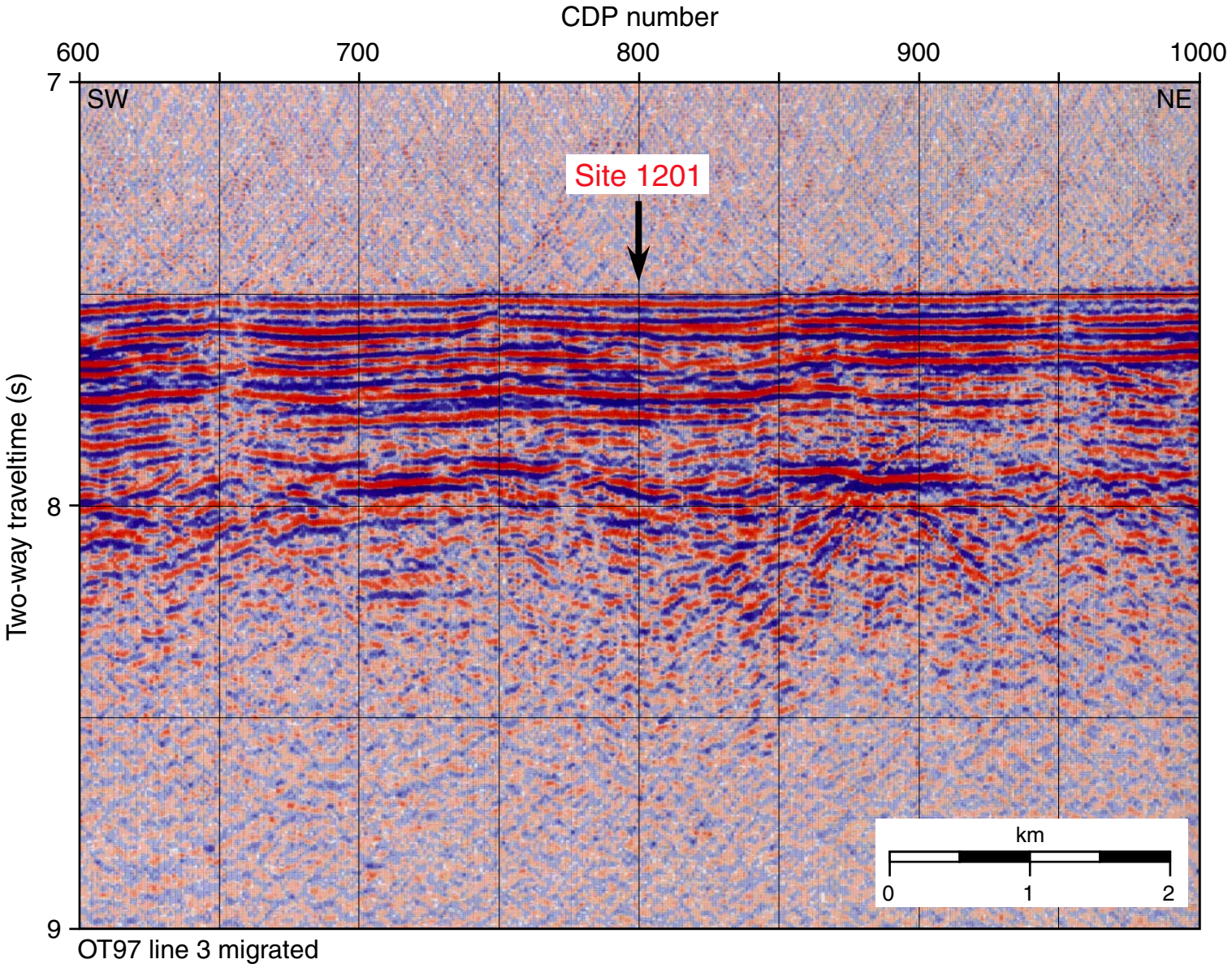

Figure F17. Borehole seismometer instrument package deployed in Hole 1201D. BIA = borehole instrument assembly, OBH = ocean borehole seismometer.

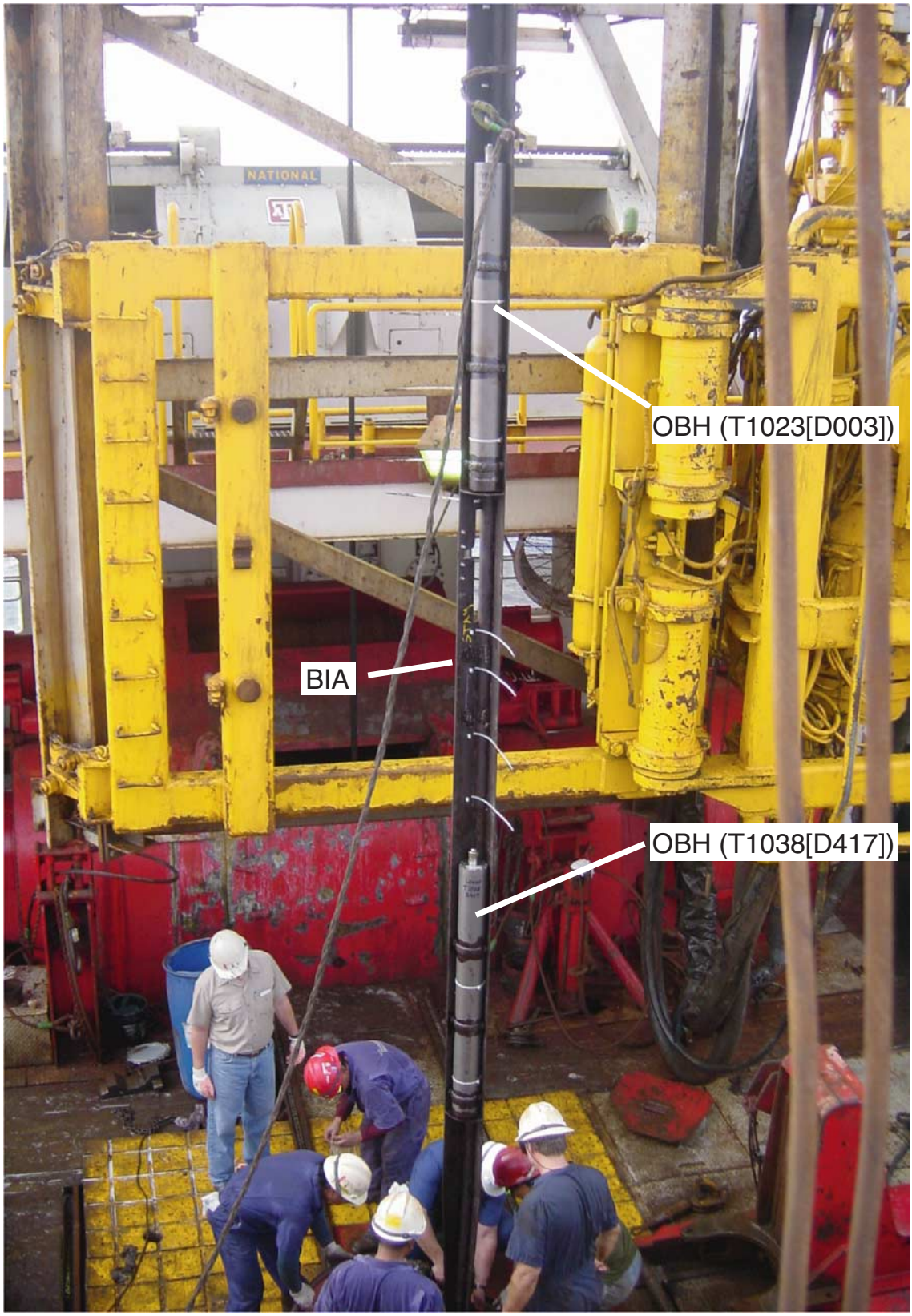

Figure F18. Configuration of reentry cone, casing, and International Ocean Network seismic observatory components at Site 1201. MEG = multiple-access expandable gateway, ROV = remotely operated vehicle, PAT = power access terminal.

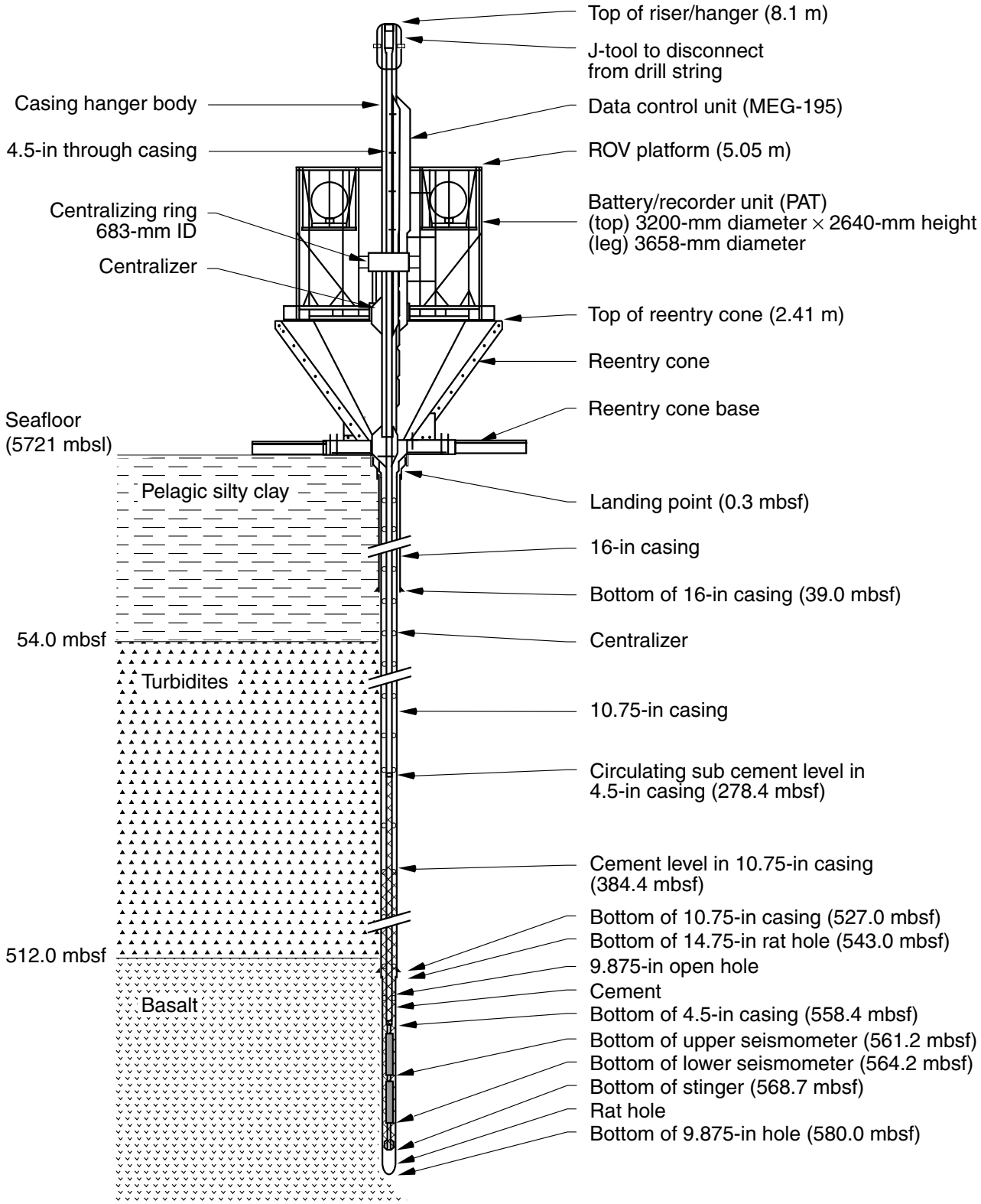

Figure F19. Remotely operated vehicle (ROV) landing platform installed in Hole 1201D. LBU = lithium battery unit, SAM = storage acquisition module, UMC = underwater mateable connector.

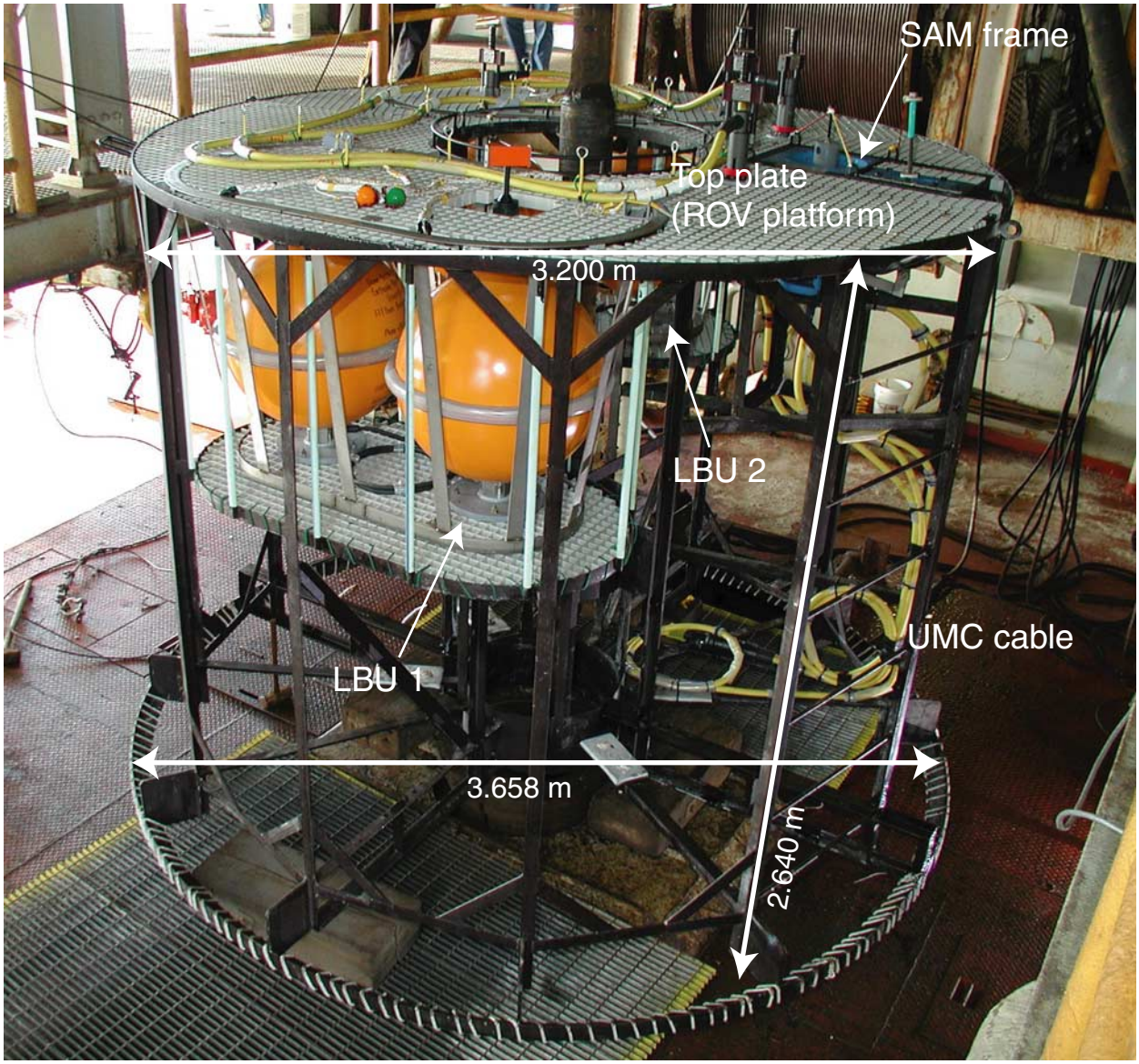

Figure F20. Lithology, color, natural gamma count, and mineralogy vs. depth and age at Site 1201. Note the increase in zeolites with depth in the turbidites. In the graphic lithology log, c = clay, s = silt, s = sand, g = gravel. a* = color reflectance parameter.

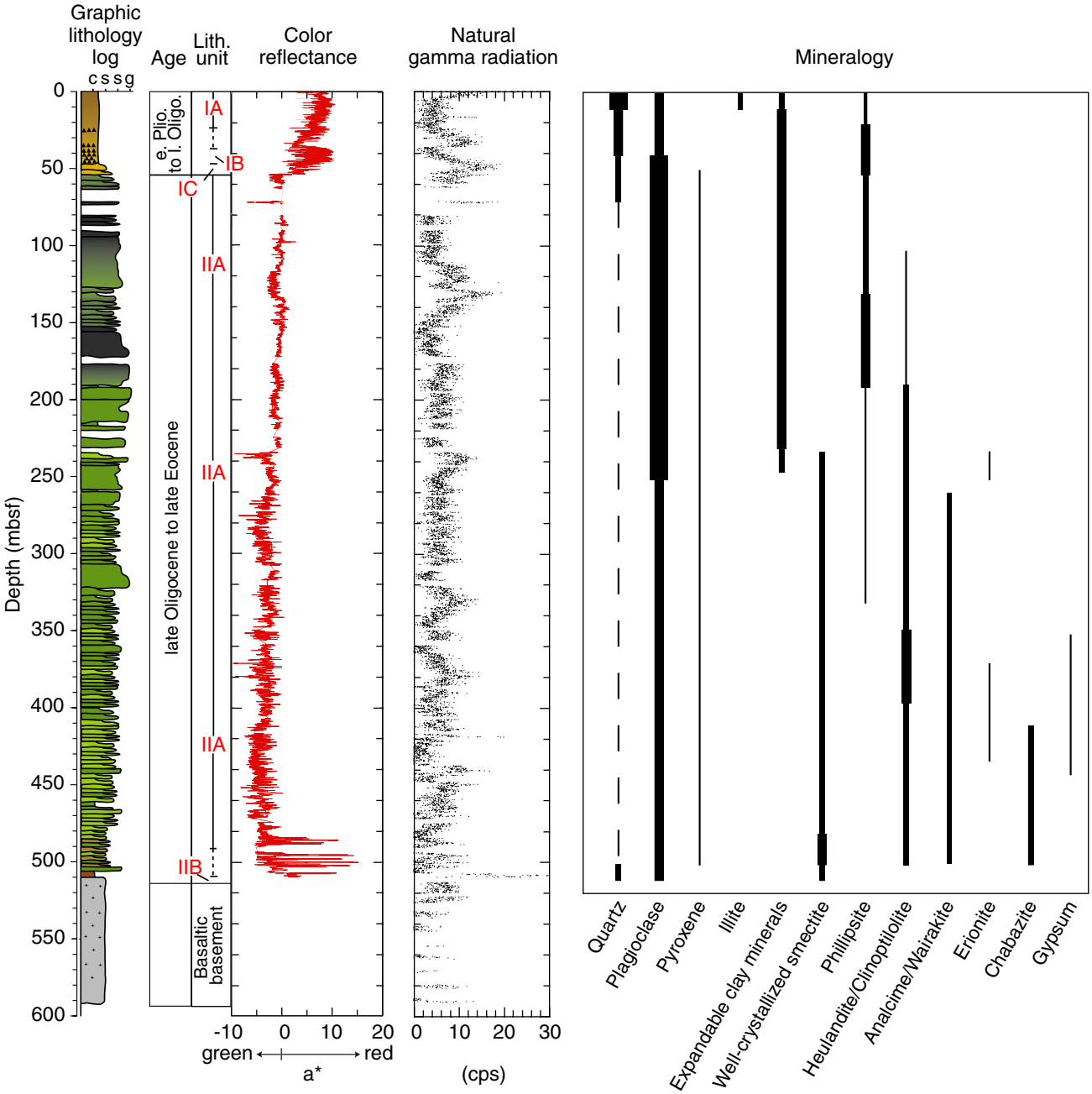

Figure F21. Laboratory multisensor track measurements of (**A**) magnetic susceptibility, (**B**) density, and (**C**) natural gamma ray emission vs. depth at Site 1201. In the graphic lithology log, c = clay, s = silt, s = sand, g = gravel.

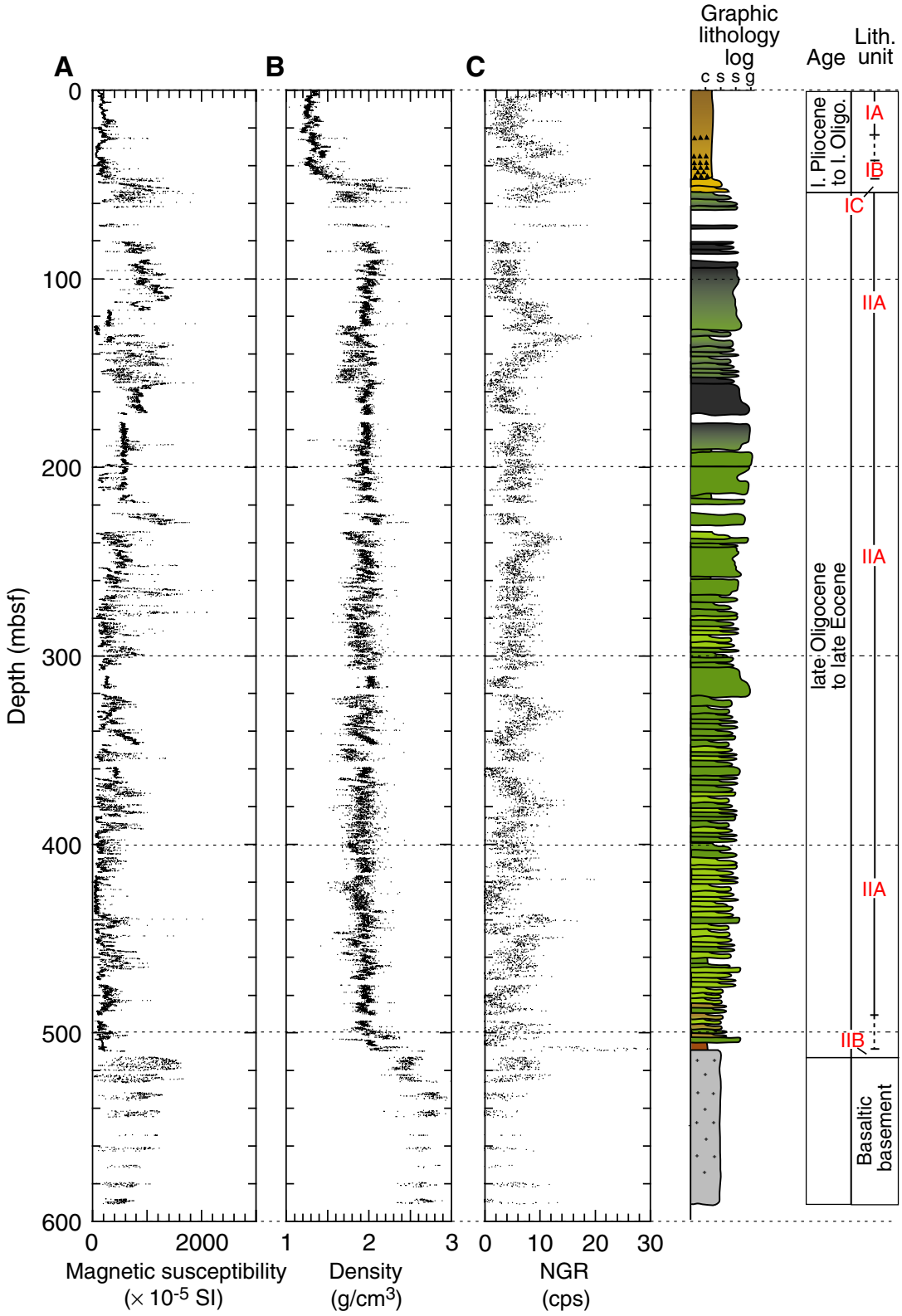

Figure F22. Logging results from Hole 1201D. Logging Units 1a–1d correspond to coarse turbidite units. In the graphic lithology log, c = clay, s = silt, s = sand, g = gravel. * = spurious data.

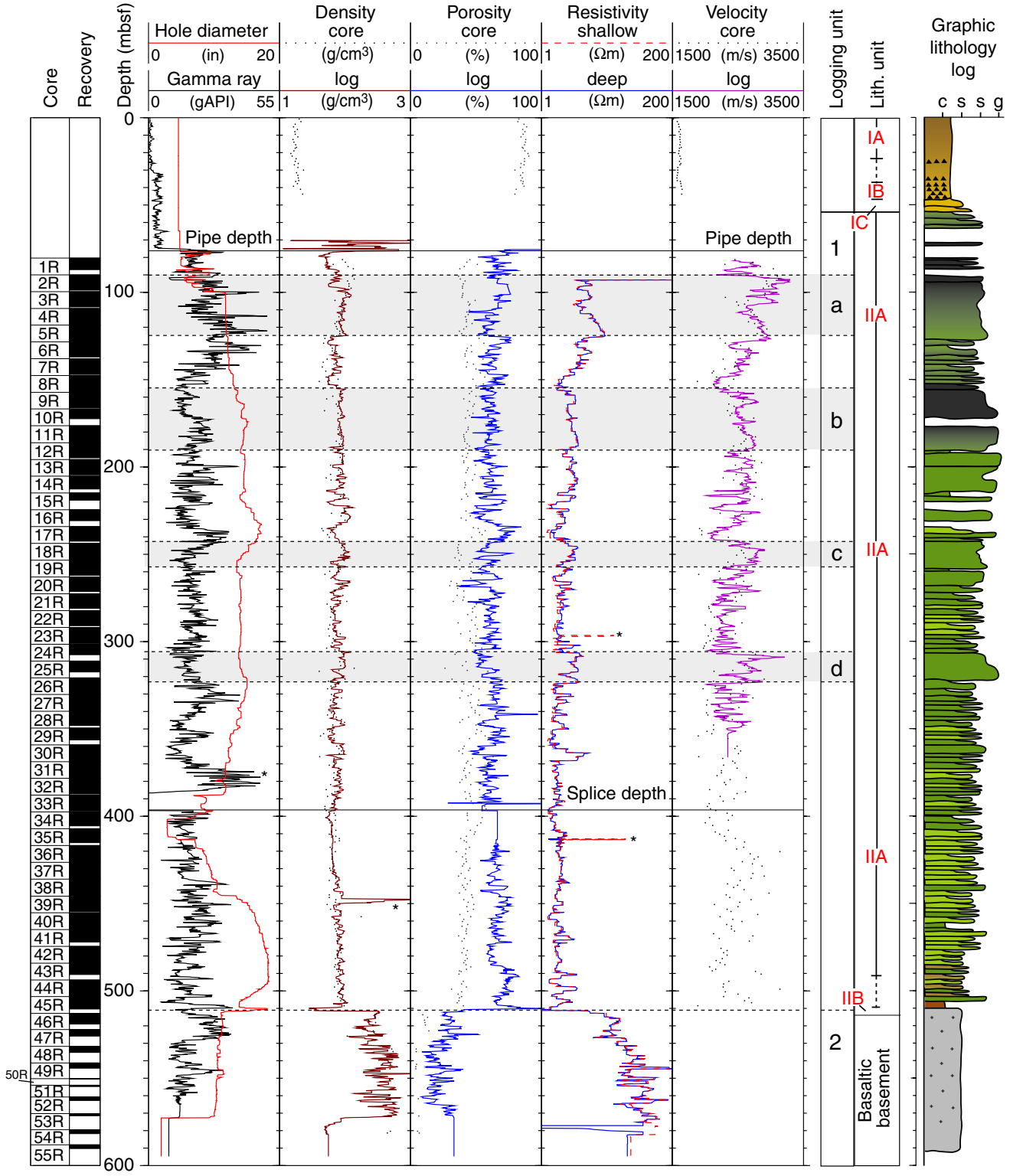

Figure F23. (**A**) Mg, (**B**) Ca, (**C**) Na, and (**D**) alkalinity vs. depth in pore waters from Site 1201. In the graphic lithology log, c = clay, s = silt, s = sand, g = gravel. Arrows = seawater values.

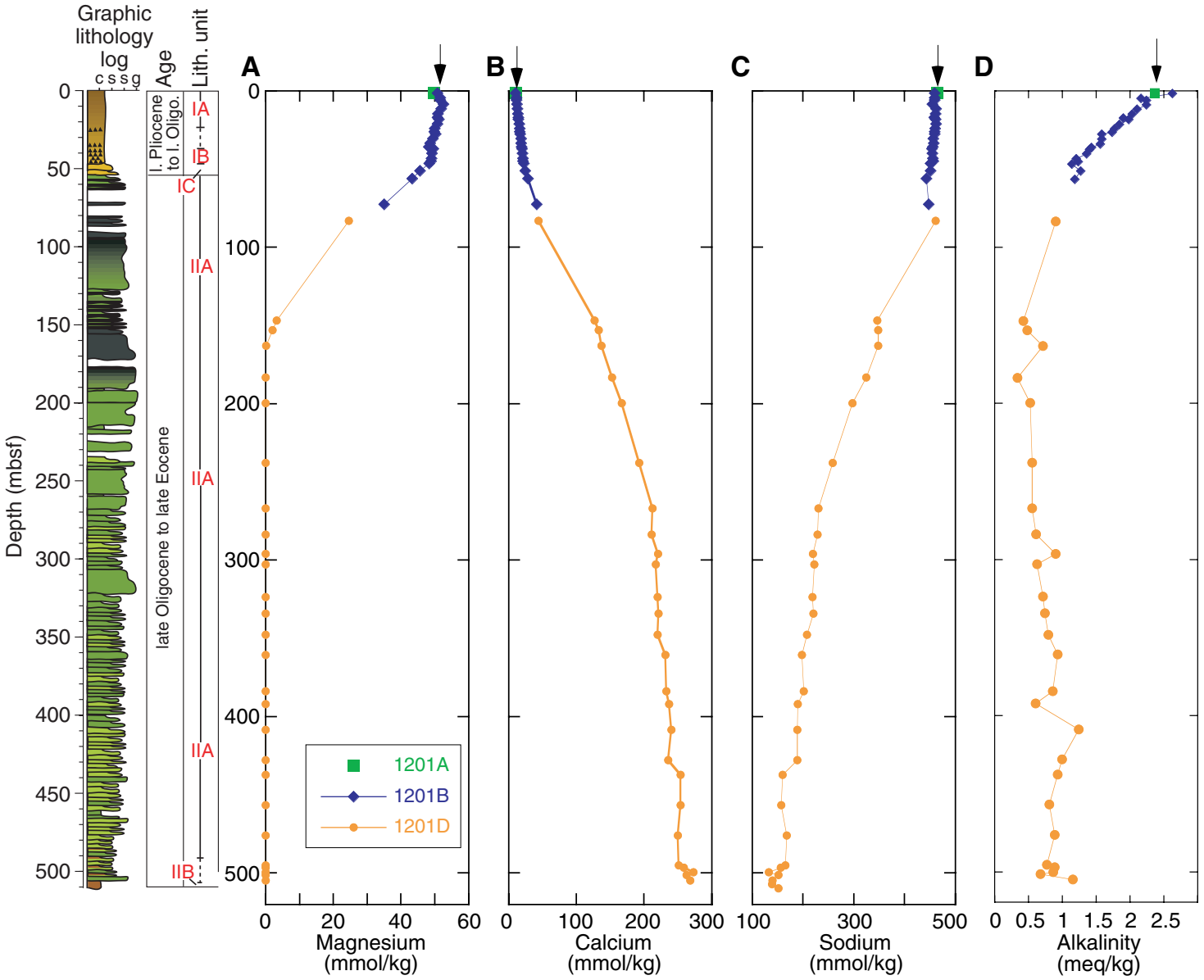

Figure F24. Nannofossil ranges at Site 1201. The upper 25 m and the lower 45 m of the section are barren except for radiolarians and fish teeth. In the graphic lithology log, c = clay, s = silt, s = sand, g = gravel.

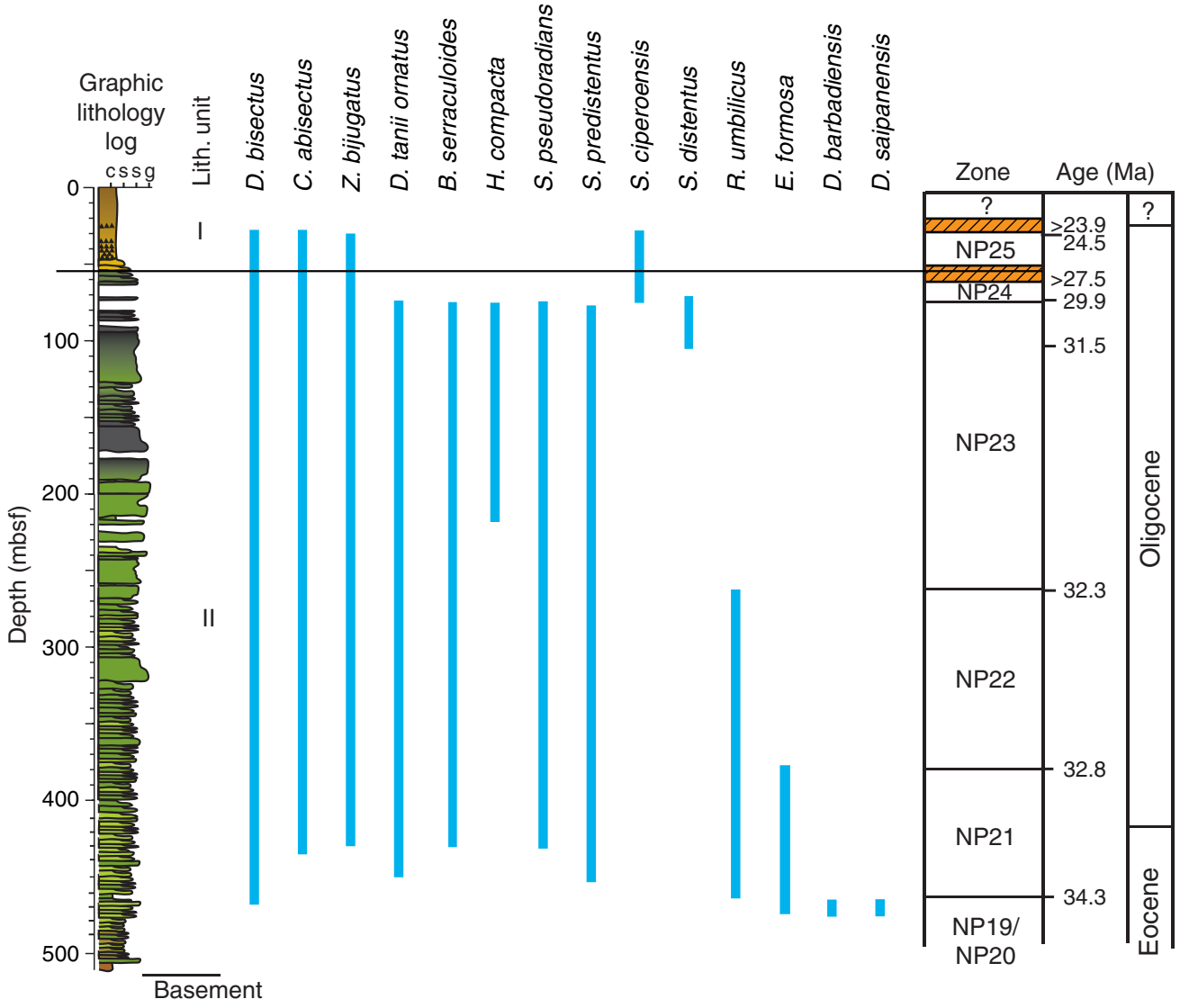

Figure F25. Continuous magnetic inclination and declination record in pelagic sediments at Site 1201 (large dots correspond to discrete samples). Also shown is the best fit to the late Oligocene through late Miocene geomagnetic polarity timescale based on paleontological markers from the site. In the polarity column, black bands = normal and white bands = reversed polarity.

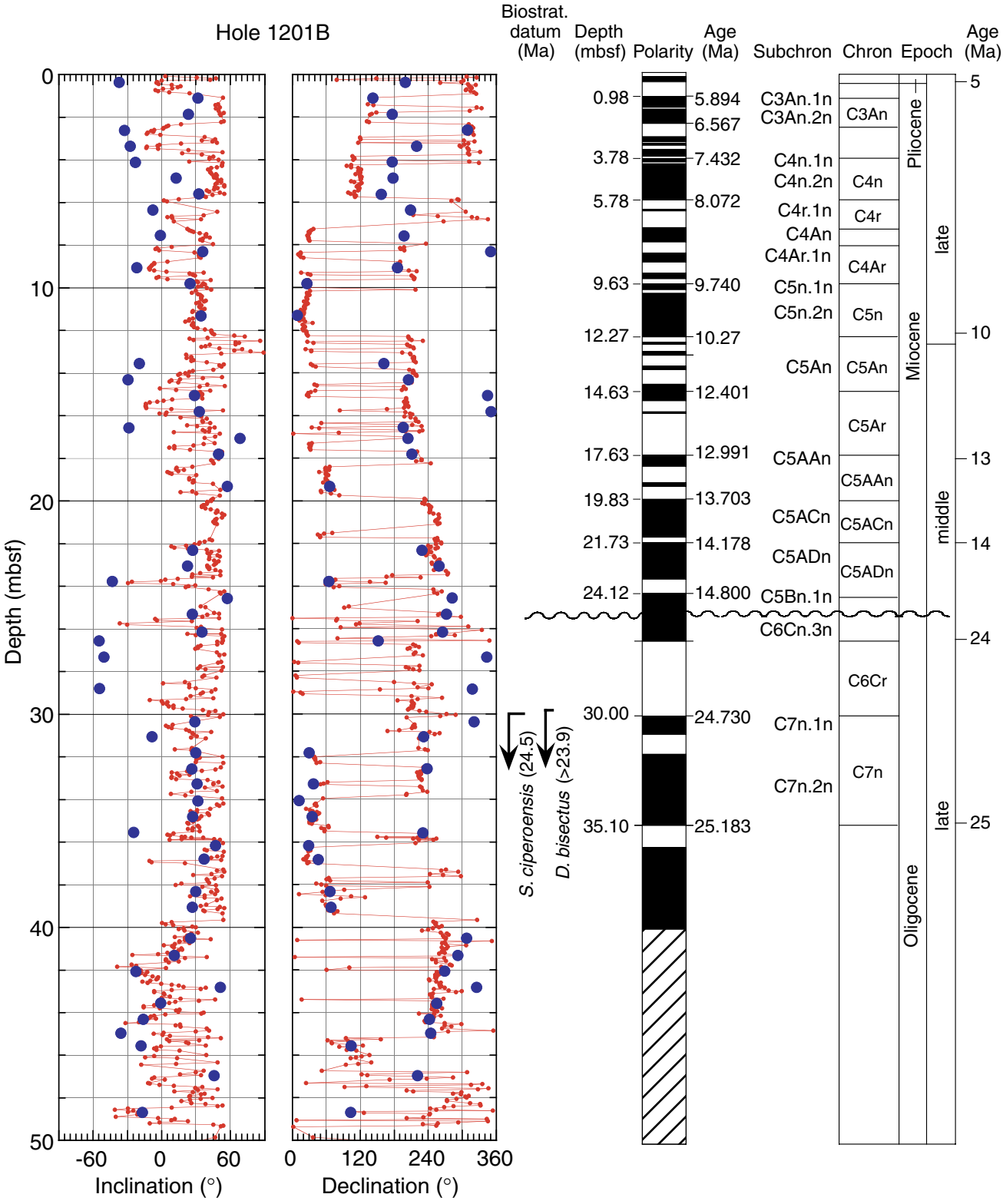

Figure F26. Sedimentation rates at Site 1201 based on biostratigraphic and magnetostratigraphic results. In the graphic lithology log, c = clay, s = silt, s = sand, g = gravel.

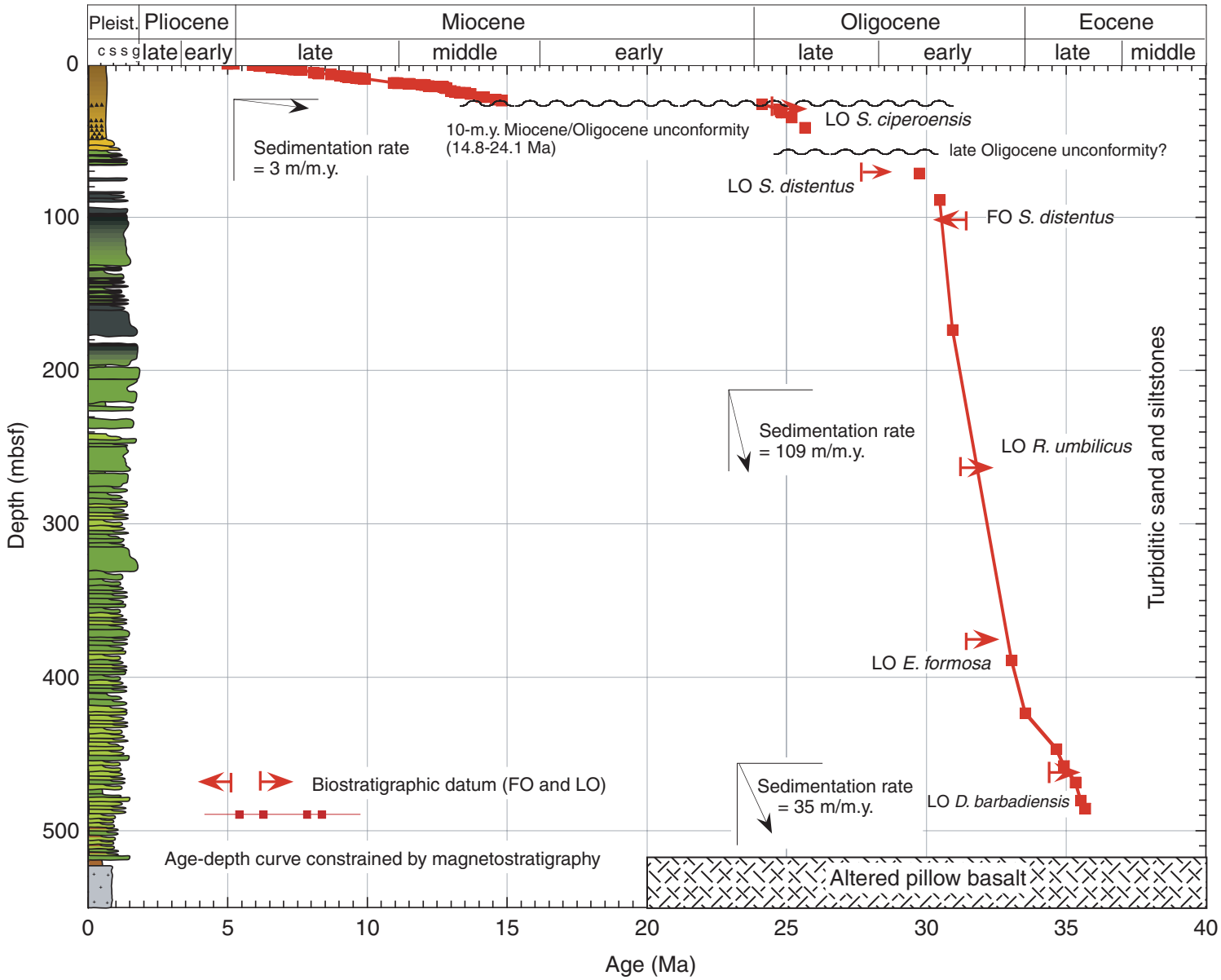

Figure F27. V vs. Ti tectonic discrimination diagram for Site 1201 basalts. The basalts at Site 1201 are transitional between arc tholeiites and mid-ocean-ridge basalts (MORB) or backarc island basalts (BABB). OIB = ocean island basalt.

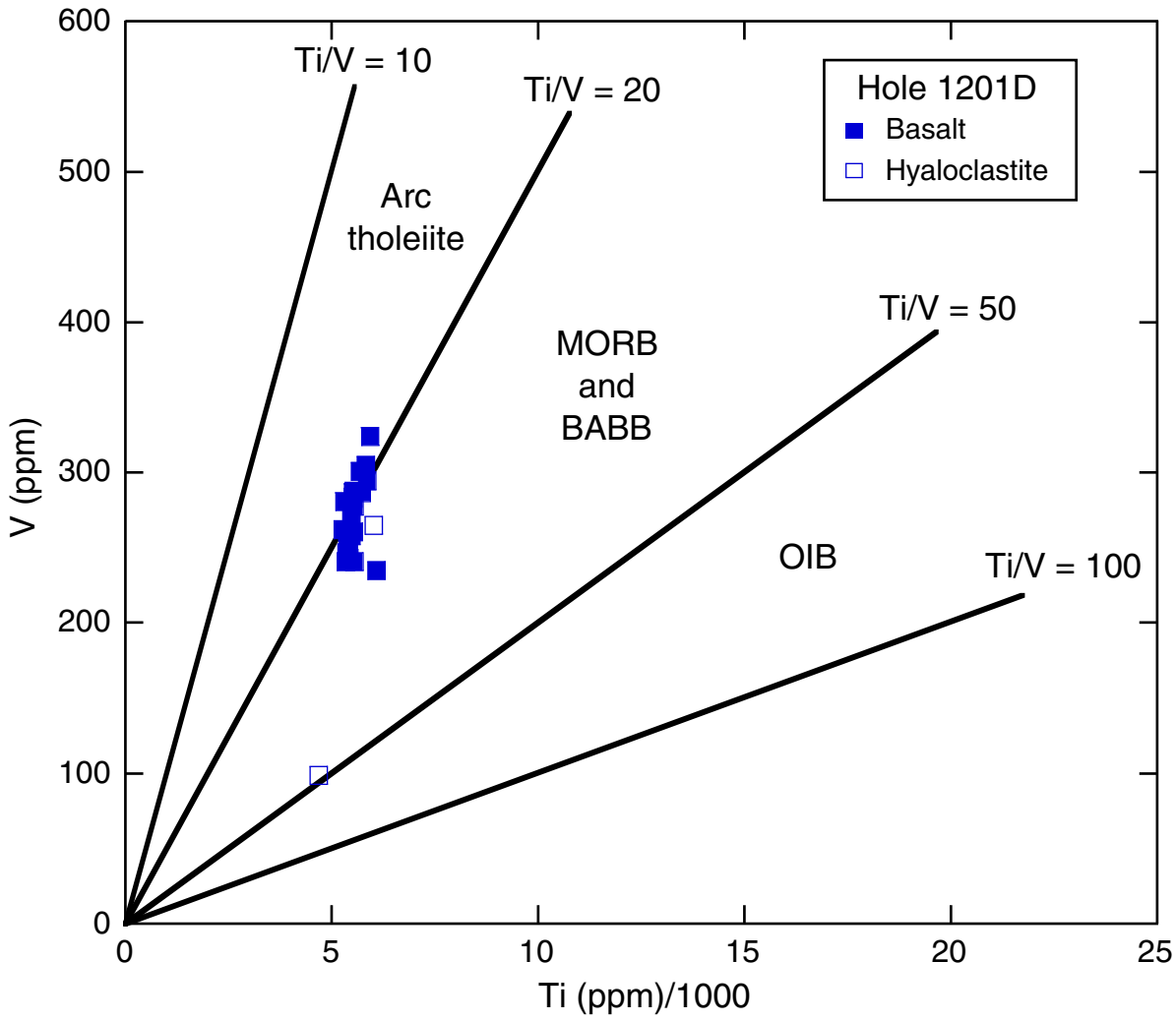

Figure F28. Geological interpretation of the sediment and basement section at Site 1201.

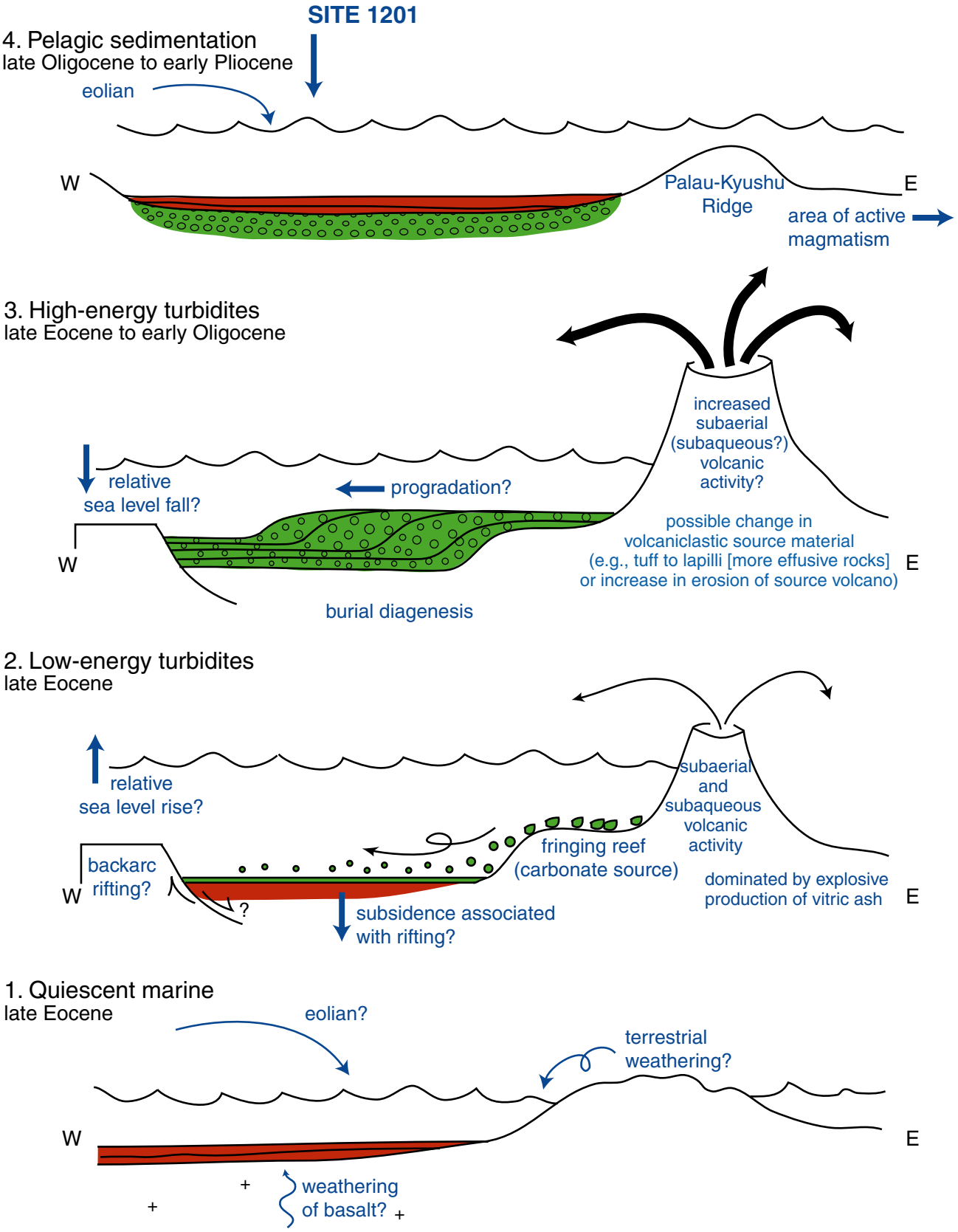

Figure F29. Location of Site 1202 in the Okinawa Trough. The seafloor in the trough under the Kuroshio Current lies above the carbonate compensation depth. Diverging arrows indicate zones of upwelling. Contour interval = 200 m.

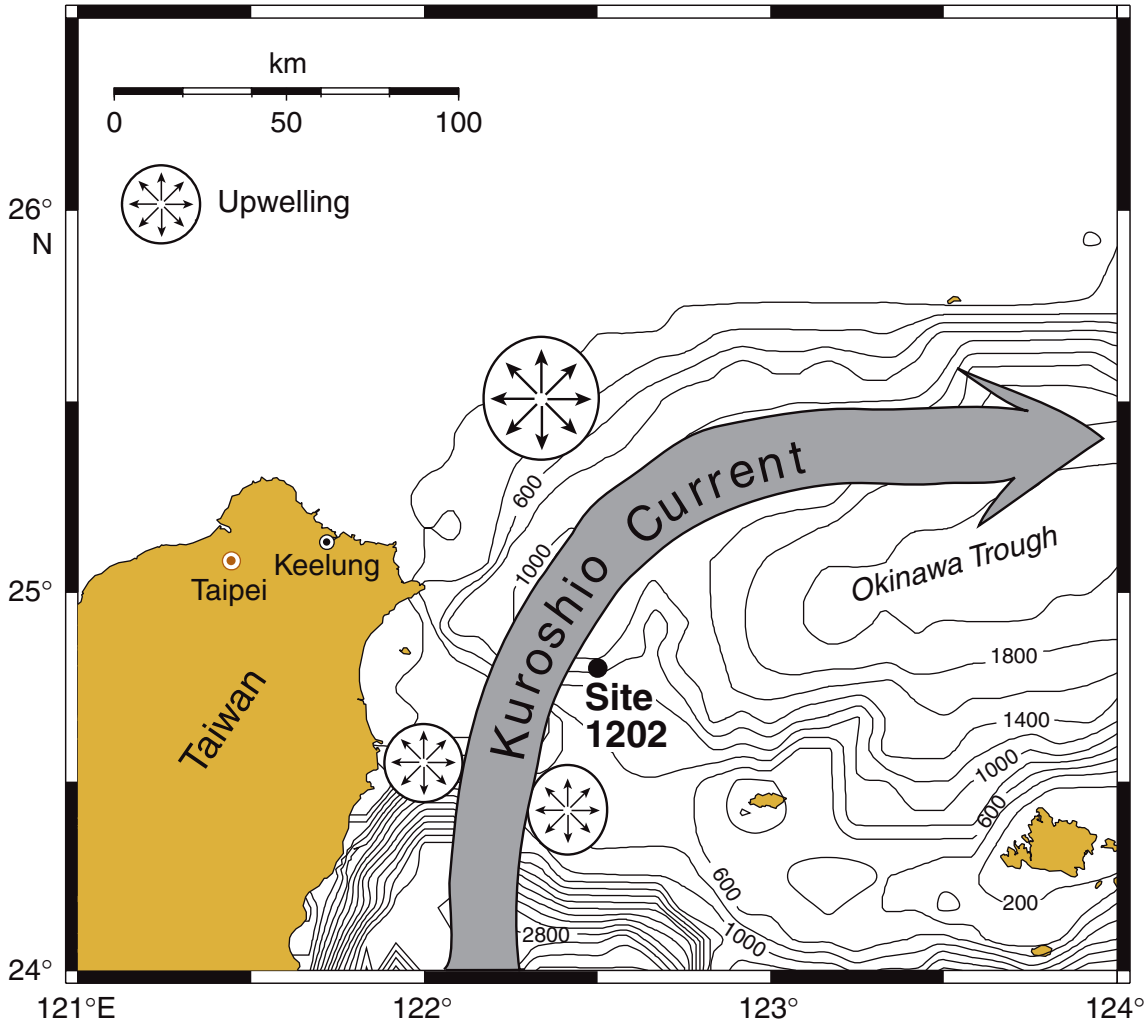

Figure F30. North-south seismic profile EW95091 at Site 1202.

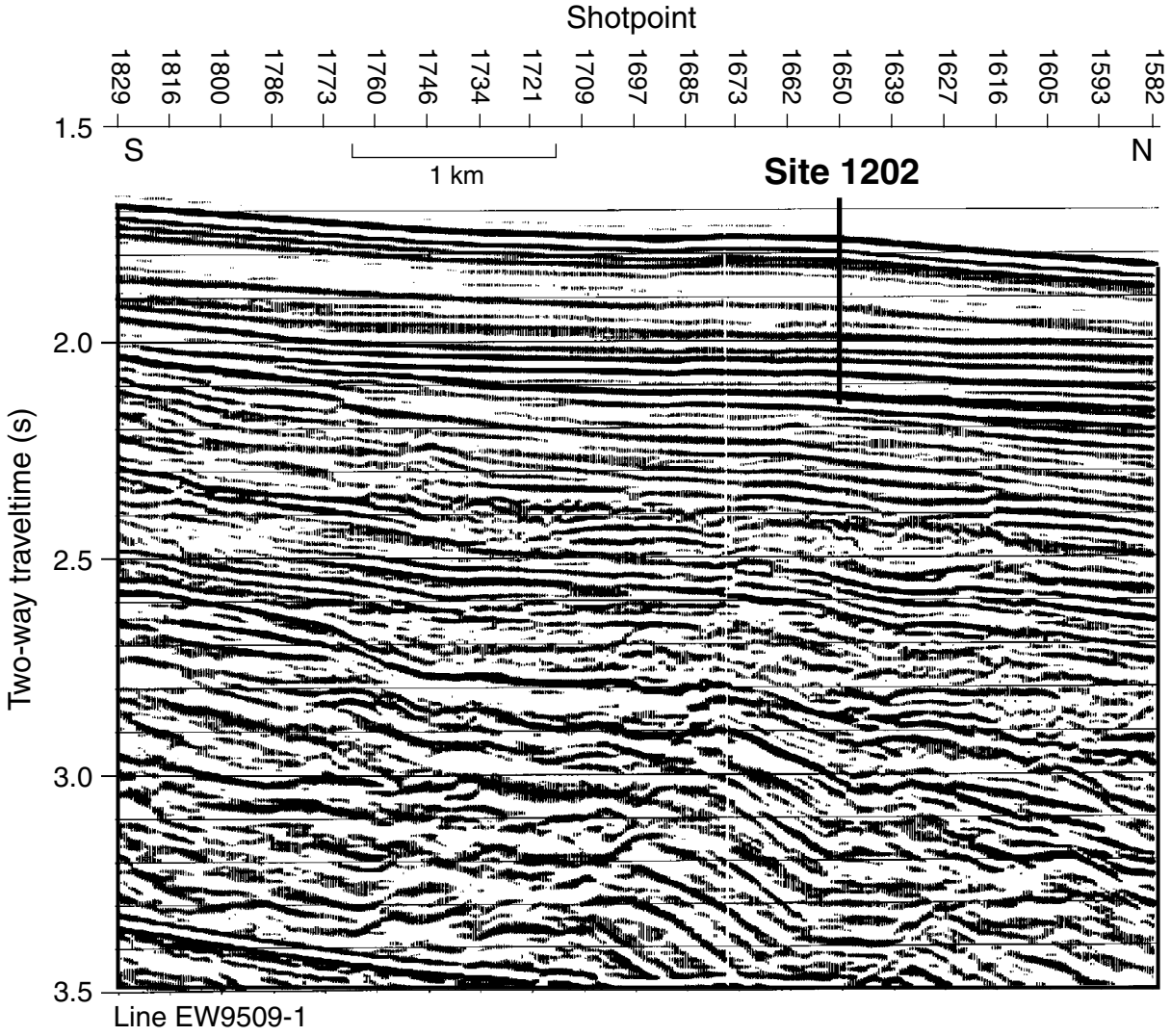

Table T1. Coring summary, Leg 195.

Hole	Latitude	Longitude	Coring technique	Water depth (mbsl)	Interval cored (m)	Core recovered (m)	Core recovery (%)
1200A	13°47.0053′N	146°0.1854′E	RCB	2910	147.2	13.8	9.4
1200B	13°47.0039′N	146°0.1981′E	RCB with center bit	2911	98.0	0.0	0.0
1200C	13°47.0724′N	146°0.1717′E	Rotary drilled for casing, reentry cone	2932	266.0	0.0	0.0
1200D	13°47.0043′N	146°0.1715′E	APC/XCB with center bit	2931	21.9	22.0	100.5
1200E	13°47.0043′N	146°0.1858′E	APC	2911	54.4	38.1	70.0
1200F	13°47.0154′N	146°0.1860′E	APC	2911	16.3	16.3	99.9
1201A	19°17.8830′N	135°5.9501′E	APC	5710	1.6	1.5	93.1
1201B	19°17.8788′N	135°5.9506′E	APC/XCB	5710	90.3	65.9	73.0
1201C	19°17.8829′N	135°5.9408′E	APC	5710	48.1	49.5	102.9
1201D	19°17.8165′N	135°5.9519′E	RCB	5709	519.6	406.8	78.3
1201E	19°17.8542′N	135°5.9491′E	Rotary drilled for casing, reentry cone	5710	580.0	0.0	0.0
1202A	24°48.2449′N	122°30.0002′E	APC	1274	119.5	127.14	106.4
1202B	24°48.2445′N	122°30.0077′E	APC/XCB	1274	140.5	143.28	102.0
1202C	24°48.2428′N	122°30.0167′E	APC/XCB	1274	97.5	100.56	105.2
1202D	24°48.2456′N	122°30.0259′E	APC/XCB	1274	410.0	321.62	78.4

Note: RCB = rotary core barrel, APC = advanced hydraulic piston corer, XCB = extended core barrel.